AD NUMBER

AD838748

NEW LIMITATION CHANGE

TO

Approved for public release, distribution unlimited

FROM

Distribution authorized to U.S. Gov't. agencies and their contractors; Administrative/Operational use; May 1968. Other requests shall be referred to Army Materiel Command, Attn: AMCRD-TV, Washington, D.C. 20315.

AUTHORITY

USAMC ltr 22 jul 1971.

AMC PAMPHLET AMCP 706-251

ENGINEERING DESIGN HANDBOOK

GUNS SERIES

MUZZLE DEVICES

STATEMENT #2 UNCLASSIFIED
This document is subject to special export controls and each transmittal to foreign governments or foreign nationals may be made only with prior approval of: Army Materiel Command, Attn: AMCRD-TV, Washington, D.C. 20315

HEADQUARTERS, U.S. ARMY MATERIEL COMMAND MAY 1968

HEADQUARTERS
UNITED STATES ARMY MATERIEL COMMAND
WASHINGTON, D.C. 20315

AMC PAMPHLET
No. 706-251

17 May 1968

ENGINEERING DESIGN HANDBOOK

GUNS SERIES
MUZZLE DEVICES

This pamphlet is published for the information and guidance of all concerned.

(AMCRD-R)

FOR THE COMMANDER:

OFFICIAL:

CLARENCE J. LANG
Major General, USA
Chief of Staff

WM. A. GREGORY
Colonel, GS
Chief, Administrative Office

DISTRIBUTION:
Special

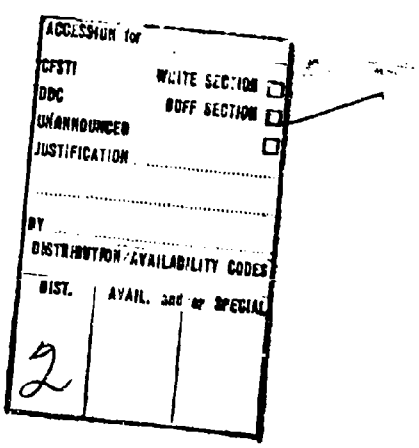

PREFACE

The Engineering Design Handbook Series of the Army Materiel Command is a coordinated series of handbooks containing basic information and fundamental data useful in the design and development of Army materiel and systems. The handbooks are authoritative reference books of practical information and quantitative facts helpful in the design and development of Army materiel so that it will meet the tactical and the technical needs of the Armed Forces.

This handbook is one of a series on Guns and presents information on the fundamental operating principles and design of muzzle devices. Because of higher priorities assigned in the past to other activities, progress in the design of bore evacuators, noise suppressors, and smoke suppressors was not shared with that of muzzle brakes, blast deflectors, and flash suppressors. Therefore, less design guidance is presented for the first group of three than for the second group. However, effort to improve all muzzle devices continues, and this effort is being augmented by studies on human behavior when exposed to the phenomena created at the gun muzzle.

This handbook was prepared by the Franklin Institute, Philadelphia, Pennsylvania, for the Engineering Handbook Office of Duke University, prime contractor to the U. S. Army Research Office—Durham. The handbook was prepared under the technical guidance and coordination of a special committee with representation from the U. S. Army Human Engineering Laboratory, U. S. Army Tank-Automotive Command, Rock Island Arsenal, U. S. Army Weapons Command, and Watervliet Arsenal.

Comments and suggestions on this handbook are welcome and should be addressed to U. S. Army Research Office—Durham, Box CM, Duke Station, Durham, North Carolina 27706.

TABLE OF CONTENTS

TABLE OF CONTENTS (CONT.)

TABLE OF CONTENTS (CONT.)

LIST OF ILLUSTRATIONS

LIST OF ILLUSTRATIONS (CONT.)

LIST OF TABLES

LIST OF SYMBOLS*

A = bore area

A_b = area of projectile passage in muzzle device

A_e = exit area of flow passage

A_h = area of perforation in smoke suppressor

A_i = inner area of baffle passage

A_n = total nozzle area

A_o = area of flash suppressor at origin of slots

A_p = port area

A_{pd} = initial port area

A_{pt} = total port area

A_t = total open area

a_o = velocity of sound in muzzle gas

B = momentum index

B_e = effective momentum index

B_T = impulse on gun at any given time

C_f = conversion factor to compute gas muzzle temperatures

C_n = thrust correction factor for projectile passageway closure

C_{pa} = specific heat of air at constant pressure

C_{pg} = specific heat of muzzle gas at constant pressure

C_{pn} = specific heat at constant pressure of muzzle gas mixture, where n indicates a particular region

C_{va} = specific heat of air at constant volume

C_{vg} = specific heat of muzzle gas at constant volume

C_λ = correction factor for thrust because of friction and turbulence

D = bore diameter of gun tube

D_b = diverter diameter of smoke suppressor

D_e = exit diameter

D_f = distance from muzzle to field position

D_h = diameter of perforation of smoke suppressor

D_o = diameter of projectile passageway in muzzle device

dB = decibel

E = energy

E_f = frictional and engraving losses

E_g = kinetic energy of gas

E_h = heat loss to gun tube

E_m = muzzle energy

E_p = kinetic energy of projectile

E_r = energy of free recoil without muzzle brake

E_{rb} = energy of free recoil with muzzle brake

E_{re} = thermal energy of gas at projectile ejection

F = propellant potential

$F( )$ = function of ( )

$F'( )$ = first derivative of $F( )$

F_a = recoil force

F_b = muzzle brake force; thrust

F_{bx} = muzzle brake force, x identifies the baffle number

F_c = 1400 ft-lb/BTU/°K (conversion factor)

F_{ct} = fraction of maximum overpressure from opposite shock center

*A consistent set of dimensions must be employed in the applicable formulas.

LIST OF SYMBOLS (CONT.)

F_m = maximum instantaneous force on individual baffle

F_n = force on muzzle brake normal to gun axis

f_b = the thrust on a specific baffle during a specific time

f_n = correction factor for computing muzzle brake thrust

f_3 = correction factor of 1.33 used as an approximation

g = acceleration of gravity

H = heat of combustion

I_g = impulse induced on gun during the muzzle gas period

I_i = impulse on muzzle brake at any given time

I_{mb} = total impulse on muzzle brake

I_n = impulse on muzzle brake normal to gun axis

I_r = resultant impulse on recoiling parts

i = number of groups of perforations to position being investigated

i_t = total number of groups of perforations

j = subscript identifying a given position in a sequence

K_{bx} = symbol representing a value of many terms in computing muzzle brake force, x identifies the baffle number

°K = degrees Kelvin

k = $(\gamma-1)/\gamma$ where γ is ratio of specific heats

L = length of recoil; length of gas cell

L_b = length of flash suppressor bar

L_c = length of cone

L_d = length of diverter

L_e = equivalent length

L_g = distance from muzzle to trunnions

L_n = distance to muzzle of evacuator nozzle

M = momentum of muzzle gas

$\dot{M}$ = rate of change of momentum

M_c = mass of propellant gas

M_e = effective mass

M_o = mass rate of flow at muzzle

M_p = mass of projectile

M_r = mass of recoiling parts

M_{rb} = mass of recoiling parts including muzzle brake

m_g = mass of gas leaving muzzle per second

m_r = total momentum of recoiling parts without muzzle brake

m_{rb} = total momentum of recoiling parts with muzzle brake

N_m = maximum number of perforations of periphery at each increment i of smoke suppressor

N_n = actual number of perforations at increment i of smoke suppressor

ΣN = total number of perforations of smoke suppressor up to and including increment i

n = number of baffles; speed-up factor; number of nozzles; molar gas volume

n_e = exit speed-up factor

n_{ej} = exit speed-up factor at baffle No. j

n_i = inner speed-up factor

n_1 = modified speed-up factor

P = pressure, general term

P_a = atmospheric pressure

P_b = breech pressure

P_d = design pressure

LIST OF SYMBOLS (CONT.)

P_{bi} = breech pressure at shot ejection

P_g = gage pressure; gas pressure

P_o = pressure at muzzle; pressure at origin of slots in flash suppressor; muzzle pressure at shot ejection

P_{os} = limit of pressure at origin of flash suppressor slots

P_r = maximum theoretical operating pressure in bore evacuator

P_s = stagnation pressure

Q = rate of flow

QE = angle of elevation of a gun

R = gas constant

°R = degrees Rankine

R_i = inside radius

R_o = outside radius

R_p = ratio of ambient to muzzle pressure at shot ejection

r = mass ratio of air to total air-gas mixture; radius of gun bore

r_b = outside radius of baffle

r_e = radius of shock envelope at baffle

r_j = ratio of baffle inlet area to total area available for flow

r_p = radius of projectile passage

r_l = fractional amount of deflected gas

SPL = sound pressure level

T = temperature of propellant gas having done no external work; isochoric flame temperature

T_a = absolute temperature of ambient air

T_b = time between shot ejection and breech opening

T_f = flame temperature

T_j = jet duration time

T_{jc} = jet duration time of check valve nozzle

x

T_n = computed temperature of muzzle gas of region indicated by digit n

T_o = average temperature of gas at shot ejection

T_s = stagnation temperature

TTS = temporary threshold shift

T_x = ignition temperatures of propellant indicated by any letter subscript

t = time, general term

V_c = chamber volume

V_p = volume of projectile and charge

V_r = reservoir volume of bore evacuator

V_t = total volume of gun tube

v_f = velocity of free recoil

v_o = muzzle velocity

v_r = velocity of recoiling parts

v_w = wind velocity

W_b = weight of gas flowing through projectile passage; weight of muzzle brake

W_c = weight of propellant

W_i = weight of gas diverted through baffle

W_{ig} = weight of igniter

W_p = weight of projectile

W_r = weight of recoiling parts

W_{rb} = weight of recoiling parts with muzzle brake

W_w = ratio of dynamic pressure to static pressure

w_s = total peripheral width of slots

x = distance from breech

x_b = distance traveled by gases from muzzle to side port exit

x_o = lateral distance from tube axis to side port exit

y = ratio of ambient pressure to stagnation pressure

LIST OF SYMBOLS (CONT.)

y_o = ratio of muzzle pressure to stagnation pressure

z_o = axial distance from muzzle to center of side port exit

GREEK LETTERS

α = baffle deflection angle

β_j = upward diverting angle of muzzle brake

γ = ratio of specific heats

Δ = expansion ratio

Δ_b = ratio of projectile passage area to total available area

Δ_{en} = divergence of gas at the baffle exit at baffle n

Δ_i = ratio of baffle inlet area to total available area

Δ_{ij} = ratio Δ_i at any baffle j

Δ_n = divergence of gas from muzzle at flow passage n

ΔT = jet duration factor

δ = heat loss to gun tube as function of shot energy; density of air

ϵ_a = actual muzzle brake efficiency

ϵ_e = efficiency of back traveling shock wave

ϵ_g = gross efficiency of muzzle brake

ϵ_i = intrinsic efficiency of muzzle brake

η = covolume

θ = a simplified term for a time expression in the gas flow equation; time of muzzle pressure drop; angular distance from muzzle to field position

θ_m = minimum breech opening time

λ = composite speed-up factor; ratio of bore to reservoir volumes

λ_d = ratio of bore to reservoir volumes used in design

λ_n = speed-up factor for baffle n

λ_u = uncorrected speed-up factor

ρ = ratio of port area to open area of smoke suppressor

ρ_a = actual value of ρ; mass density of air

ρ_d = theoretical designe value of ρ

ρ_g = ratio of gas entering filter of smoke suppressor

Σ = summation

ϕ = semi-angle of nozzle; inclination of bore evacuator nozzle to bore axis

χ = heat transfer factor

ψ = angular divergence of brake flow passage

ψ_1 = angular distance from horizontal to bottom plate of free periphery brake

ψ_2 = angular distance from horizontal to top plate of free periphery brake

ψ_3 = deflection angle of bottom plate of free periphery brake

ω = speed-up factor for force normal to bore axis; ratio of nozzle area to bore area of a bore evacuator

ω_c = ratio of charging nozzle area to bore area

ω_d = design value of ω in a bore evacuator

ω_{de} = ratio of discharging nozzle area to bore area

ω_n = speed-up factor for normal thrust at baffle n

ω_u = uncorrected speed-up factor for force normal to bore axis

CHAPTER 1

INTRODUCTION

1—1 PURPOSE

This design handbook provides a convenient and ready reference of: (1) fundamental and practical design information, and (2) procedures for use by engineers to select or adapt existing designs or to evolve modified or new designs for achieving the intended performance characteristics of various gun muzzle devices.*

1—2 SCOPE

Present warfare tactics require a high degree of weapon mobility as well as means by which the personnel and equipment may achieve added protection either from their own weapon or from the enemy. Muzzle devices that will reduce the forces acting on a carrier will effectively reduce the massiveness of its supporting structure, thereby increasing its mobility. Those devices that eliminate or reduce detectable phenomena emanating from a gun will improve weapon concealment. A device that reduces disturbing effects on personnel will increase efficiency and morale. All these features are available to some degree in the field of muzzle devices. Each distinct type has its own characteristics, some of which may overlap those of another device. Unfortunately, all desirable performance characteristics of any two, let alone all devices, cannot be incorporated into one assembly. For instance, a muzzle brake may also reduce flash; it cannot suppress noise. Although dual purposes may be managed, no confusion should arise as to the identity or specific purpose of any given muzzle device.

This handbook presents basic and applied information on the general characteristics of guns with particular attention to the behavior of gases when in the bore and when discharged from the muzzle. It discusses both harmful and helpful aspects of those gases, and describes those devices that have been developed to minimize the harmful and utilize the helpful aspects. It explains convenient and generally reliable design methods and procedures from early concept to experimental verification, including comments on reliability of scaling size and performance. It contains material, manufacturing, and maintenance phases that contribute to successful designs. It also has the more sophisticated design procedures programmed for a digital computer. A comprehensive bibliography, glossary, and list of contributors completes the contents and may assist the engineer in this technological field when a problem is not readily amenable to solution by procedures or with data in this handbook.

1—3 GENERAL DESCRIPTION OF GUN MUZZLE DEVICES

1—3.1 MUZZLE BRAKES

1—3.1.1 History

Despite the lack of a strong incentive for its invention before 1888 (the advent of the recoil mechanism), the first muzzle brake appeared in 1842 in France built by Colonel de Beaulieu. A crude affair, it consisted of a series of holes in the muzzle region of the barrel. The holes were sloped rearward to divert the expanding gases in that direction. Twenty-one years later, the French military conducted tests with a 106 mm gun with 36 holes of 60 mm diameter inclined rearward at 45°. Data published by de Beaulieu disclosed the great success of doubling the accuracy and having the recoil distance reduced to 25 percent of its normal distance with only a 6 percent loss in muzzle velocity. Reservations should be

*Prepared by Martin Regina, Franklin Institute Research Laboratories, Philadelphia, Pa.

made with respect to the reliability and accuracy of these claims unless all data are available. However, this first official attempt did establish the muzzle brake as a practical and useful component of a gun.

The first attempt was followed by inventions of Hartley (1871), de Place (1885), Maxim (1890), Simpson (1902), and Smith (1903). During the latter years, several agencies began to devote efforts toward muzzle brake development, thus lending encouragement to the individuals interested in this field. This activity was not monopolized by one country. The United States, England, France, and Germany, all were keenly aware of its potential and did much to advance the technique in design procedure through the years before and during World War I. Muzzle brakes of assorted descriptions and sizes appeared during this period with enough claims of fantastic proportions to excite continued interest in building and testing new hardware. But, not until after the war, when Rateau developed his theory, was any concerted effort made to apply scientific principles to existing mechanical techniques in order to rationalize muzzle brake design concepts. Rateau's theory, still useful, became the basis of our present theoretical and practical design procedures.

1—3.1.2 Purpose

When a gun is fired, the burning propellant and the subsequent gas activity are the sole influences on gun structure and projectile. While in the bore, the projectile offers the inertial and frictional resistance commensurate with the thermodynamics of the propellant. After it leaves the muzzle, the projectile loses further influence. On the other hand, the gas exerts pressure on the gun tube while the projectile is being propelled and after, until this pressure becomes ambient. The pressure forces on the bore surface are balanced and have no external influence. Although of short duration, the pressure force on the breech creates an impulse on the gun tube that is equivalent and opposite to that on the projectile. This rearward impulse is responsible for recoil, an undesirable but controllable phenomenon of all closed-breech guns. There are any number of ways of achieving this control. If the gun is rigidly fixed to its structure and foundation, everything remains motionless and all resultant forces are transmitted directly to the foundation. If the gun is free to move, the impulse will induce a rearward velocity to the movable parts which eventually must be stopped. The magnitude of the resistance determines the recoil distance. Most guns provide this resistance by some type of recoil mechanism, from the application of a person's body when firing shoulder or hand guns to the elaborate recoil mechanisms of artillery. A recoil mechanism moderates the recoil force by diluting the propellant gas impulse with a reaction extended over a comparatively long period of time. The recoil force may be reduced further by reducing the recoiling mass momentum with a muzzle brake.

1—3.1.3 Description

A muzzle brake is a device that is attached to, or is integral with, the muzzle of a gun. Usually the brake has a series of baffles either perpendicular or nearly perpendicular to the gun tube axis. The brake is generally closed on the bottom to prevent escaping gases from endangering or annoying the gun crew. To maintain symmetrical peripheral loading and therefore balance, the top also is closed, leaving the sides open for the gases to escape after impinging on the baffles. Some standard configurations, adhering to either theoretical or empirical practice, have evolved through years of application.

1—3.1.4 Theory of Operation

Immediately as the projectile clears the muzzle, the propellant gases follow, no longer restrained by tube wall or projectile, but still having an appreciable pressure and a velocity equal to or slightly exceeding that of the projectile. If left alone, the gases expand into air and reduce to atmospheric pressure. However, if the gun has a muzzle brake, a different sequence of

events ensues. The projectile while passing through the brake continues to restrain, to some extent, gas flow in the axial direction. But the side ports in the brake offer little resistance to the expanding gas which can now flow between the baffles. The general direction of flow is therefore changed. The resultant direction of this gas flow is no longer diagonally forward, but is radial or actually rearward. By diverting the flow in these directions, the gas must impinge on the baffles and induce a forward thrust. This thrust generates an impulse which is opposite in direction to the recoil momentum, thereby reducing that momentum by the amount of the muzzle brake impulse. Unfortunately, the muzzle brake does not perform while the projectile is still in the bore. The recoiling parts almost reach their full momentum during this time, thus consigning the function of the brake to the analogous role of a corrective rather than a preventive performer.

1—3.1.5 Advantages

The principal advantage of a muzzle brake is its ability to decrease the momentum of the recoiling parts of a gun. How this advantage is exploited depends on the weapon assignment. If low weight is the dominating criterion and knowing that recoil force is inversely proportional to length of recoil, a conventional length of recoil can be retained with subsequent low recoil forces that lead toward lighter supporting structures. In tanks, where space is at a premium, short recoil lengths only are possible but recoil forces remain correspondingly high thus offering little opportunity to reduce structural weight. Some secondary advantages of a muzzle brake include the ability to suppress flash to some extent, and help gun stability during recoil partly by the effect of the additional mass and partly by the thrust generated by the muzzle gases. A few tests indicated an accuracy increase but conclusive data are lacking.

1—3.1.6 Disadvantages

Perhaps the principal disadvantage of a muzzle brake is the deleterious effect that the muzzle blast has on the crew, particularly excessive overpressure. Air disturbances or propellant gas moving at high velocity, loud noise, and heat can be disconcerting if not outright injurious. The resulting obscuration is a primary objection. Damage to camouflage and the danger of flying debris are two undesirable products of the blast. Noise is always increased although at least one model had the ability to muffle sounds which seems contrary to the inherent characteristics of a muzzle brake but, until more substantiating data are available, increased noise will continue to be listed as a disadvantage. A minor disadvantage is the added weight at the muzzle. This weight increases muzzle preponderance and further burdens the elevating mechanism, particularly in older guns that were not initially designed for a muzzle brake. Newly designed guns eliminate this problem with a suitable equilibrator.

1—3.1.7 Current State of the Art

The present consensus among users has the advantages of muzzle brakes outweighed by the disadvantages. As yet, its objectionable muzzle blast has not been eliminated from artillery but noted success has been achieved with small arms. A high degree of effectiveness is usually accompanied by strong muzzle blasts which always suggests a compromise in design. Although improvements are continuing, the designer is handicapped by the unwanted blast. If the gun crew is shielded, as in a tank, muzzle blast has little effect. However, artillery crews must be shielded or some means developed to divert the blast away from the crew. Even so, shielding does little to protect support personnel in the general weapon area. Some effort has been directed toward this development, but no real improvement has been achieved. Much progress remains to be made in the muzzle brake field but, aside from structural requirements, secondary effects cause the greatest concern. Muzzle brake efficiency and effectiveness have reached highly acceptable levels. Empirical and theoretical design procedures are available beginning with somewhat elementary but

effective initial design approaches and ending with the more sophisticated electronic computer routines programmed for highly theoretical approaches.

1—3.1.8 Types

Basically there are two types of muzzle brake—the closed and the open. A third type, free periphery, is an outgrowth of either of the other two. The closed type, shown schematically in Fig. 1—1, derives its name from the spacing of the baffles, said spacing being too short to permit the natural expansion of the gas before it is diverted by the baffles. The open type (Fig. 1—2) has its baffle spacing large enough to permit the gas to expand relatively freely before striking the baffle and being diverted. The free periphery is so named because it offers little restriction to gas flow around the periphery of the baffles. Whatever restriction it does offer comes from the structure that is needed to assemble the baffle system into the rigid, integral structure that forms the muzzle brake. When not of the free periphery type, the muzzle brakes (closed on top and bottom) discharge the gas through side ports thus creating a resultant external reaction of zero around the periphery.

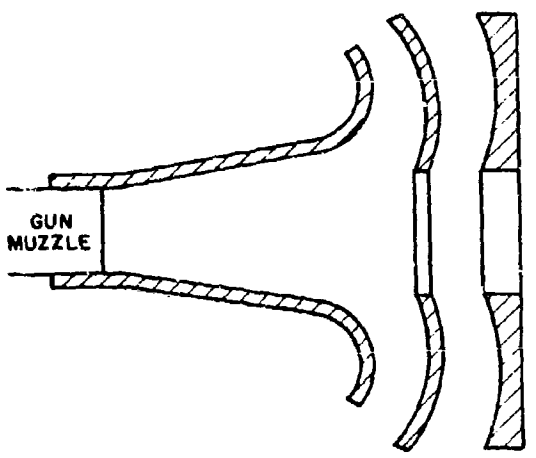

FIGURE 1–1. SCHEMATIC OF CLOSED MUZZLE BRAKE

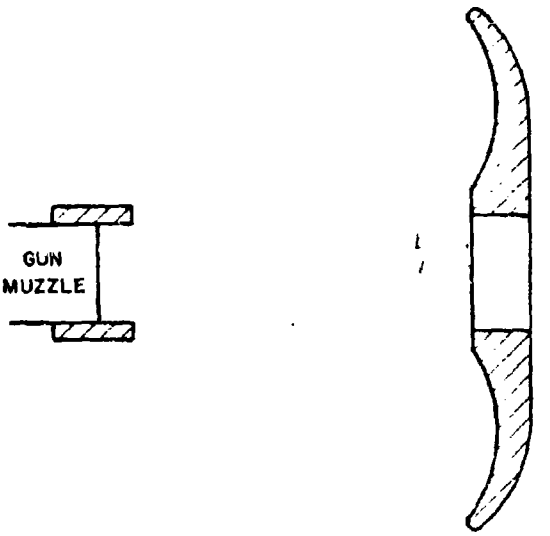

FIGURE 1–2. SCHEMATIC OF OPEN MUZZLE BRAKE

1—3.2 BLAST DEFLECTORS

1—3.2.1 History

The inception of the blast deflector had to occur simultaneously with the muzzle brake regardless of the intent of the inventor. Both operate on the same principle, however, the degrees of success usually diverge although successful combinations of brake and deflector have been realized. Early attempts at blast deflector design followed the empirical approach, and success in the areas of deflector or brake was achieved through trial and error. One type (OMCF 2722), not only reduced the size of dust clouds experienced during normal firing, but it also reduced flash and the length of recoil. In contrast, the Gallot muzzle brake, the R.H.S. Hughes Recoil Control, Blast Deflectors AD-C537, AD-C538, AD-C544 were failures. The successful blast deflectors were outright muzzle brakes or modified versions. Of all those made and tested, the 76 mm Muzzle Brake M2, double

baffle type, showed the most promise with respect to operational requirement and acceptable size. The most successful, from the operational point of view alone, consisted of a muzzle assembly that had twin ducts, one on each side and parallel to the gun tube, or a single duct above the tube. These ducts carried the propellant gases rearward and discharged them at the trunnions. A 90° bend upward in each duct directed the discharge away from both gun and crew. This type also performed well as a muzzle brake.

1—3.2.2 Purpose

A blast deflector has a twin function—to minimize obscuration and to lessen the effect of muzzle blast on the crew if the gun has a muzzle brake. Both these functions need not apply simultaneously to all weapon installations. The tank crew is shielded from muzzle blast but the dust cloud raised by the blast can hide the target, thus interfering with precise sighting. On the other hand, the muzzle blast on long range guns may be extremely disconcerting or physically harmful to the gun crew but obscuration presents no sighting problem inasmuch as the target is usually beyond visual range. For short-range weapons, where targets are visible, the blast deflector must exercise its dual function, but only if the gun has a muzzle brake.

1—3.2.3 Description

The blast deflector is similar to the muzzle brake. In fact, either may also function as the other. It is attached to the muzzle and is so constructed that propellant gas will be diverted away from the ground and gun crew. The deflector has ports through which the propellant gas flows. The ports may be an arrangement of simple baffles or may be more complex with channels of circular, elliptical, or other cross-sections, leading outward, usually perpendicular to the bore, or canted slightly rearward. If antiobscuration is the primary function, the surface facing the ground should be closed. If balance of forces is needed, the top also should be closed.

1—3.2.4 Theory of Operation

The blast deflector operates similarly to the muzzle brake by controlling the flow direction of the expanding propellant gas as it leaves the muzzle. By changing the direction of the resultant of the gas momentum, the deflector must develop a component of the resultant in the axial direction opposite to that of the recoil momentum, thereby inducing a muzzle brake effect. If used for antiobscuration purposes only, the deflector diverts the gas upward and outward but not toward the ground. In so doing, thrust is generated in the direction opposite to the diverted gas flow. This thrust can be balanced by providing equal and opposite gas flow, readily achieved with side ports for lateral stability. Vertical stability can be achieved not only by closing the top of the deflector at the muzzle region but by ducting the gas rearward and discharging it upward at the trunnions. If the blast deflector is an adjunct of the muzzle brake, it must direct the rearward flow of propellant gas at an angle that reduces the impact on the crew to a limit that can be tolerated.

1—3.2.5 Advantages

A blast deflector reduces obscuration which in turn increases the effectiveness of the gun by keeping the target visible. It reduces the muzzle blast effects to limits that can be tolerated by the gun crew.

Both foregoing advantages are morale boosters. From one point of view, a target obscured by one's own gun fire is a source of frustration. From another, the effect that obscures the target may reveal the gun's position and, in a sense, create overexposure to enemy fire. An unabated muzzle blast is analogous to inflicting self-injury, a factor that does not promote either confidence or efficiency.

1—3.2.6 Disadvantages

The disadvantages are usually related to the adverse effects produced on other

equipment. Blast deflectors generally reduce the efficiency of muzzle brakes and may overload the elevating mechanism. Some models have a tendency to increase flash.

1—3.2.7 Current State of the Art

The development of the blast deflector is almost congruous with that of the muzzle brake. Although its primary purpose is to dilute the effect of the muzzle blast created by the muzzle brake, one of the more acceptable deflectors is a muzzle brake. Many types of blast deflectors have been proposed, built, and tested. Most have been found wanting; some because of structural weakness, some because of massiveness or awkwardness in construction, and some because of poor performance. The successful deflectors were those that redirected the gas flow away from the crew area but these invariably caused a decrease in brake efficiency. Those that were made for antiobscuration only and were considered successful have not been recommended for general usage. However, the degree of success of either blast deflector or muzzle brake has always been relative, comparing the performance of the new with its predecessors. Muzzle brakes of relatively high efficiency are available, but the shock overpressures on gun crews are objectionable. Reducing the shock is the main challenge to the blast deflector designer. Some attempts have been made to attenuate the shock induced by artillery fire but were not totally successful. Development in this direction is continuing.

1—3.2.8 Types

There are several types of blast deflector, some are actually muzzle brakes; others were designed for their own particular function.

1. Baffle-type. This type is a natural outgrowth of the baffle-type brake. The muzzle brake has good antiobscuration characteristics provided that the gas flow is diverted from the ground. This type is one of the most successful.
2. Perforated-type. Originally designed as a muzzle brake (Swiss Solothurn) this type proved unsuccessful on artillery. Its structure was tubular, circular, elliptical, rectangular, cross-section, or any other configuration that appealed to the designer. Horizontal holes, usually five, traversed the device. Propellant gases, escaping through the ten exits, were to reduce obscuration. One model performed well, the others proved to have little or no significant effect.
3. T-type. This blast deflector is merely a one-baffle muzzle brake. Its baffle is a flat plate with a circular hole in the center to permit projectile passage. The baffle plate is held, top and bottom, by two other plates that are fixed to a housing that attaches to the muzzle. This type performs well as an obscuration deterrent.
4. Duct-type. A rather massive affair, this type, attached to the muzzle, diverts the gas rearward through one or two ducts and discharges into the air above the trunnions. The discharge direction is upward, perpendicular to the bore, so that the induced reaction passes through the trunnions and thus spares the elevating gear an additional burden. Ideal as an obscuration deterrent and holding promise as a muzzle brake, this type has still to be accepted because of its massiveness and, when applied to artillery weapons, the gas discharge is in close proximity to the crew; therefore, during high Q. E. firing, gas discharge is directed toward the crew area.

1—3.3 FLASH SUPPRESSORS

1—3.3.1 History

Military authorities were cognizant of the problem presented by muzzle flash before 1900 but did not attach material significance to it until World War I. Betrayal of gun position soon became evident to both sides and was exploited accordingly.

The search for a flash eliminator or suppressor during this war became almost as intense as the search for a higher performing gun; however, flash research always lagged research on other gun phenonema. For one reason, stimulants, such as the two World Wars which revealed the dire need for a flash suppressant, ceased before an effective suppressor could be found or invented. Perhaps a better explanation of this lag was that flash behavior was never fully understood. The pressure of other war needs and the lack of adequate instruments gave the technical investigators little more than empirical procedures. (For a discussion of the spectral characteristics of muzzle flash see Ref. 21.)

Earliest attempts at flash suppression involved additives to the propellant. These additives varied from small amounts of black powder to inorganic salts or any other compound that struck the fancy of the experimenter. During World War I, the French used a propellant for machine gun ammunition consisting of nine parts smokeless powder and one part black powder. For the same reason, the German loaded cotton or silk bags with potassium chloride and attached these to the base of the projectile. Both were effective in suppressing secondary flash but, as happened with many similar suppressants, smoke increased while the ballistic properties of the propellant suffered.

Research in flash suppression continued in the interim between the two World Wars but little progress was achieved. Beside the additives as suppressants, muzzle brakes and blast deflectors appeared to have some effect on flash. This observation led to organized attempts to learn the mechanics of the muzzle blast and flash. Since World War II, considerable data have been accumulated, and mechanical flash hiders and flash suppressors have been developed with various degrees of success. However, a great deal of progress is still needed to achieve an efficient, practical flash suppressor either mechanical or chemical.

1—3.3.2 Purpose and Description of Types

A flash hider or suppressor reduces muzzle flash to the extent that the illumination does not reveal a gun position to the enemy. The muzzle device may be a cone-type (Fig. 1—3) or a bar-type (Fig. 1—4). The former is sometimes called a flash hider but irrespective of their labels, both function according to the same physical principles. Each is a simple device.

1—3.3.3 Theory of Operation

In Chapter 2, five types of flash are defined—preflash, primary, muzzle glow, intermediate, and secondary. To summarize:

1. *Muzzle flash* is a sequence of events created by the propellant gas as it issues from the muzzle.
2. *Preflash* is the burning of the gas that leaks past the projectile before the rifling fully engraves the rotating band or jacket and therefore before obturation is complete, or in worn guns where obturation is never complete.
3. *Primary flash* is the flame of continued burning of the propellant or the incandescent gas at the muzzle. Neither preflash nor primary flash can be influenced by mechanical means except by obscuration methods.
4. *Muzzle glow* is the illuminated gas inside the shock bottle.

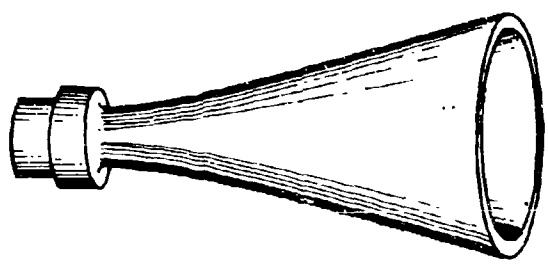

FIGURE 1-3. CONE FLASH HIDER

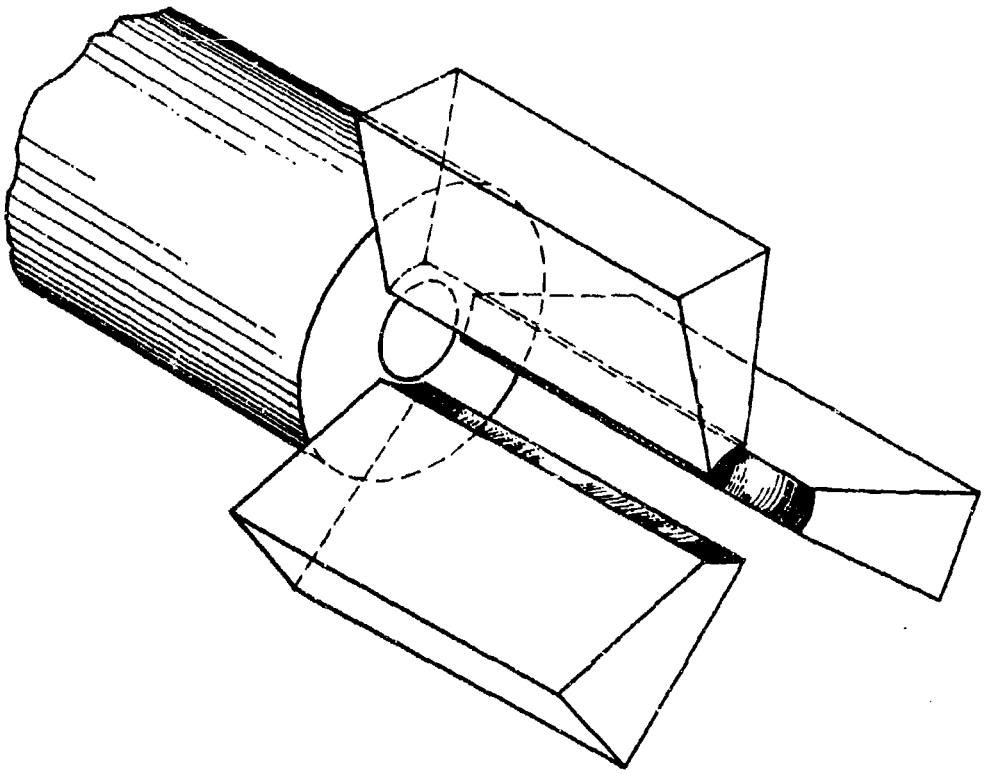

FIGURE 1-4. BAR FLASH SUPPRESSOR

5. *Intermediate flash* is the illuminated gas in front of the normal shock caused by the increased pressure and temperature as the gas passes through the shock.

6. *Secondary flash* is the intense flare of burning propellant gas after the gas has mixed with air and is ignited by the preliminary flash or by the elevated temperature after the gas has passed through the shock front.

Muzzle glow, intermediate flash, and secondary flash are controllable mechanically by destroying the shock boundaries that are responsible for the flash. Fig. 1—5 shows this effect when comparing it with Fig. 1—6. Fig. 1—5 is a shadowgraph of uncontrolled flash. The shock bottle and normal shock are discernible, indicating that the entire area is brilliantly illuminated. Fig. 1—6 is a shadowgraph taken under the same general conditions except for the bar flash suppressor. Neither shock bottle nor normal shock are present with the resulting effect of far less illumination being indicated. Fig. 1—7 contains two photographs, each illustrating the respective features of Figs. 1—5 and 1—6, the brilliant flash and the barely visible suppressed flash. Either hider or bar suppressor serves the purpose for all three types of flash, with one exception. Secondary flash will occur if the prevailing conditions at the muzzle defy any sort of control. These conditions involve the richness of the air-gas mixture and the ignition temperature of each mixture. If the richness r is expressed in terms of the percentage of air in the mixture, then r will vary from

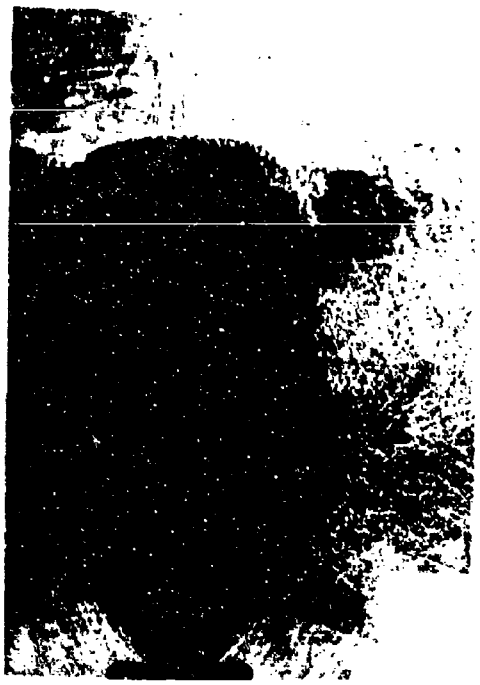

FIGURE 1-5. UNSUPPRESSED FLASH

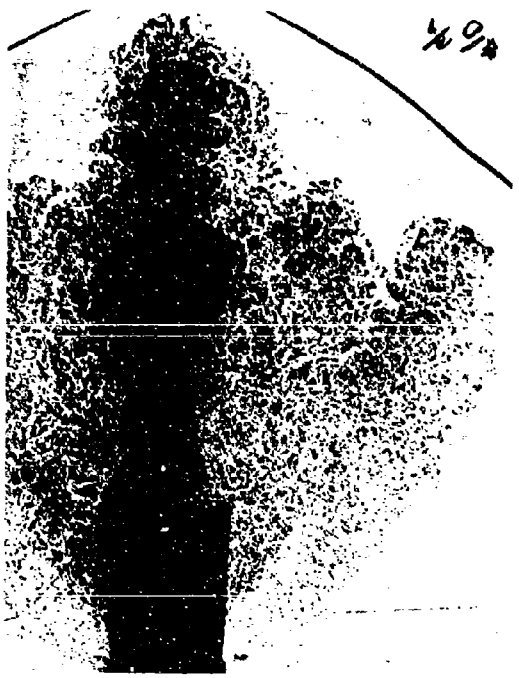

FIGURE 1-6. EFFECTS OF FLASH SUPPRESSOR

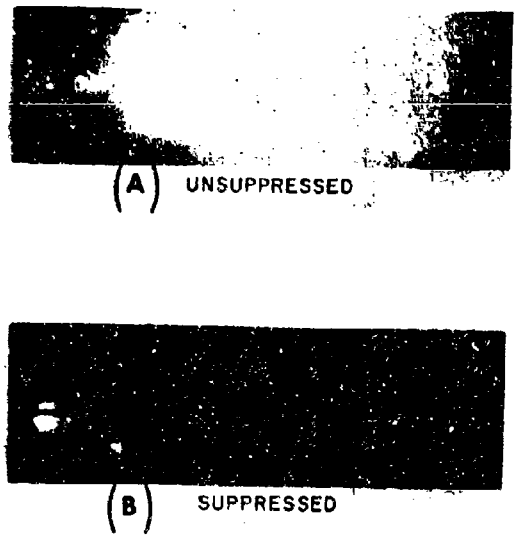

FIGURE 1-7. EXAMPLE OF FLASH SUPPRESSION

zero at the muzzle where the gas is undiluted to almost 100 sometime later when the gas has practically disappeared. Each mixture has its minimum ignition temperature. The mixture will ignite only if the actual temperature of the mixture coincides with or exceeds the minimum ignition temperature. Fig. 1—8 illustrates the probability. If T_i is the minimum ignition temperature and T_a the actual temperature of the gas-air mixture, mechanical devices will have no effect on secondary flash between f_1 and f_2. However, secondary flash may still not develop between these limits. Although the ignition limit may be met, the temperature history of the gas mixture must meet its ignition period requirement. Should the mixture pass through the high temperature regions fast enough, the gas may not have enough time to ignite and cause secondary flash.

1—3.3.4 Advantages and Disadvantages

The advantages of a successful flash suppressor are almost obvious. A flashless gun, by not generating visible light, does not immediately reveal its position to the enemy. The absence of glare benefits the

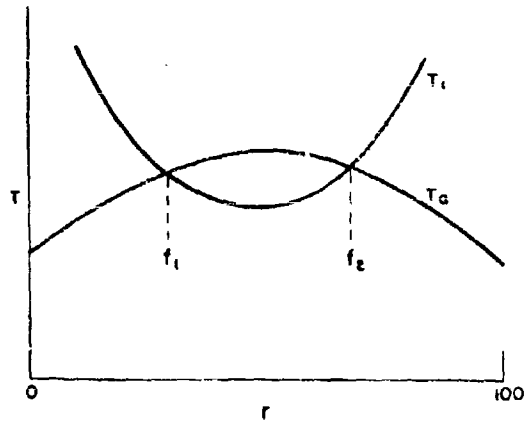

FIGURE 1-8. FLASH PREDICTION TEMPERATURE CURVES

crew by not hampering visibility. The suppressor's primary disadvantage is its tendency to generate more smoke than otherwise would be emitted. Other disadvantages, secondary in nature, are added weight, added costs, and susceptibility to damage during handling.

1—3.4 SMOKE SUPPRESSORS

1—3.4.1 History

Gunpowder ceased to be a powder about 1860 when General T. J. Rodman discovered the principle of progressive combustion. Propellants thereafter came in grains the sizes of which were compatible with the size of the gun. Although ballistics improved after this change, black powder was still unsatisfactory because, among other undesirable effects, it produced large amounts of smoke. The smoke problem was reduced considerably in 1886 when nitrocellulose was introduced as a smokeless propellant, however, enough smoke was generated by other ammunition components to perpetuate the search for a smoke suppressant. The emphasis on flash suppression by propellant additives did not help because these additives usually generated more smoke. Unfortunately, additives that reduce smoke generally contribute to more intensive flash, thus directing the search toward a mechanical smoke suppressor.

Gun smoke is formed by the presence of small particles suspended in muzzle gases. These particles may condense from a gas to a solid or liquid state, or may be minute particles of metal or metallic oxides, derived from cartridge case, projectile, and barrel. Water vapor and carbon particles are also present in the propellant gas. When exposed to the atmosphere, the water vapor may condense and increase the density of the smoke. Air temperature and relative humidity will influence the formation and longevity of this contribution to the density. Gun smoke can be suppressed by removing some or all of these particles from the gas. Before 1947, little research effort was made for this purpose. An extensive literature survey at this time on flash and smoke found over 900 references, of which only four dealt with gun smoke[1*]. From the survey, the conclusion was reached that gun smoke was derived primarily from the projectile, primer, and flash suppressant and contained both water-soluble and insoluble particles. Copper, lead, zinc, antimony, and iron are the principal elements of the insoluble particles, whereas compounds of potassium, copper, chlorine, sulfur, and sodium predominate in the soluble particles. Collecting the smoke for the analysis was difficult. Mechanical filters were unsuitable but attempts at collecting smoke particles proved very efficient with electrostatic precipitators. After the literature survey, a research program was organized to ascertain the sources, and the qualitative and quantitative nature of the smoke particles to form a firm basis for the development of efficient smoke suppressors.

1—3.4.2 Purpose, Description, and Operation

Smoke suppressors should be capable of removing the visible particles from the propellant gases without inducing or contributing to other deleterious effects such as flash. The particles are removed by filtration. In the laboratory, successful filtering

*Superscript numbers refer to References at the end of this handbook.

has been achieved electrostatically. This technique is not readily applicable for field use. Generally, the smoke suppressor is a long annular chamber the inside diameter of which is larger than the gun tube bore so as not to impede the radial expansion of the propellant gas as it leaves the muzzle. The inner wall is perforated for the gas to pass through it and enter the chamber which is packed with a porous medium. Since the size of a smoke particle is 0.5 micron or less, a filter which would screen out this size material would be impractical, sufficient time not being available for the filter to accept the total flow. In addition, the filter passages would soon be clogged and useless. To avoid these deficiencies, the filter is made much more porous to permit a more generous flow of gas. However, no straight channels exist; hence the smoke particles must continuously impinge, or bounce, from one solid filter element to another, eventually losing all momentum and stopping. The gas continues to flow into the chamber until the muzzle gas pressure falls below the suppressor chamber pressure, then flow reverses and exits from the inner cylinder. The mechanics of operation are related more to the function of a settling tank rather than to a filter.

1—3.4.3 Advantages and Disadvantages

An efficient smoke suppressor is advantageous if it fulfills its purpose and may be of further use by suppressing flash. One disadvantage stems from the ability, at times, of inducing flash. Other disadvantages are the usual—added weight, added cost, and probably frequent maintenance, particularly the cleaning or replacing of filter elements.

1—3.4.4 Types

Two general types of smoke suppressors have been used successfully, the electrostatic type which thus far is confined to the laboratory, and the filter or impingement type. The latter may be subdivided into three categories. The first makes no attempt to control the flow, for the perforations are spaced evenly around and along the inner wall. The second may have perforations of one size evenly spaced around the periphery but becoming more dense in the axial direction of flow, or may be the same in number but increasing in size in this same direction. In this way, accessibility to the chamber increases as pressure drops along the axis thus making an attempt to equalize the flow into the chamber at all points. The third category is the tapered bore suppressor. Experience shows that the perforations nearest the gun muzzle frequently become clogged with copper and other smoke particles. To relieve this tendency, the inner diameter of the suppressor is made larger than would otherwise be necessary while the exit diameter would be of conventional size, thereby providing a conical inner surface. In theory, this construction distributes the impinging properties of the perforations evenly along the length of the suppressor or at least delays the clogging of those nearest the muzzle.

1—3.5 NOISE SUPPRESSORS

The report or noise of a firing gun is numbered among the various objectionable phenomena that develop at the muzzle. Noise is closely associated with flash and muzzle blast inasmuch as attempts to attenuate any of the three will unquestionably have some influence on the other two. On the other hand, if no controlling measures are taken, secondary flash may prolong the duration of report and muzzle blast but not necessarily increase their intensity. And, since muzzle gas pressures are related to all three, noise and blast intensity may be assumed to influence flash.

Noise produced by weapon firing can be hazardous to hearing, cause communication interference, and aid the enemy in detection. A blast deflector offers relief to the crew by diverting the harmful pressure waves away from the crew area but without reducing the intensity to the extent where it becomes undetectable. A flash suppressor, however, can incorporate features that reduce the intensity of the noise.

If this type muzzle device can be developed to the point where both flash and noise can be reduced to acceptable limits, two knotty problems become solved simultaneously. A large amount of effort has been expended on flash suppressors; considerably less on noise inhibitors. A measure of success has been achieved in the suppression of noise through experimentation. No general design procedures, either theoretical or empirical, have been developed for a noise suppressor, primarily because no appreciable effort was ever assigned to develop this type of muzzle device. A measure of success has been achieved in the suppression of noise but usually as a by-product of the development of another type of muzzle device, such as a flash suppressor.

1—3.6 BORE EVACUATORS

Rapid fire tank or closed-cab mounted guns have a tendency to discharge propellant gases into the cab when the breech is opened to receive the next round. This reverse flow not only is disconcerting to the crew but also reduces its effectiveness by impairing sight and breathing. Further damage is sustained on the occasions when flashback occurs. To dispel the accumulation of breech gas flow, large installations such as naval gun turrets resort to rapid ventilation methods. However, this method of removing the objectionable gas requires bulky equipment, not readily adaptable to the already overcrowded tank compartments.

Preventive measures, usually more attractive than corrective ones, are available in the bore evacuator. The evacuator is simply a gas reservoir that is attached to the gun tube. Gas flow between reservoir and bore is achieved through one or more nozzles that connect the two chambers. From the time the projectile passes the nozzles until it leaves the muzzle, propellant gas flows into the evacuator. When the pressure in the bore drops below that in the evacuator, the stored gas reverses its earlier flow and, by being directed by the nozzles toward the muzzle, exits there at an appreciable velocity. The flow of gas from evacuator toward muzzle creates a partial vacuum in this region which induces clean air to enter the breech. This air, under the influence of the differential pressure, continues to flow toward the muzzle to flush the bore of residual gas, thereby precluding reverse propellant gas flow into the gun compartment.

CHAPTER 2

MUZZLE GAS FLOW

2—1 MUZZLE GAS PHENOMENA

As it leaves the muzzle, the projectile is followed by what appears to be a violent eruption of propellant gases. This eruption is called muzzle blast. Actually, the blast is gas activity that adheres to a definite sequence of events. It is a jet of short duration formed by hot, high pressure gases that follows a well-defined series of stages as it grows and decays. Descriptively, muzzle blast is a system of normal and oblique shock waves that form the boundaries of the region in which the principal expanding and cooling of gases occur. Surrounding the shock boundary is a turbulent shell and outside this shell is a turbulent "smoke ring" that moves radially and advances forward. Fig. 2—1 is a sketch of the muzzle blast after 25 calibers of bullet travel from the muzzle. It shows all the phenomena of the blast in their relative positions except for the weak shock caused by the air pushed ahead of the bullet. Fig. 1—5 is a shadowgraph of a muzzle blast. The normal shock, barely visible, is in the center of the blast area.

The main traveling shock is formed in the air by the released propellant gases when they flow past the projectile and induce a succession of weak shocks in the relatively still air behind the first, but weaker projectile-induced shock. This succession soon merges into a strong shock ahead of the projectile. In the meantime, the projectile, by interfering with the direct gas flow, causes a strong shock to form behind it. This shock eventually becomes the quasi-stationary normal shock and with the oblique shock, forms the central supersonic region, dubbed *shock bottle*, of the jet. The flow into the bottle starts at the muzzle where the gas is luminous. This visible light, extending only a short distance, is called *primary flash* and may be white light, indicative of actual burning, or it may be the red glow of luminous solids in the gas. It is the white dot in Figs. 2—2 and 2—3.

The principal expansion of the jet is confined to the shock bottle where the flow, starting at the muzzle with a Mach number close to one, is practically adiabatic. As the gas continues to move until checked by the shock boundaries, both Mach number and absolute velocity increase rapidly with a corresponding decrease in pressure density and temperature; the temperature being low enough most of the time so that the gas ceases to radiate visible light. When the light is visible, the illumination fills the shock bottle but does not extend outside it. This light, muzzle glow (Fig. 2—4), is very weak and rarely observed. Flow stream lines are straight and diverge from the muzzle as in point source flow, but density and pressure at any plane normal to the bore axis drop uniformly from the axis outward. In the region just outside the oblique shocks, the gas that has crossed these shocks still has supersonic velocities and temperatures that have dropped below the luminous range. On the other hand, the gas moving ahead through the normal shock decelerates to subsonic velocity, compresses, and consequently has its temperature elevated to approximate that at the muzzle. This temperature is high enough to cause *intermediate flash*, a red or reddish-orange cone of light (Figs. 2—2 and 2—3). The base of the cone is on the normal shock; the apex points away from the muzzle. Not nearly as intense as secondary flash, intermediate flash casts enough light to reveal position during night firing.

Surrounding the layer of supersonic gases is a turbulent shell in which propellant gas containing large amounts of hydrogen and carbon monoxide mix with air

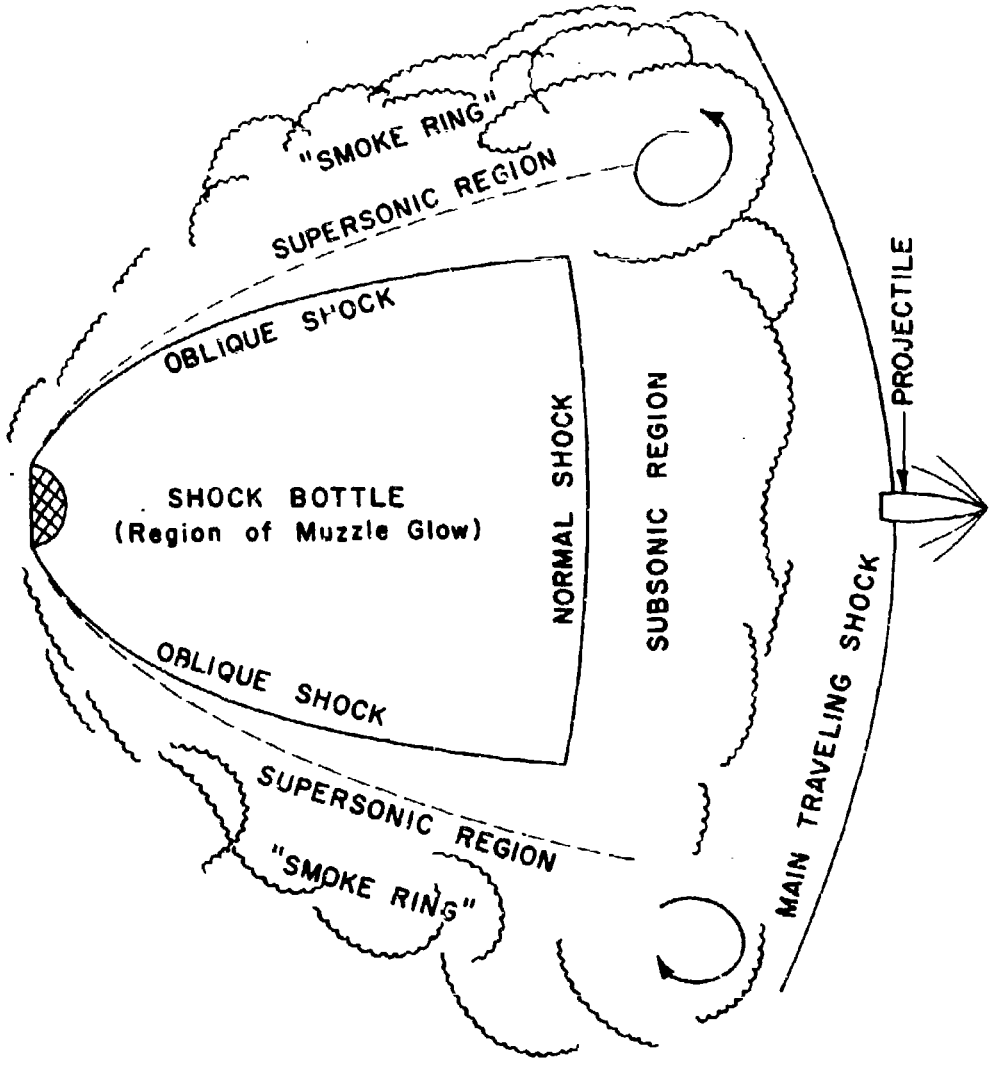

FIGURE 2-1. MAXIMUM VOLUME STAGE OF SHOCK BOTTLE

drawn into this shell. This mixture of entrained air and gas is the "smoke ring" mentioned earlier. It is a highly turbulent vortex that grows radially and advances forward until dissipated by air currents or some obstacle. Or it may ignite and become a large, voluminous flash known as *secondary flash*, the most intense, by far, of all flash phenomena. With a proper mixture of air and gas, ignition may be induced by the same factors responsible for intermediate flash, i.e., increased pressure and temperature after gases have passed the shock fronts. Ignition may be also caused by *preflash* (Fig. 2—3), a phenomenon not usually associated with muzzle blast inasmuch as it precedes the projectile from the barrel. It is the burning of low pressure gas that has leaked ahead of the projectile while still in the bore. If the leakage is

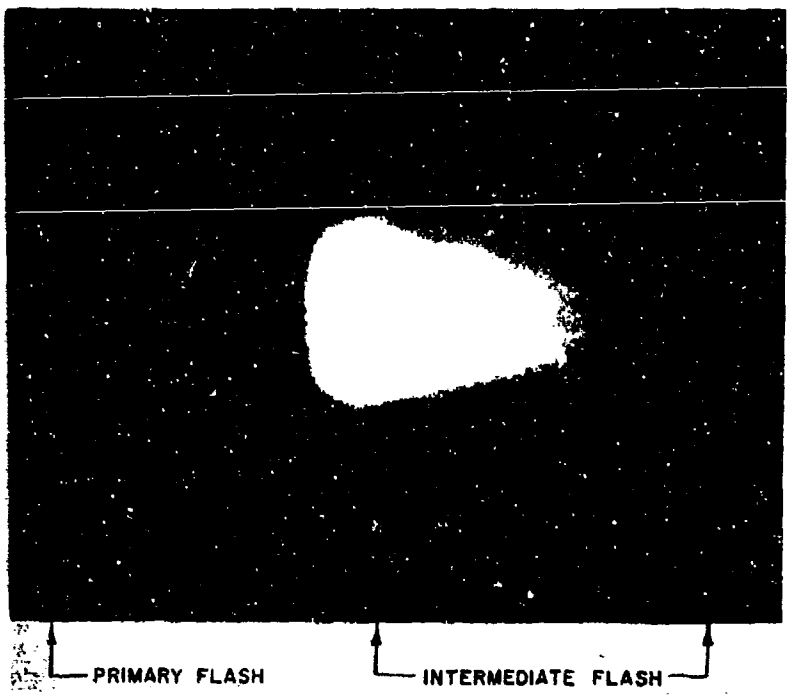

FIGURE 2-2. PRIMARY AND INTERMEDIATE FLASH

copious and the burning duration long, the air-gas mixture can overtake it and thus become ignited. Gas leakage of this nature usually happens only in worn guns and is not considered a major problem.

Flash is a by-product of muzzle blast and, regardless of its appearance or intensity, does not greatly influence the evolution of the jet which is divided into two periods — the growth and decay of the shock bottle. Although gas discharge from the gun decays steadily, the activity of the bottle offers a convenient vehicle for a qualitative analysis of the sequential events. The growth, already discussed, is complete when the bottle attains its maximum volume (Fig. 2—1). Hereafter, the bottle goes through two well-defined periods of evolution. During the first, the normal shock remains stationary about 15 calibers from the muzzle, but the projected area diminishes until the bottle reaches steady-state proportions, having a shape similar to the outline sketched in Fig. 2—5. The last evolutionary period begins after the steady-state condition. It involves the steady shrinking of the bottle without apparent change in shape.

Another phenomenon associated with the decay of the jet has considerable influence on obscuration activity. This is a rarefaction wave that starts at the time of shot ejection and travels from muzzle to breech, reflected toward the muzzle to emerge eventually in the jet. While this is going on, the normal shock moves toward the muzzle. Shock and rarefaction front will meet somewhere ahead of the muzzle. The events that happen afterward simulate the rupture of a membrane restraining compressed gas in a tube. The shock pressure drops and the bottle collapses to complete the final phase of the blast phenomenon.

2—2 RAISING OF DUST BY A GUN BLAST

The raising of a dust cloud when a gun is fired too close to dry ground involves lifting the dust off the ground and its subsequent diffusion. Two forces are responsible, the pressure gradient surrounding the dust

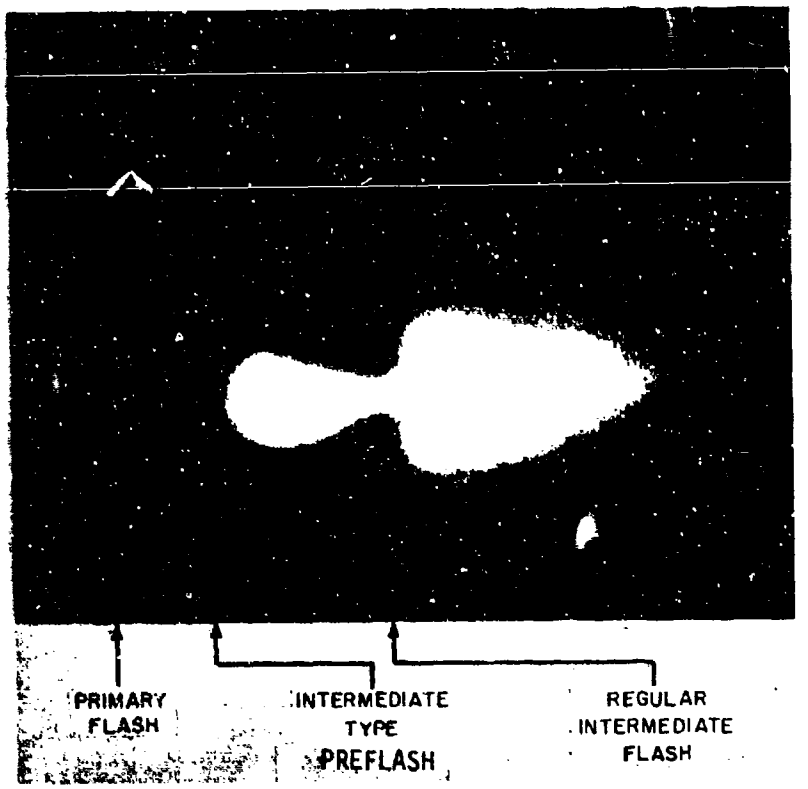

FIGURE 2-3. THREE TYPES OF FLASH

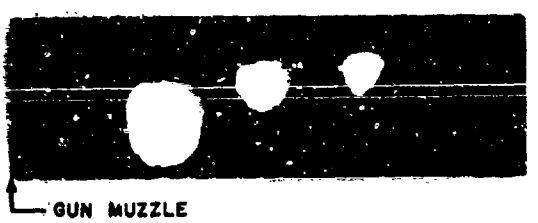

FIGURE 2-4. DEVELOPMENT OF MUZZLE GLOW

particles, and the drag of the gas as it moves past them. A muzzle blast contains both. The shock that precedes the blast prepares the ground by loosening and raising it a short height. The high speed central jet then scours the surface, picking up the raised dust but not diffusing it to any great extent. The upward drift of the blast's dust-laden eddies is very slow. However, the highly turbulent gas that surrounds the central jet, the "smoke ring", quickly raises the dust high above the ground. The rarefaction wave that follows also picks up and carries dust to considerable heights. However, its contribution is small in comparison with the preceding blast but, being least susceptible to control, the rarefaction wave may be one of the limiting factors of the deflector's effectiveness.

2-3 MECHANICS OF MUZZLE GAS FLOW

The quantitative analysis of the flow of propellant gases at the muzzle begins with the energy equation of interior ballistics[2]

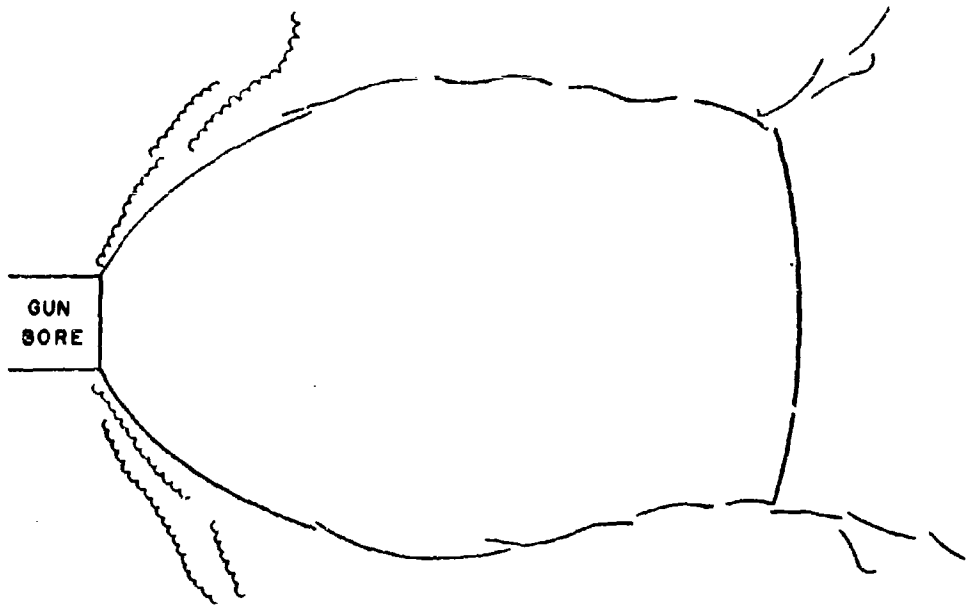

FIGURE 2–5. STEADY-STATE SHAPE OF SHOCK BOTTLE

$$\frac{W_c}{\gamma - 1}(RT - RT_o) = \frac{1}{2} W_p v_o^2 (1 + \delta) + \frac{1}{6} W_c v_o^2 \qquad (2—1)$$

where

R = gas constant, ft-lb/lb/°R

T = temperature of propellant gas having done no external work, °R

T_o = average temperature of gas at shot ejection, °R

v_o = muzzle velocity, ft/sec

W_c = weight of propellant, lb

W_p = weight of projectile, lb

γ = ratio of specific heats

δ = fractional heat loss to gun tube as function of shot energy

Weight W is a force, a defined term, and is expressed in pounds (lb). Mass is a computed term $M = W/g$, lb-sec^2/ft (slugs) where g is the acceleration of gravity. Other dimensions may be used provided that proper conversion of factors are used.

Eq. 2—1 is the application of Resal's equation at the instant of shot ejection provided that all the propellant has burned. A similar equation exists that includes the propellant gas energy[3]. Either may be used, the choice involves only the value of δ. In Eq. 2—1, by substituting $\frac{1}{7}$ for δ and 1.26 for γ (a good approximation), and solving, the equation becomes[4]

$$RT_o = RT - 0.26\,(1/6 + 4W_p/7W_c\, v_o^2 \qquad (2—2)$$

Appropriate values of RT, a characteristic of the propellant, are available in thermochemical tables. In some ballistic operations, RT is called specific impetus the dimensions of which are ft-lb/lb; and $RT/(\gamma - 1)$, of the same dimensions, is the potential of the propellant. Numerically, $RT/(\gamma - 1)$ is about 1.5×10^6 ft-lb/lb. However, to be dimensionally compatible, RT in Eqs. 2—1 and 2—2, contains the acceleration of gravity, so that RT in these and subsequent equations has the dimensions of ft^2/sec^2. Values of RT for some service propellants are listed in Table 2—1.

TABLE 2-1. RT OF SERVICE PROPELLANTS

Propellant	M1	M2	M6	M8	M9
RT, $(ft^2/sec^2)\ 10^{-6}$	9.83	11.69	10.13	12.31	12.30
Propellant	**M10**	**M15**	**M17**	**T28**	**IMR**
RT, $(ft^2/sec^2)\ 10^{-6}$	10.90	10.82	11.22	11.48	11.18

After computing RT_o, the pressure at any position in the bore at the instant of shot ejection[5]

$$p = \frac{12\,RT_o}{g\left(\frac{V_t}{W_c} - \eta\right)}\left[1.0 + \frac{W_c}{6W_p}\left(1.0 - \frac{3\,A^2\,x^2}{V_t^2}\right)\right], \text{ psi} \qquad (2\text{—}3)$$

where

A = bore area, $in.^2$

V_t = total volume of bore and chamber, $in.^3$

x = distance from breech, in.

g = acceleration of gravity, ft/sec^2

η = covolume, usually dimensioned $in.^3/lb$

RT_o = ft^2/sec^2

At the breech where $x = 0$,

$$p_b = \frac{12\,RT_o}{g\left(\frac{V_t}{W_c} - \eta\right)}\left(1.0 + \frac{W_c}{6W_p}\right), \text{ psi} \qquad (2\text{—}4)$$

at the muzzle where $Ax = V_t$,

$$p_o = \frac{12\,RT_o}{g\left(\frac{V_t}{W_c} - \eta\right)}\left(1.0 - \frac{W_c}{3W_p}\right), \text{ psi} \qquad (2\text{—}5)$$

2—4 MUZZLE GAS MOMENTUM

Hugoniot's gas flow theory, although accurate within a few percent, has been modified to calculate the flow and momentum of the propellant gases after shot ejection. The rate of flow, by neglecting the second and higher powers of W_c/W_p which is compatible with the general accuracy of all the equations, is

$$Q = \frac{12W_cA}{V_t}\left(1.0+\frac{W_c}{6\gamma W_p}\right)\left(1.0+\frac{t}{\theta}\right)^{\frac{1+\gamma}{1-\gamma}}\sqrt{\gamma RT_o\left[1.0+\frac{(\gamma-1)W_c}{6\gamma W_p}\right]\left(\frac{2}{\gamma+1}\right)^{\frac{\gamma+1}{\gamma-1}}} \qquad (2—6)$$

where

$$\theta = \frac{V_t}{6A(\gamma-1)}\sqrt{\frac{\left(\frac{\gamma+1}{2}\right)^{\frac{\gamma+1}{\gamma-1}}}{\gamma RT_o\left(1.0+\frac{(\gamma-1)W_c}{6\gamma W_p}\right)}} \qquad (2—7)$$

and the rate of change of momentum

$$\dot{M} = \frac{12ART_oW_c\gamma}{gV_i}\left(1.0+\frac{W_c}{6W_p}\right)\left(\frac{2}{\gamma+1}\right)^{\frac{\gamma}{\gamma-1}}\left(1.0+\frac{t}{\theta}\right)^{\frac{2\gamma}{1-\gamma}} \qquad (2—8)$$

where g = acceleration of gravity, ft/sec^2.

If the variables in Eqs. 2—6, 2—7, and 2—8 are assigned the dimensions of Eq. 2—3

Q = lb/sec

θ = sec

$\dot{M}$ = lb-sec/sec

The momentum equation of the gas at the muzzle is the integral of Eq. 2—8 at any given time t, provided that the second and higher powers of W_c/W_p are neglected. Retaining the above dimensions,

$$M = \frac{W_c}{g}\sqrt{RT_o}\left(\frac{2}{\gamma+1}\right)^{3/2}\left(1.0 + \frac{(\gamma+1)\,W_c}{12\gamma W_p}\right)\left[1.0 - \left(1+\frac{t}{\theta}\right)^{\frac{1+\gamma}{1-\gamma}}\right], \text{ lb-sec} \qquad (2—9)$$

CHAPTER 3

MUZZLE BRAKES

3—1 THEORY OF GUN GAS DEFLECTION

3—1.1 NOZZLE FLOW

The passages in a muzzle brake are treated by the one-dimensional theory of nozzles, without allowance for friction at the walls. Furthermore, the gas is assumed to fill the nozzle completely; true only if the nozzle is so designed that there is no break away from the walls. To prevent this, the semi-angle of a conical nozzle should never exceed 30°, a rather large angle. Smaller angles result in larger nozzles, thereby increasing muzzle brake weight. If more weight can be tolerated, a smaller semi-angle of about 20° is preferred. Semi-angles below 15° offer no appreciable advantage over their immediate larger counterparts.

Fig. 3—1 is a schematic of a one-baffle brake but is adequate for defining the geometry and the flow.

A = bore area

A_b = area of projectile passage

A_e = exit area of baffle passage

A_i = inner area of baffle passage

n_e = exit speed-up factor

n_i = inner speed-up factor

v_o = muzzle velocity

α = baffle deflecting angle

ϕ = semi-angle of nozzle

Because of the projectile passage, not all of the gas will go through the baffle passage, a portion will continue straight ahead, the amount depending on the ratio of exit areas. The weight of the quantity of gas diverted through the baffles is expressed as

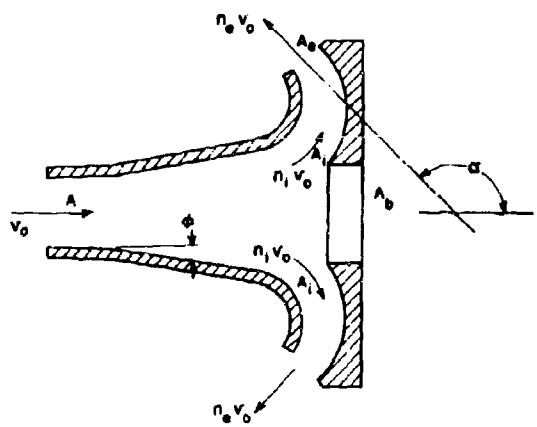

FIGURE 3-1. MUZZLE BRAKE GAS FLOW DIAGRAM

$$W_i = \frac{A_i}{A_i + A_b} W_c = \Delta_i W_c \qquad (3—1)$$

where W_c = weight of the propellant

$\Delta_i = \dfrac{A_i}{A_i + A_b}$, ratio of baffle inlet area to total available area.

The weight of gas flowing through the projectile passage

$$W_b = \frac{A_b}{A_i + A_b} W_c = \Delta_b W_c \qquad (3—2)$$

where $\Delta_b = \dfrac{A_b}{A_i + A_b}$, the ratio of projectile passage area to total available area.

The area of the baffle passage should diverge smoothly from inside to exit following a straight line function or a smooth

curve. The divergence of gas from muzzle to the first flow passages

$$\Delta_1 = \frac{A_j + A_b}{A} \qquad (3—3)$$

The divergence of the gas at the baffle exit

$$\Delta_{e1} = \Delta_1 \frac{A_e}{A_i} \qquad (3—4)$$

The velocity reaches its maximum value when the nozzle area diverges to about 25 times the throat area, in this application, the bore area. In practice, both nozzle and baffles normally would be too large to achieve the optimum condition. Fig. 3—2 shows the relation between speed-up factor n and divergence Δ. The speed-up factor is the ratio of exit to the entrance velocity of a flow passage. Examination of the curve shows that the gain in efficiency is small while the increase in size and weight of the muzzle brake is large for a divergence larger than 5.

The change in momentum, or thrust, of the muzzle gas is computed in Eq. 2—8. However, only a portion of the total gas impinges on the baffle. According to Eq. 3—1, if m_g is the mass of gas issuing from the muzzle per second, the mass flow per second impinging on the baffle

$$\Delta_i m_g = \frac{W_i}{W_c} m_g \qquad (3—5)$$

The thrust on that baffle during that second

$$f_b = \Delta_i m_g (v_i - v_e \cos \alpha) \qquad (3—6)$$

but $v_i = n_i v_o$ and $v_e = n_e v_o$, therefore

$$f_b = \Delta_i m_g (n_i v_o - n_e v_o \cos \alpha) = \lambda_u m_g v_o \qquad (3—7)$$

where λ_u is the uncorrected speed-up factor

$$\lambda_u = \Delta_i (n_i - n_e \cos \alpha) \qquad (3—8)$$

3—1.2 THRUST CALCULATIONS

3—1.2.1 Discussion

When computing the value of λ, a correction is needed to compensate for previously neglected friction and turbulence. Experiments show that the computed λ_u is too large and should be reduced by a correction factor C_λ so that

$$\lambda = \lambda_u / C_\lambda \qquad (3—9)$$

Examples of C_λ determined from firing tests are listed in Table 3—1.

Unfortunately, Table 3—1 offers little but qualitative values because test models are few and parameters are lacking. A value of $C_\lambda = 1.5$ should be adequate for initial design concepts.

The maximum thrust on a muzzle brake occurs at $t = 0$, thus providing a convenient means for computing λ. By substituting $t = 0$, $\gamma = 1.26$, $g = 32.2$, ft/sec^2 in Eq. 2— the thrust in pounds becomes

$$F_b = \left[\lambda C_t \frac{12 \times 1.26\, A W_c R T_o}{32.2\, V_t} \left(\frac{2}{2.26} \right)^{4.85} \times \left(1.0 + \frac{W_c}{6 W_p} \right) \right], \text{ lb} \qquad (3—10)$$

where C_t = thrust correction factor

$$F_b = 0.26 C_t \frac{W_c}{V_t} A R T_o \left(1.0 + \frac{W_c}{6 W_p} \right) \gamma, \text{ lb} \qquad (3—11)$$

The dimensions of A and V_t are expressed in inches. The value of λ may be readily computed from Eq. 3—11 for either single or multiple baffle brakes.

By assuming that all needed parameters are given or estimated, the computation for λ follows the procedure outlined below for a 3-baffle brake such as shown in Fig. 3—3.

TABLE 3-1. λ CORRECTION FACTORS

Type of Brake	3G, ϕ = 30° 2 or 4 Baffles	3G, ϕ = 15° 2 or 4 Baffles	German Single Baffle	German Double Baffle
C_λ	1.45	1.25	1.60	1.60

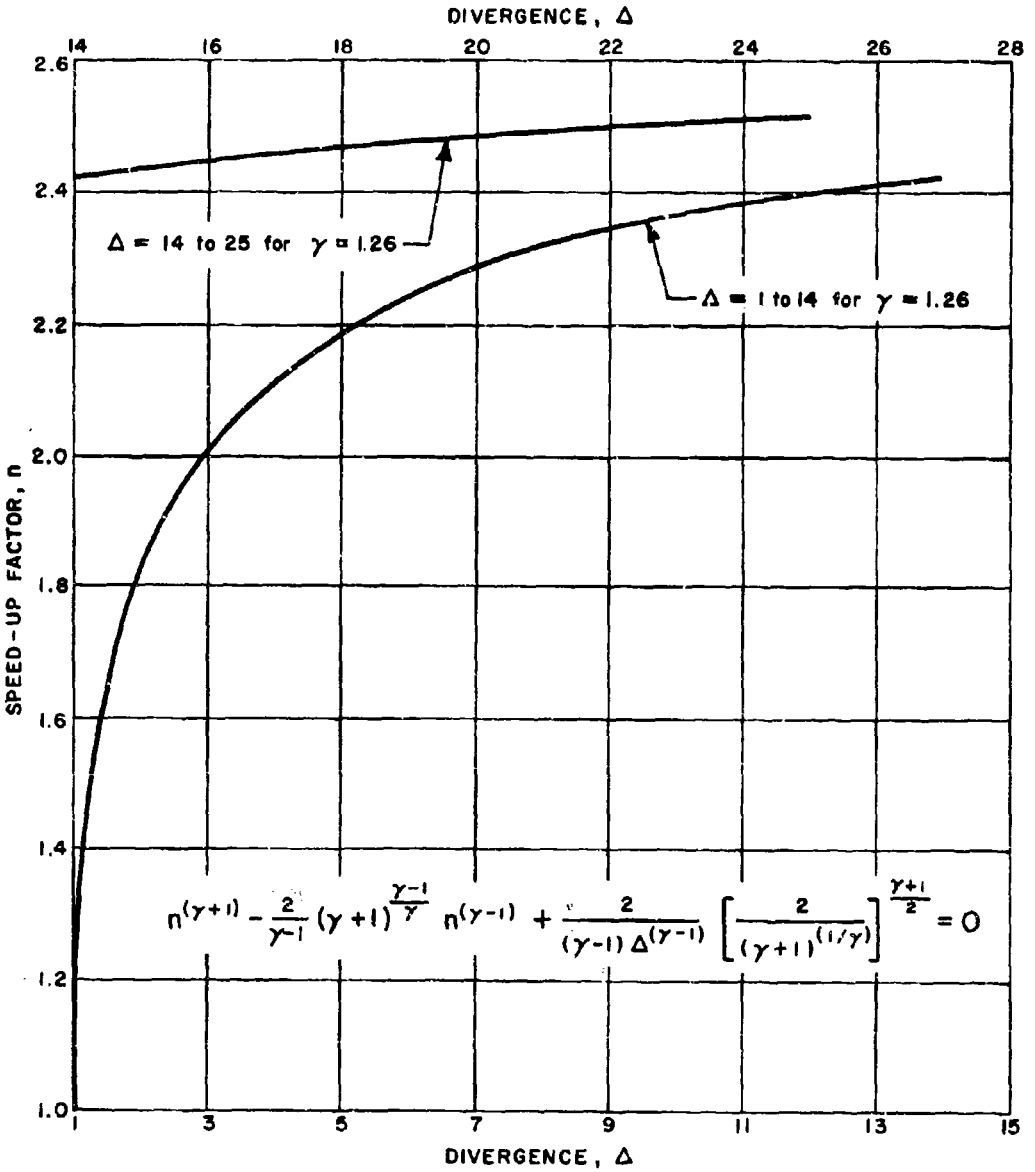

FIGURE 3-2. SPEED-UP FACTOR VS DIVERGENCE

Given or estimated data

Gun: W_c, W_p, V_t, v_o A, RT

Muzzle Brake: A_b, A_e, A_i, α, ϕ

(Subscripts 1, 2, 3, indicate the respective baffles)

After solving for RT_o in Eq. 2—2, the thrust on any baffle becomes (Eq. 3—11)

$$F_{bx} = K_{bx}\ \lambda_x \qquad (3-12)$$

For the first baffle:

Solve for Δ_{i1} and Δ_{b1} of Eqs. 3—1 and 3—2

Solve for Δ_1 and Δ_{e1} of Eqs. 3—3 and 3—4

From Fig. 3—2, read n_{i1} and n_{e1} corresponding to Δ_1 and Δ_{e1}. Now insert the known values into Eqs. 3—8 and 3—9

$$\lambda_1 = \Delta_{i1}\ (n_{i1} - n_{e1} \cos \alpha_1)/C_\lambda \qquad (3-13)$$

For the second baffle:

$$\Delta_{i2} = \Delta_{b1} \frac{A_{i2}}{A_{i2} + A_{b2}} \qquad (3-14)$$

$$\Delta_{b2} = \Delta_{b1} \frac{A_{b2}}{A_{i2} + A_{b2}} \qquad (3-15)$$

$$\Delta_2 = \Delta_1 \frac{A_{i2} + A_{b2}}{A_{b1}} \qquad (3-16)$$

$$\Delta_{e2} = \Delta_2 \frac{A_{e2}}{A_{i2}} \qquad (3-17)$$

Find the values of n_{i2} and n_{e2} that correspond with Δ_2 and Δ_{e2} from Fig. 3—2 and insert the appropriate values in Eq. 3—8

$$\lambda_2 = \Delta_{i2}\ (n_{i2} - n_{e2} \cos \alpha_2)/C_\lambda \qquad (3-18)$$

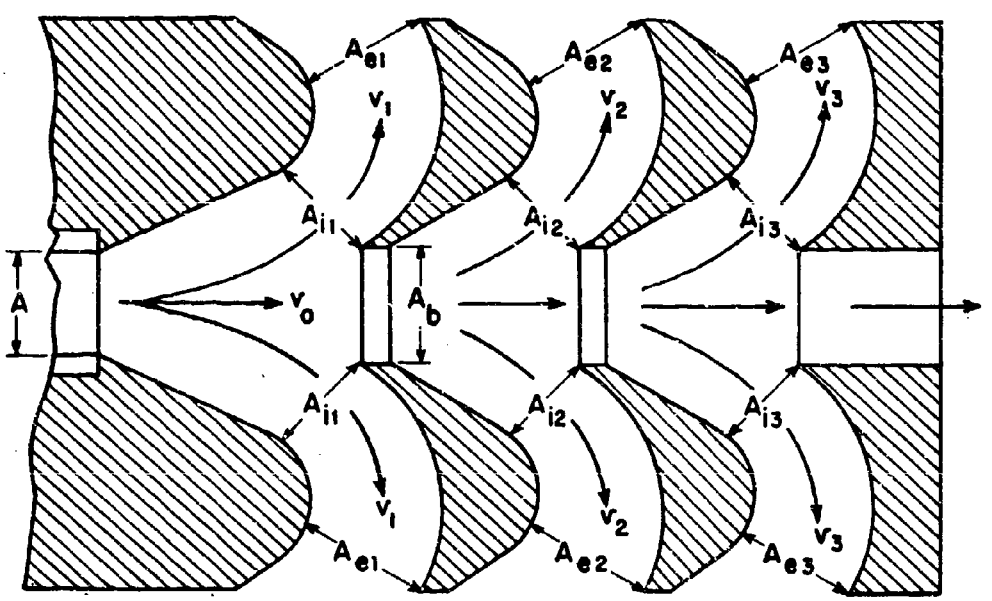

FIGURE 3-3. SCHEMATIC OF MUZZLE BRAKE GAS FLOW

For the third baffle:

$$\Delta_{i3} = \Delta_{b2} \frac{A_{i3}}{A_{i3} + A_{b3}} \qquad (3\text{—}19)$$

$$\Delta_{b3} = \Delta_{b2} \frac{A_{b3}}{A_{i3} + A_{b3}} \qquad (3\text{—}20)$$

$$\Delta_{3} = \Delta_{2} \frac{A_{i3} + A_{b3}}{A_{b2}} \qquad (3\text{—}21)$$

$$\Delta_{e3} = \Delta_{3} \frac{A_{e3}}{A_{i3}} \qquad (3\text{—}22)$$

Find the values of n_{i3} and n_{e3} that correspond with Δ_3 and Δ_{e3} in Fig. 3—2 and insert the appropriate values in Eqs. 3—8 and 3—9

$$\lambda_3 = \Delta_{i3}(n_{i3} - n_{e3} \cos \alpha_3)/C_\lambda$$

The value of λ for the muzzle brake

$$\lambda = \lambda_1 + \lambda_2 + \lambda_3 \qquad (3\text{—}23)$$

If more baffles are used, the above procedure merely continues the sequential pattern so that

$$\lambda = \lambda_1 + \lambda_2 + \text{----} + \lambda_{n-1} + \lambda_n \qquad (3\text{—}24)$$

The practice of adding many baffles is discouraged by the fact that the increase of baffles follows the law of diminishing returns. The two charts in Fig. 3—4 illustrate this principle. Here, the thrust on both individual and series of baffles is measured in proportion to the maximum thrust had 100 percent of the gases been utilized and then plotted for the percentage of gas tapped from zero to 100%. Through the lower range (0 — 35%) of the amount of gas tapped, multiple baffles are needed for an effective muzzle brake indicating poor design and inefficiency. In the upper range (above 35%), only two will be almost as effective as any number of baffles exceeding two.

The modified Hugoniot theory embodies inaccuracies in thrust computation during the decay period of the muzzle gas; too low at the beginning and too high at the end. To correct for the thrust at the beginning when the thrust is highest and therefore loads are critical, the thrust is increased by 70 percent. Fig. 3—5 shows the comparison between the computed and actual thrust. The 70 percent increase is included for strength considerations. However, for the total momentum during the entire period, the inaccuracies in the modified theory are compensating and are reasonably accurate without additional corrections. Another correction for the thrust involves the effect of closing the projectile

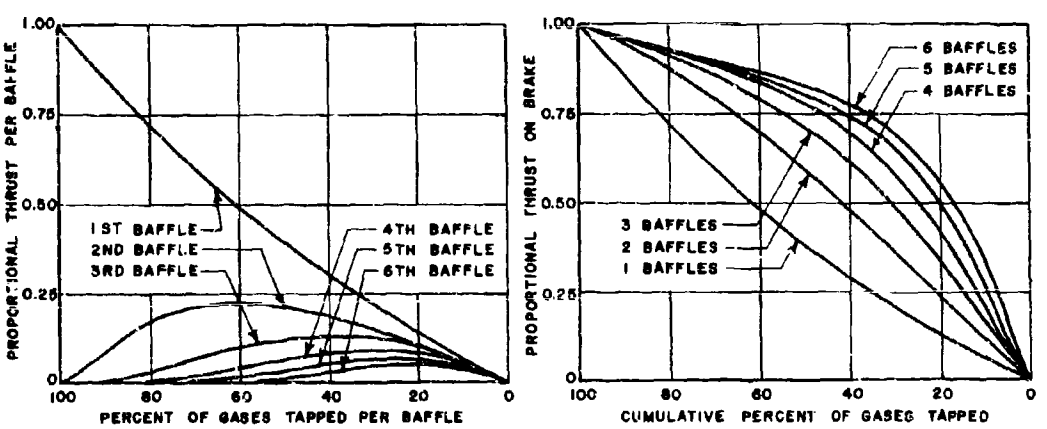

FIGURE 3-4. EFFECTIVENESS OF MULTIPLE BAFFLES

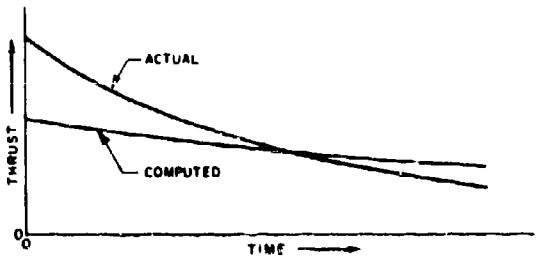

FIGURE 3-8. THRUST COMPARISON

passage as the projectile passes through it. This correction for any given baffle is

$$C_n = \left[\Sigma\lambda_{n-1} + \frac{\lambda_n(A_i + A_b)}{A_i}\right]^{\lambda^{-1}} \qquad (3\text{—}25)$$

The thrust correction factor now becomes

$$C_t = 1.70\, C_n \qquad (3\text{—}26)$$

3—1.2.2 Example Problem

Gun data:

A = 7.34 in.^{2}, bore area

RT = 10.6 x 10^6 ft^2/sec^2, type N. H. propellant

v_o = 3000 ft/sec, muzzle velocity

V_t = 1357 in.^{3}, bore volume

W_c = 8 lb, propellant weight

W_p = 17 lb, projectile weight

Muzzle Brake data:

A_b = 8.0 in.^{2}, area of projectile passage

A_e = 14.25 in.^{2}, exit area of flow passage

A_i = 11.0 in.^{2}, inlet area of flow passage

C_λ = 1.5 speed-up factor correction

α = 135°, angle of gas deflection

$\cos\alpha$ = −0.70711

ϕ = 30°, semi-angle of nozzle

n = 4, number of baffles, all baffles and passages are identical

From Eq. 2—2,

$$RT_o = RT - 0.26\left(\frac{1}{6} + \frac{4}{7}\cdot\frac{17}{8}\right)v_o^2$$

$$= \left(10.6 - 2.34\frac{29}{21}\right)10^6 = 7.37 \times 10^6 \text{ ft}^2/\text{sec}^2$$

The total thrust in terms of λC_t (Eq. 3—11)

$$F_b = 0.26\,\lambda C_t \frac{W_c}{V_t} A R T_o \left(1.0 + \frac{W_c}{6W_p}\right)$$

$$= 0.26\,\frac{8}{1357}\,7.34 \times 7.37 \times 10^6 \left(1.0 + \frac{8}{102}\right)\lambda C_t$$

$$= 89400\,\lambda C_t, \text{ lb} \qquad (3\text{—}27)$$

From Eq. 3—3

$$\Delta_1 = \frac{A_i + A_b}{A} = \frac{11 + 8}{7.34} = 2.5888$$

To save space and avoid repetitious algebra, the values for the various computed data from Eqs. 3—1 to 3—26 are listed in Table 3—2. The maximum instantaneous load on the muzzle brake occurs when the projectile has cleared the first baffle and is passing through the second. On the assumption that the brake force is distributed in direct proportion to λ_n/λ, the maximum instantaneous force on the individual baffles as the projectile is passing through that baffle is

$$F_m = F_b \frac{\lambda_n}{\lambda} \qquad (3\text{—}28)$$

TABLE 3-2. COMPUTED DATA FOR MUZZLE BRAKE THRUST

Data	1st Baffle	2nd Baffle	3rd Baffle	4th Baffle
A_b	8.0	8.0	8.0	8.0
A_e	14.25	14.25	14.25	14.25
A_i	11.0	11.0	11.0	11.0
$A_i/(A_i+A_b)$	0.579	0.579	0.579	0.579
$A_b/(A_i+A_b)$	0.421	0.421	0.421	0.421
$(A_i+A_b)/A_{b-1}$	2.588	2.375	2.375	2.375
A_e/A_i	1.295	1.295	1.295	1.295
Δ_i	0.579	0.244	0.102	0.043
Δ_b	0.421	0.177	0.075	0.032
Δ	2.59	6.15	14.61	34.70
Δ_e	3.35	7.96	18.92	44.93
n_i	1.94	2.25	2.43	2.57
n_e	2.05	2.32	2.47	2.60
$n_e \cos \alpha$	−1.45	−1.64	−1.75	−1.84
λ_n	1.308	0.633	0.84	0.12
λ	1.308	1.941	2.225	2.352
$\lambda_n (A_i+A_b)/A_i$	2.258	1.093	0.490	0.219
C_n	1.727	1.237	1.093	1.038
C_t	2.936	2.103	1.858	1.765
F_b	343,000	365,000	369,000	371,000
F_m	343,000	119,000	47,000	20,000

The large loads appearing on the first and second baffles are clear evidence why muzzle brakes must be rugged structures.

3—2 PERFORMANCE CALCULATIONS

3—2.1 IMPULSE

Although only the maximum force is needed to establish the size of the structural components, the decreasing brake force throughout the decay period of the muzzle gas activity performs the essential function of a muzzle brake, producing the impulse that reduces the momentum of the recoiling parts. The momentum of the muzzle gas at any time t (Eq 2—9), when multiplied by the speed-up factor λ, gives the impulse of the brake during that time

$$I_i = \lambda \frac{W_c}{g} \sqrt{\gamma R T_o} \left(\frac{2}{\gamma+1}\right)^{3/2} \left[1.0 + \frac{(\gamma+1)\ W_c}{12\gamma\ W_p}\right] \left[1.0 - \left(1 + \frac{t}{\theta}\right)^{\frac{1+\gamma}{1-\gamma}}\right], \text{ lb-sec} \qquad (3-29)$$

Except for detailed recoil analysis, these incremental impulses are not needed. However, the sum of these increments is needed for the total effect on recoil for preliminary design and may be found by substituting the limits of $t = 0$ to $t = \infty$ thereby reducing the expression

$$\left[1.0 - \left(1 + \frac{t}{\theta}\right)^{\frac{1+\gamma}{1-\gamma}}\right]$$

to 0.0 and 1.0. The total impulse induced on the muzzle brake

$$I_{mb} = \lambda \frac{W_c}{g} \sqrt{\gamma R T_o} \left(\frac{2}{\gamma+1}\right)^{3/2} \left[1.0 + \frac{(\gamma+1)\ W_c}{12\gamma\ W_p}\right] \qquad (3-30)$$

Substituting 1.26 for γ and 32.2 ft/sec^2 for g

$$I_{mb} = 0.029\ \lambda W_c \sqrt{R T_o} \left(1.0 + \frac{0.15\ W_c}{W_p}\right), \text{ lb-sec} \qquad (3-31)$$

The impulse induced on the gun during this same period

$$I_g = \frac{W_c}{g} \sqrt{R T_o} \sqrt{1-k} \left[\frac{2-k}{2(1-k)}\right]^{\frac{2-3k}{2k}} \left(1 + \frac{0.15\ W_c}{W_p}\right) \left[1 - \left(1 + \frac{t}{\theta}\right)^{\frac{k-2}{k}}\right]^{*}, \text{ lb-sec} \qquad (3-32)$$

*Based on Eqs. 6.312 and 6.404 of Reference 5.

The resultant impulse on the recoiling parts

$$I_r = I_g - I_{mb} \tag{3—33}$$

$$I_r = \frac{W_c}{g}\sqrt{RT_o}\sqrt{1-k}\left[\frac{2-k}{2(1-k)}\right]^{\frac{2-3k}{2k}}(1-B)\left(1+\frac{0.15\,W_c}{W_p}\right)\left[1-\left(1+\frac{t}{\theta}\right)^{\frac{\gamma+1}{1-\gamma}}\right] \tag{3—34}$$

where

$$B = \frac{\lambda}{(1-k)}\left[\frac{\gamma(1-k)}{2-k}\right]^{1/k} = \lambda\gamma\left(\frac{2}{\gamma+1}\right)^{\frac{\gamma}{\gamma-1}} = 0.696\lambda \tag{3—35}$$

$k = (\gamma-1)/\gamma$

$\gamma = 1.26$

Operating within the limits of $t = 0$ to $t = \infty$

$$I_r = 0.0417\,(1-B)\,W_c\sqrt{RT_o}\left(1.0+\frac{0.15\,W_c}{W_p}\right), \text{ lb-sec} \tag{3—36}$$

Except for the parenthetical expression (1—B), Eq. 3—34 is identical to Eq. 3—32, therefore by observation

$$I_r = (1-B)\,I_g \tag{3—37}$$

3—2.2 EFFICIENCY OF A MUZZLE BRAKE

3—2.2.1 Discussion

There are generally three types of efficiency designations of a muzzle brake. The first measure of efficiency is the momentum index B that is zero if the gun has no muzzle brake. According to Eq. 3—36, as B increases, the residual impulse on the recoiling parts decreases after the projectile leaves the muzzle. The intrinsic efficiency and the gross efficiency are the other two types. The gross efficiency is the percentage reduction of recoil energy caused by the brake.

The total momentum m_r of the recoiling parts is equal to the momentum of the projectile and gas just as the projectile emerges from the muzzle, plus the impulse of the gas afterwards

$$m_r = M_r v_r = M_p v_o + \frac{1}{2} M_c v_o + I_g \qquad (3\text{—}38)$$

$$m_r = M_e v_o + I_g$$

where

M_c = mass of propellant gas

$M_e = M_p + \frac{1}{2} M_c$, effective mass

M_p = mass of projectile

M_r = mass of recoiling parts

v_r = velocity of recoil

With a muzzle brake, the total momentum of the recoiling parts

$$m_{rb} = M_r v_{rb} = M_p v_o + \frac{1}{2} M_c v_o + I_r \qquad (3\text{—}39)$$

$$m_{rb} = M_e v_o + I_r$$

Converting momentum to velocity of recoiling parts

$$v_r = \frac{\Sigma(Mv)}{M_r} \qquad (3\text{—}40)$$

Since energy $E = \frac{1}{2} Mv^2$ and since the gross efficiency is based on the reduced recoil energy, the gross efficiency

$$\epsilon_g = \left(\frac{m_r^2 - m_{rb}^2}{m_r^2} \right) 100 \qquad (3\text{—}41)$$

The intrinsic efficiency is the gross efficiency corrected by the weight of the muzzle brake

$$\epsilon_i = \epsilon_g \frac{W_{rb}}{W_r} - \frac{100\, W_b}{W_r} \qquad (3\text{—}42)$$

where

W_b = weight of muzzle brake

W_r = weight of recoiling parts

W_{rb} = weight of recoiling parts with muzzle brake

Fig. 3—6 is a curve indicating the intrinsic efficiency for various values of the momentum index.

3—2.2.2 Example Problem

The computed effectiveness of a muzzle brake here illustrated is for the same gun and brake that were used to compute the thrust. The given and computed data in Table 3—2 are also used. Before the performance can be computed, characteristic weights must be estimated for the recoiling parts and the muzzle brake. The muzzle energy

$$E_m = \frac{1}{2} M_p v_o^2 = \frac{1}{2} \times \frac{17}{32.2} \times 9 \times 10^6 = 2{,}376{,}000 \text{ ft-lb}$$

The recoiling weight[6]

$$W_r = 8.2 \times 10^{-4}\, E_m = 1950 \text{ lb}$$

Muzzle brake weight: 1–baffle, 150 lb; 2–baffle, 220 lb, 3–baffle, 260 lb; 4–baffle, 360 lb

From Eq. 3—38

$$I_g = 0.0417\, W_c \sqrt{RT_o} \left(1.0 + \frac{0.15\, W_c}{W_b} \right)$$

$$= 0.0417 \times 8 \times 2715 \left(1.0 + \frac{0.15 \times 8}{17} \right)$$

$$= 905.7 \times 1.07 = 969 \text{ lb-sec}$$

From Eq. 3—37,

$$I_r = 969(1 - B)$$

(This relationship is only approximately correct for normal guns and for the order of velocity used to determine this relationship.)

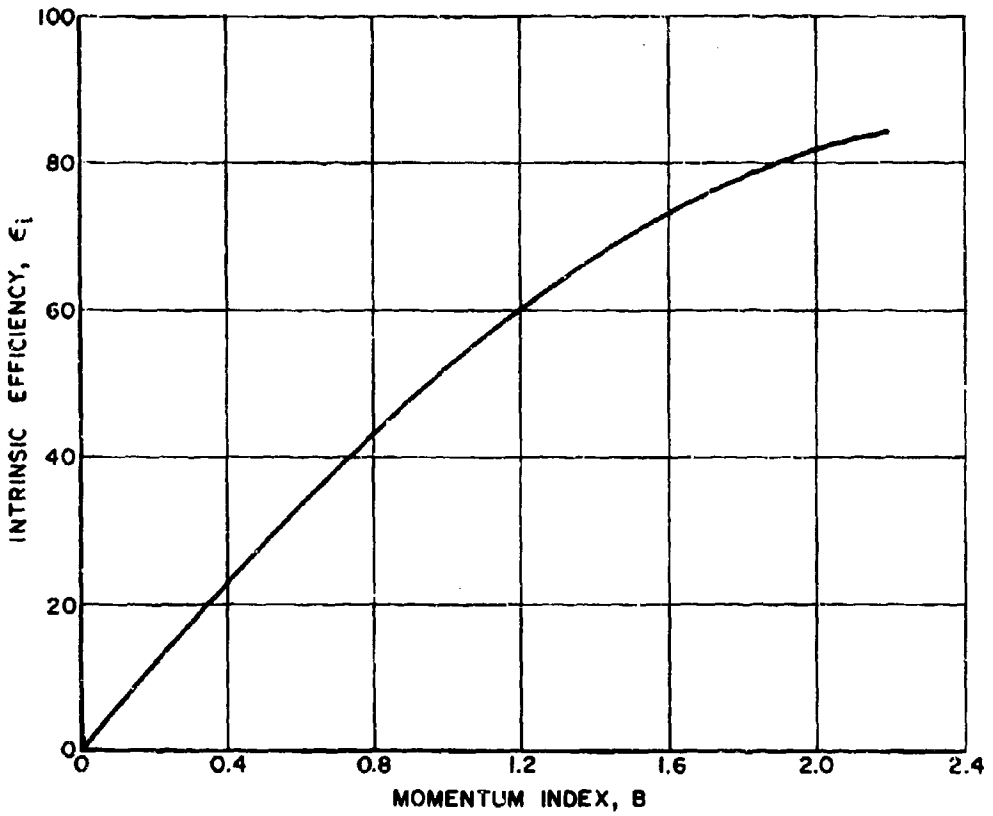

FIGURE 3-6. PREDICTED APPROXIMATE EFFICIENCY

From Eq. 3—38

$$M_e v_o = \left(\frac{17 + 8/2}{32.2}\right) 3000 = 1957 \text{ lb-sec}$$

$$m_r = M_e v_o + I_g = 2926 \text{ lb-sec}$$

$$m_r^2 = 8.561 \times 10^6 \text{ lb}^2\text{-sec}^2$$

As indicated earlier from the thrust in Table 3—2 the efficiencies of Table 3—3 show that little is to be gained by using the third and fourth baffles.

3—2.3 EFFECTS ON RECOIL

3—2.3.1 Discussion

A muzzle brake may affect either recoil force, recoil length, or both. There are infinite variations but only two limits are demonstrated. After acceptable values for the two parameters are established for a gun without a muzzle brake, variations in recoil force are computed for a constant length of recoil. Then, holding the force constant, variations in length of recoil are computed. Earlier, Eqs. 3—38 and 3—39 showed that the momentum of the recoiling

TABLE 3-3. COMPUTED DATA FOR MUZZLE BRAKE EFFICIENCY

Data	1-Baffle	2-Baffle	3-Baffle	4-Baffle
W_b	150	220	260	300
W_{rb}	2,100	2,170	2,210	2,250
λ	1.308	1.941	2.225	2.352
B	0.910	1.351	1.549	1.637
1-B	0.090	−0.351	−0.549	−0.637
I_r	87	−340	−532	−617
m_{rb}	2,044	1,617	1,425	1,340
$m_{rb}^2 \times 10^{-6}$	4.178	2.615	2.031	1.796
W_{rb}/W_r	1.077	1.113	1.133	1.154
$100\ W_b/W_r$	7.7	11.3	13.3	15.4
ϵ_g	51.2	69.5	76.3	79.1
ϵ_i	47.4	66.1	73.1	76.1

parts was equal to the combined momentum and impulse of projectile and propellant gas. The velocity of free recoil (i. e., no resistance offered while the propellant gas is still effective)

$$v_f = \frac{m_{rb}}{M_{rb}} \qquad (3\text{—}43)$$

The energy of free recoil

$$E_{rb} = \frac{1}{2} M_{rb} v_f^2 \qquad (3\text{—}44)$$

Note that m_{rb}, M_{rb}, and E_{rb} are equivalent to m_r, M_r, and E_r, respectively, when the gun has no muzzle brake.

On the assumption that the gun is firing horizontally, the recoil force

$$F_a = \frac{E_{rb}}{L} \qquad (3\text{—}45)$$

where L = length of recoil

More accurate detailed methods are available for recoil analyses[7] but are not needed for this demonstration. A limit of either F_a or L establishes the limit of the other.

The actual efficiency based on recoil energy

$$\epsilon_a = 100\ (1.0 - E_{rb}/E_r) \qquad (3\text{—}46)$$

where

E_r = free recoil energy without muzzle brake

E_{rb} = free recoil energy with muzzle brake

When the recoil force is held constant, the length of recoil varies and is expressed as

$$L = \frac{E_{rb}}{F_a} \qquad (3\text{—}47)$$

3—2.3.2 Example Problem

Continuing with the same gun and muzzle data of the two early examples, from

Eq. 3—43, the velocity of free recoil with no muzzle brake

$$v_f = \frac{m_r}{M_r} = \frac{2926 \times 32.2}{1950} = 48.3 \text{ ft/sec}$$

The energy of free recoil (Eq. 3—44)

$$E_r = \frac{1}{2} \times \frac{1950}{32.2} \times 2333 = 70{,}649 \text{ ft-lb}$$

Assuming a 30-in. (2.5 ft) length of recoil, the recoil force (Eq. 3—45)

$$F_a = \frac{70640}{2.5} = 28{,}250 \text{ lb}$$

For the 1-Baffle brake when the recoil force is the same as that for the brakeless gun, the length of recoil (Eq. 3—47)

$$L = \frac{12 \times 31950}{28250} = 13.6 \text{ in.}$$

The actual efficiency according to Eq. 3—46 is

$$\epsilon_a = 100 \left(1.0 - \frac{31950}{70640}\right) = 54.8\%$$

From the point of view of recoil effects, most of the gain is experienced with a muzzle brake of one or two baffles. In keeping with the observations for thrust and efficiency, any further increase in the number of baffles is discouraged; the returns do not justify the effort. Note that the more accurately estimated efficiencies of Table 3—4 are slightly higher than those estimated in Table 3—3 but the difference may be considered as not significant. Fig. 3—7 has curves graphically depicting these trends.

3—3 ANALYSIS OF SPECIFIC TYPES

3—3.1 CLOSED MUZZLE BRAKE

3—3.1.1 Discussion

The computation of axial thrust and the subsequent performance analysis of the

TABLE 3-4. EFFECT OF MUZZLE BRAKE ON RECOIL

Data	No Brake	1-Baffle	2-Baffle	3-Baffle	4-Baffle
W_{rb}(lb)	1,950	2,100	2,170	2,210	2,250
m_{rb}(lb-sec)	2,926	2,044	1,617	1,425	1,340
v_f(ft/sec)	48.3	31.3	24.0	20.9	19.1
E_{rb}(ft-lb)	70,640	31,950	19,410	14,990	12,750
L (in.)*	30.0	30.0	30.0	30.0	30.0
F_a(lb)*	28,250	12,780	7,760	6,000	5,100
F_a(lb)**	28,250	28,250	28,250	28,250	28,250
L (in.)**	30.0	13.6	8.2	6.4	5.4
ϵ_a(%)	0.0	54.8	72.5	78.8	81.9

*Constant recoil distance; variable recoil force
**Constant recoil force; variable recoil distance

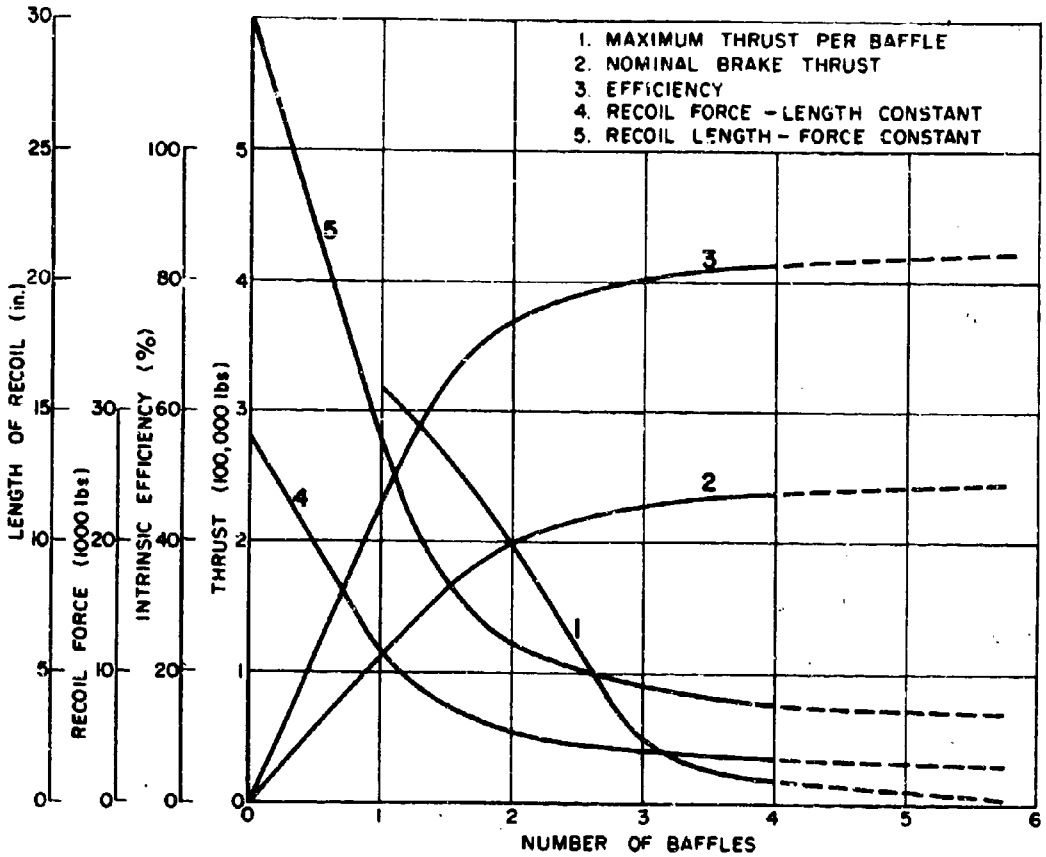

FIGURE 3-7. EFFECTIVENESS OF MUZZLE BRAKES

muzzle brake were those for a closed muzzle type and they need not be repeated. However, unless the brake is symmetrical, unbalanced forces and impulses normal to the bore axis will occur. Since the muzzle gas is usually diverted upwards when the brake is asymmetric, induced force and impulse will be downward. Fig. 3—8 is a schematic front view of an asymmetric, closed brake. According to Eq. 4—27 of Reference 8, the normal nondimensional brake force

$$\omega = \frac{1}{f_n} \sum_{j}^{N} f_j \, n_{2j} \cos \beta_j \qquad (3—48)$$

where $f_n = C_\lambda$ of Eq. 3—9, $\omega = \lambda$, and β_j is the diverting angle measured from the vertical. Express the values in Eq. 3—48 to correspond with those of the preceding equations so that Eq. 3—8 becomes

$$\omega_u = \Delta_i n_e \cos \beta \qquad (3—49)$$

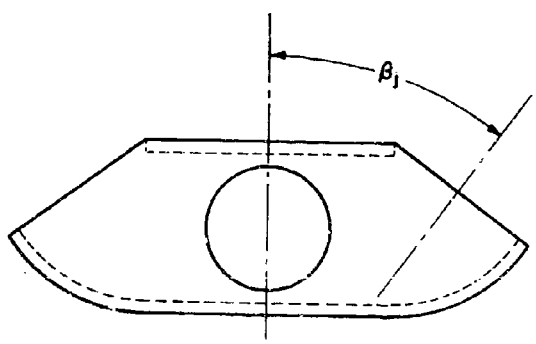

FIGURE 3-8. SCHEMATIC OF ASYMMETRIC CLOSED BRAKE

Following Eqs. 3—1 through 3—26

$$\omega = \left(\Delta_{i1} n_{e1} \cos \beta_1 + \Delta_{i2} n_{e2} \cos \beta_2 + \text{---} + \Delta_{ij} n_{ej} \cos \beta_j \right) / f_n \qquad (3\text{—}50)$$

3—3.1.2 Example Problem

Assume that all baffles are of equal size and shape

$$\beta = 30^\circ, \; f_n = 1.5, \; \cos \beta / f_n = 0.577$$

The remaining data are those listed in Table 3—2

$$\omega = \left(\Delta_{i1} n_{e1} + \Delta_{i2} n_{e2} + \ldots + \Delta_{ij} n_{ej} \right) 0.577 \qquad (3\text{—}51)$$

Based on Eq. 3—25

$$C_n = (\Sigma \omega_{n-1} + 1.727 \; \omega_n)/\omega \qquad (3\text{—}52)$$

where

$$\frac{A_i + A_b}{A_i} = \frac{11.0 + 8.0}{11.0} = 1.727$$

The maximum brake force normal to the bore axis is computed from Eq. 3—27, with C_t being computed from Eq. 3—26. The impulse normal to the axis is computed from Eq. 3—31. Substituting ω for λ

$$F_n = 89400 \omega C_t \qquad (3\text{—}53)$$

$$I_n = 0.029 \omega W_c \sqrt{RT_o} \left(1.0 + \frac{0.15 \, W_c}{W_p} \right) \qquad (3\text{—}54)$$

$$= 0.029 \times 8 \times 2715 \times 1.0705 \omega = 675 \omega, \text{ lb-sec}$$

The available and computed data are listed in Table 3—5.

TABLE 3-5. FORCE AND IMPULSE NORMAL TO BORE AXIS OF CLOSED MUZZLE BRAKE

Data	1st Baffle	2nd Baffle	3rd Baffle	4th Baffle
Δ_i	0.579	0.244	0.102	0.043
n_e	2.05	2.32	2.47	2.60
ω_n	0.685	0.327	0.145	0.065
ω	0.685	1.012	1.157	1.222
$1.727\omega_n$	1.182	0.564	0.250	0.112
C_n	1.727	1.232	1.093	1.037
C_t	2.936	2.095	1.858	1.762
F_n	180,000	190,000	192,000	194,000
I_n	463	684	780	825

3—3.2 OPEN MUZZLE BRAKE

3—3.2.1 Discussion

Open muzzle brakes depend on the free expansion of gas before impinging on, and being deflected by the baffle[8]. The rigid connection between baffle and muzzle confines the flow to some extent but even without special physical means, confinement of flow is assumed to be achieved by the shock envelope. Fig. 3—9 is a schematic of the muzzle, baffle, and outline of the shock envelope with pertinent dimensions. If the radius of the shock envelope does not exceed the radius of the baffle when the gas contacts the baffle, the fraction of gas deflected is

$$r_1 = 1.0 - \left(\frac{r_p}{r_e}\right)^2 ; (r_e \leq r_b) \qquad (3—55)$$

where

r_b = outer radius of baffle

r_e = radius of shock envelope at baffle

r_p = radius of projectile passage

If the shock envelope is larger than the baffle, the fraction of deflected gas

$$r_1 = 1.0 - \frac{\psi}{\pi} + \left(\frac{\psi}{\pi} r_b^2 - r_p^2\right)/r_e^2 \qquad (3—56)$$

where ψ = angular divergence of brake flow passage. According to Eq. 5—10 of Reference 8, the muzzle brake force

$$F_b = M_o a_o n_1 r_1 (1.0 - \cos \alpha)/f_3 \qquad (3—57)$$

where

a_o = velocity of sound in muzzle gas

f_3 = 1.33 (approximately) correction factor

M_o = mass rate of flow at muzzle

n_1 = modified speed-up factor

α = baffle deflection angle

$$a_o = \sqrt{\gamma R T_o} \qquad (3—58)$$

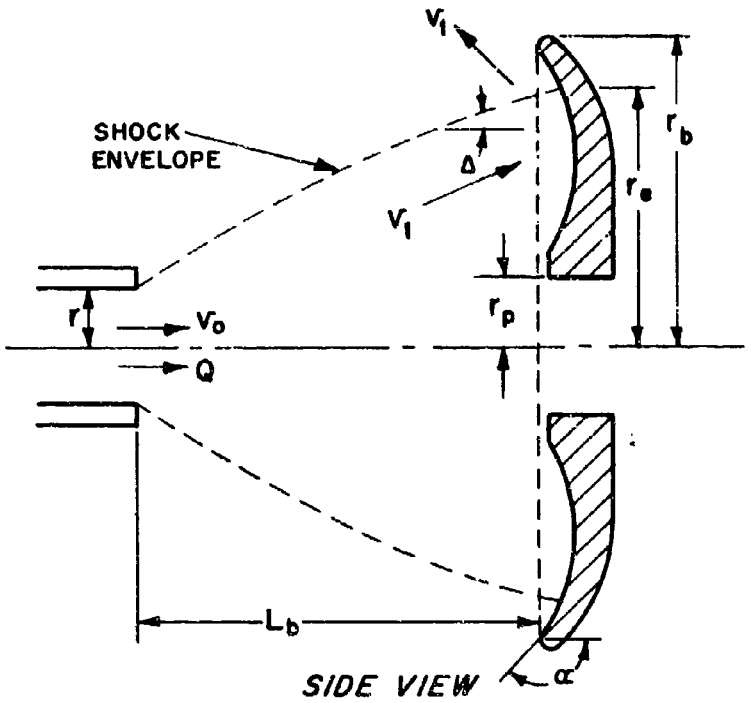

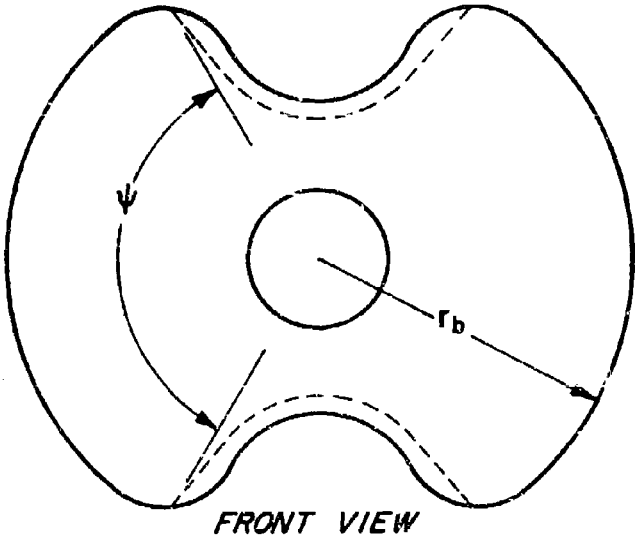

FIGURE 3-9. SCHEMATIC OF OPEN BRAKE

From Eq. 2—6

$$M_a = \frac{Q}{g} \tag{3—59}$$

From Eqs. 5.8b and 5.8c of Reference 8, the expansion ratio

$$\Delta \cong 1 + \frac{\psi}{\pi}\left(\frac{r_c}{r}\right)^2 \tag{3—60}$$

n is found from the expression

$$n^{(\gamma+1)} - \frac{2}{\gamma-1}(\gamma+1)^{\frac{(\gamma-1)}{\gamma}} n^{(\gamma-1)} + \frac{2}{(\gamma-1)\Delta^{(\gamma-1)}}\left[\frac{2}{(\gamma+1)^{1/\gamma}}\right]^{\frac{\gamma+1}{2}} = 0^* \tag{3—61}$$

The impulses induced on the gun at any time according to Eq. 3.40 of Reference 8, $B_T = Ap_{bi}\Phi_T/\alpha_T$. If we substitute known values for the variables, the impulses on the gun are

$$I_g = \frac{W_c}{g}\sqrt{\frac{RT}{\gamma}}\left(\frac{\gamma+1}{2}\right)^{\frac{3-\gamma}{2(\gamma-1)}}\left\{1 - \left[\frac{\gamma-1}{2}\gamma\left(\frac{2}{\gamma+1}\right)^{\frac{\gamma+1}{2(\gamma-1)}}\frac{Agp_{bi}}{W_c\gamma RT}t + 1\right]^{\frac{\gamma+1}{1-\gamma}}\right\} \tag{3—62}$$

where

A = bore area

P_{bi} = breech pressure at shot ejection

W_c = total weight of propellant

From $t = 0$ to $t = \infty$, the expression for the impulse becomes

$$I_g = \frac{W_c}{g}\sqrt{RT}\left(\frac{\gamma+1}{2}\right)^{\frac{3-\gamma}{2(\gamma-1)}} \tag{3—63}$$

Eq. 3—62 is practically identical to Eq. 3—32, thus demonstrating the close correspondence between two sources of information. The resulting impulse on the recoiling parts from the influence of the muzzle brake

*This equation was determined from Eq. 3.71 of Reference 8 by substitution.

$$I_r = I_g(1 - B_e) \qquad (3—64)$$

where B_e is the effective momentum index. B_e is not readily computable but based on an existing brake performance $B_e = .97$ (approximate).

3—3.2.2 Example Problem

The sample calculation for an open muzzle brake is based on the same gun data that were used earlier for the multiple-baffle closed brake.

Gun Data

r = 1.528 in., bore radius

RT = 10.6×10^6 ft^2/sec^2, type AH propellant

RT_o = 7.37×10^6 ft^2/sec^2, at muzzle (Eq. 2—2)

W_c = 8 lb, total weight of propellant

Muzzle Brake Data

r_b = 6.0 in., radius of baffle

r_e = 4.584 in., radius of envelope-baffle contact

r_p = 1.68 in., radius of projectile passage

α = 135°, baffle deflecting angle

$\psi = \frac{1}{2}\pi$, divergence angle

From Eq. 2—6, the rate of flow of gas when $t = 0$

$$Q = \frac{12W_cA}{V_t}\left(1.0 + \frac{W_c}{6\gamma W_p}\right)\sqrt{\gamma RT_o\left(1.0 + \frac{(\gamma-1)W_c}{6\gamma W_p}\right)\left(\frac{2}{\gamma+1}\right)^{\frac{\gamma+1}{\gamma-1}}}$$

$$= \frac{12\times8\times7.34}{1357}\left(1 + \frac{8}{6\times1.26\times17}\right)\sqrt{1.26\times7.37\times10^6\left(1 + \frac{0.26\times8}{6\times1.26.17}\right)\left(\frac{2}{2.26}\right)^{\frac{2.26}{0.26}}}$$

$$= 0.551 \times 3072 \times 0.588 = 995.5 \text{ lb/sec}$$

The mass rate of flow (Eq. 3—59)

$$M_o = \frac{Q}{g} = \frac{995.5}{32.2} = 30.92 \left(\frac{\text{lb-sec}^2}{\text{ft}}\right) \text{sec}^{-1} \text{ or slugs/sec}$$

The expansion ratio (Eq. 3—60)

$$\Delta = 1 + \frac{\psi}{\pi}\left(\frac{r_e}{r}\right)^2 = 1 + \frac{1}{2}\left(\frac{4.584}{1.528}\right)^2 = 5.5$$

The speed-up factor of $n_1 = 2.2$ is read from Fig. 3—2 for $\Delta = 5.5$.

The fraction of gas deflected (Eq. 3—55)

$$r_1 = 1.0 - \left(\frac{r_p}{r_e}\right)^2 = 1.0 - \left(\frac{1.68}{4.584}\right)^2 = 0.866$$

The maximum muzzle brake force (Eq. 3—57)

$$F_b = M_o \sqrt{\gamma R T_o}\ n_1 r_1 (1.0 - \cos 135°)/f_3$$

$$= 30.92 \times 3047 \times 2.2 \times 0.866 \times 1.707/1.33 = 230{,}000 \text{ lb}$$

The additional impulse induced by the propellant gas acting on the breech (Eq. 3—62)

$$I_g = \frac{W_c}{g}\sqrt{\frac{RT}{\gamma}}\left(\frac{\gamma+1}{2}\right)^{\frac{3-\gamma}{2(\gamma-1)}} = \frac{8}{32.2}\sqrt{\frac{10.6\times10^6}{1.26}}\left(\frac{2.26}{2}\right)^{\frac{1.74}{0.52}}$$

$$= 0.248 \times 2900 \times 1.505 = 1080 \text{ lb-sec}$$

The resultant impulse because of muzzle brake (Eq. 3—64)

$$I_r = I_g(1 - B_e) = 1080 \times 0.03 = 32 \text{ lb-sec}$$

The total momentum of the recoiling parts (Eq. 3—39)

$$m_{rb} = M_e v_o + I_r = 1957 + 32 = 1989 \text{ lb-sec}$$

If we assume that the muzzle brake weighs 200 lb, the total weight of the recoiling part is

$$W_{rb} = 1950 + 200 = 2150 \text{ lb}$$

The velocity of free recoil (Eq. 3—43)

$$v_f = \frac{m_{rb}}{M_{rb}} = \frac{1989 \times 32.2}{2150} = 29.8 \text{ ft/sec}$$

The energy of free recoil

$$E_{rb} = \frac{1}{2} \frac{W_{rb}}{g} v_f^2 = \frac{2150}{64.4} \times 888 = 29{,}650 \text{ ft-lb}$$

With a 30-in. (2.5 ft) length of recoil, the recoil force

$$F_a = \frac{E_{rb}}{L} = \frac{29650}{2.5} = 11{,}860 \text{ lb}$$

By maintaining a recoil force of 28,250 lb for no brake, the length of recoil

$$L = \frac{E_r}{F_c} = \frac{29650}{28250} \times 12 = 12.6 \text{ in.}$$

The brake efficiency (Eq. 3—46)

$$\epsilon_a = 100 \left(1.00 - \frac{E_{rb}}{E_r}\right) = 100 \left(1.00 - \frac{29650}{70640}\right) = 58.0\%$$

where E_{rb} = 70640 ft-lb (see Table 3—4)

Comparison of these results with those in Table 3—3 shows that the open muzzle brake is about as effective as the one-baffle closed muzzle brake.

3—3.3 FREE PERIPHERY MUZZLE BRAKE

3—3.3.1 Discussion

About half the periphery of a free periphery muzzle brake is open for gas discharge—provided that the bottom deflector-support is of conventional size, closing about 40 percent of the periphery, with the top support closing about 10 percent. Other supports are radial and do not interfere materially with the flow. Fig. 3—10 shows a schematic front view of this type brake. Because of the difference in area between top support and bottom area, the gas flow produces a downward thrust normal to the bore axis. This thrust, according to Eqs. 4.4a and 6.5b of Ref. 8

$$F_n = M_o a_o \omega \qquad (3—65)$$

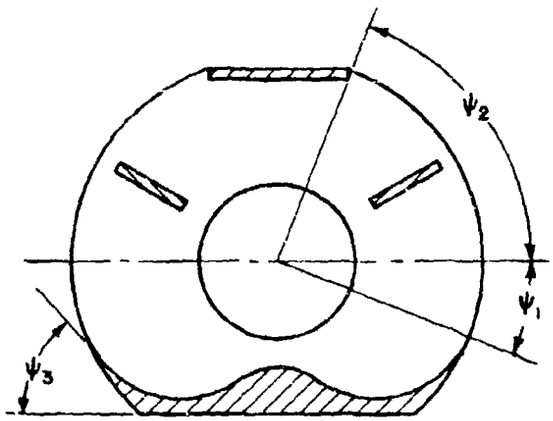

FIGURE 3-10. SCHEMATIC FRONT VIEW OF FREE PERIPHERY MUZZLE BRAKE

For a single baffle brake (Eq. 6.6 of Ref. 8)

$$\omega = \frac{\pi n_e}{\pi} \left[(\cos\psi_1 - \cos\psi_2) + \left(\frac{\pi}{2} - \psi_1\right) \sin\psi_3 \right] \qquad (3\text{—}66)$$

For multiple baffle brake (Eq. 6.7 of Ref. 8)

$$\omega = \frac{1}{\pi} \sum_{j}^{N} n_{ej} r_j \left[(\cos\psi_{1j} - \cos\psi_{2j}) + \left(\frac{\pi}{2} - \psi_{ij}\right) \sin\psi_{3j} \right] \qquad (3\text{—}67)$$

According to Eq. 2—9, the momentum of the gas at the muzzle from $t = 0$ to $t = \infty$ when $\gamma = 1.26$ is

$$M = 0.029 W_c \sqrt{RT_o} \left(1.0 + \frac{0.15 W_c}{W_p} \right) \qquad (3\text{—}68)$$

The impulse, normal to the bore axis, that is created by the deflector is

$$I_n = \omega M \qquad (3\text{—}69)$$

3—3.3.2 Example Problem

Assume that the given and computed data of earlier sample calculations still apply, then the muzzle brakes have values

a_o = 3047 ft/sec

M = 675 lb-sec (See Eq. 3—54)

M_o = 30.92 slugs/sec or $\left(\frac{\text{lb-sec}^2}{\text{ft}}\right)$ sec^{-1}

r_1 = 0.866

The free periphery angles: $\psi_1 = 20°,\ \psi_2 = 70°, \psi_3 = 40°, \psi = \frac{\pi}{2} = 90°$

According to Eq. 3—60, the expansion ratio

$$\Delta = 1 + \frac{\psi}{\pi}\left(\frac{r_e}{r}\right)^2 = 1 + \frac{1}{2}\left(\frac{4.854}{1.528}\right)^2 = 5.5$$

In Fig. 3—2, the speed-up factor corresponding to $\Delta = 5.5$ is $n_e = 2.2$. From Eq. 3—66

$$\omega = \frac{rn_e}{\pi}(\cos 20° - \cos 70°) + \left(\frac{\pi}{2} - \frac{20}{180}\pi\right)\sin 40°$$

$$= 0.605\ (0.940 - 0.342 + 1.222 \times 0.643) = 0.840$$

The normal force (Eq. 3—65)

$$F_n = M_o a_o \omega = 30.92 \times 9047 \times 0.84 = 79{,}100 \text{ lb}$$

The normal impulse (Eq. 3—69)

$$I_n = \omega M = 0.84 \times 675 = 567 \text{ lb-sec}$$

For the four-baffle brake, assume all baffles of the same size and shape wit' the same periphery angles as above. Then, according to Eq. 3—67,

$$\omega = 0.441 \sum_{j=1}^{4} n_{ej}\, r_j$$

where r_j corresponds with Δ_i of Table 3—2 and n_{ej} is obtained from Fig. 3—2. The given and computed data of a free periphery closed muzzle brake are listed in Table 3—6.

TABLE 3-6. NORMAL FORCES AND IMPULSES OF FREE PERIPHERY - CLOSED MUZZLE BRAKE

Data	1st Baffle	2nd Baffle	3rd Baffle	4th Baffle
r_j	0.579	0.244	0.102	0.043
Δ_e	3.35	7.96	18.92	44.93
n_e	2.05	2.32	2.47	2.60
$n_e r_j$	1.19	0.57	0.25	0.11
$\Sigma n_e r_j$	1.19	1.76	2.01	2.12
ω	0.525	0.776	0.886	0.935
F_n	49,500	73,100	83,500	88,000
I_n	335	524	598	632

CHAPTER 4
BLAST DEFLECTORS

4—1 DESIGN PROCEDURE

Blast deflectors are designed according to the same general procedures as muzzle brakes. Although a blast deflector has inherent muzzle brake characteristics, the converse is not always true. By directing the muzzle blast away from the gun crew area, the deflector does not alter the basic behavior of gas flow within the structure. The equations of Chapters 2 and 3 that describe this flow apply also to blast deflectors; the braking properties are merely a welcome by-product. Studies have been made and methods have been developed to analyze the pressures of the blast field in an effort to establish guidance during the early stages of the design.

4—2 OVERPRESSURE ANALYSIS OF THE BLAST FIELD

4—2.1 DISCUSSION OF PROCEDURE

A method for assessing muzzle blast of artillery during the development of a design concept is a decided asset in minimizing time, effort, and cost. At this stage, the designer can investigate the effect of any proposed design detail on the static overpressure in the crew area. The details include tube length, propellant charge, and muzzle brake characteristics. Such investigations permit the designer to use a brake of maximal efficiency consistent with tolerable overpressure limits. These pressure limits are presented in Chapter 9. Furthermore, parts of costly test programs for overpressure measurements can be avoided. An energy allocation based upon the heat of the burning propellant determines the available thermal energy remaining in the gases at projectile ejection. This is the overwhelmingly large portion of the energy available for shock formation.

A large portion of the propellant gas ejects through the side ports of the muzzle brake. In the mathematical model, two centers of spherical shock are assumed to form on each side of the muzzle brake. The positions of the two point sources of shock are located by applying the law of conservation of momentum and by finding the center of gravity of the gases expelled when the shock is fully developed[9]. Allocating a portion of half of the total available thermal energy to each of the two point sources permits calculating the scale of the shock decay which depends only on energy released and static ambient pressure of 14.7 psia.

A relation for pressure decay from each of the effective point sources was obtained by fitting the experimental shock data for a TNT explosion in air[10]. The fit is adequate over the range 1—15 psi overpressure. To evaluate the overpressure for a point in the crew area, the distances to the effective centers of shock must first be computed, i.e., N the distance to the near shock sphere, and O the distance to its counterpart on the other side of the gun. The static pressure contributed by each shock center at the field point is computed from the shock decay relationship. Shock waves reflected or refracted from hard surfaces or obstructions are not considered. Thus, the theoretical model is not valid for distant shock fields[11]. The two pressure components combine according to Eq. 36 of Ref. 11 which accounts for phase, i.e., time arrival, differences in the two components.

Isobars offer a clear way of displaying overpressure calculations. However, to compute the pressure explicitly for a given field position is a more convenient arrangement than to compute its converse (field position for a given pressure). Therefore,

since the value of each is known by selection, the procedure for computing the position of any given pressure becomes iterative. A digital computer program written in FORTRAN has been prepared to locate the static overpressure isobars in the blast field.

The program uses interior ballistic, gun, and muzzle brake data of the 105 mm XM103 Howitzer for the example. Computer isobars compare favorably with experimental values under a variety of conditions. Any realistic set of values for the isobars may be chosen. A suggested set is 7, 6, 5, 4, 3, 2.5, 2, 1.5, 1 psi.

Experimental peak overpressures are usually located in a polar coordinate system whose origin coincides with the center of the muzzle when the gun tube is at QE = 0° angle of elevation. This point remains the pole under all conditions.

To facilitate comparison with experimental data, the same coordinate system is used as that in the theoretical analysis coordinate system. The plane of the computed isobars is parallel to and at a specified height h above the horizontal plane that passes through the gun trunnion axis. Locations in the crew area of the blast field are also identified by f the horizontal distance behind the trunnion axis. Thus, the coordinate solution includes the height h, the angle relative to the gun axis θ, and the polar distance D_f of Fig. 4—1.

4—2.1.1 Definition and Dimensions of Symbols

A = bore area, in.^{2}

B = momentum index

D_f = distance from muzzle to field position at 0° elevation, ft

E_f = frictional and engraving losses, BTU

E_g = kinetic energy of gas, BTU

E_h = heat loss to gun tube, BTU

E_p = kinetic energy of projectile, BTU

E_r = kinetic energy of recoiling parts, BTU

E_{te} = thermal energy in gas at projectile ejection, BTU

F = propellant potential, ft-lb/lb

F_{ct} = fraction of maximum overpressure contributed by opposite shock center

H = heat of combustion, BTU/lb

L_g = distance of muzzle from trunnions, in.

n = moles of gas

p_g = average gas pressure at projectile ejection, psi

QE = angle of elevation, degrees

R = gas constant, ft-lb/lb, °K

T = isochoric flame temperature, °K

V_c = chamber volume, in.^{3}

V_p = volume of projectile and charge, in.^{3}

V_t = total internal volume of tube, in.^{3}

v_o = muzzle velocity, ft sec

W_c = weight of charge, lb

W_{ig} = weight of igniter, lb

W_p = weight of projectile, lb

W_r = weight of recoiling parts, lb

x_b = effective distance traveled by gases from muzzle to side port exit, in.

x_o = lateral distance from axis of gun tube to side port exit, in.

z_o = axial distance from muzzle to center of side port exit, in.

γ = ratio of specific heats

ϵ_e = efficiency of energy conversion to the back traveling shock wave

θ = angle between tube axis and line from muzzle to field position, deg

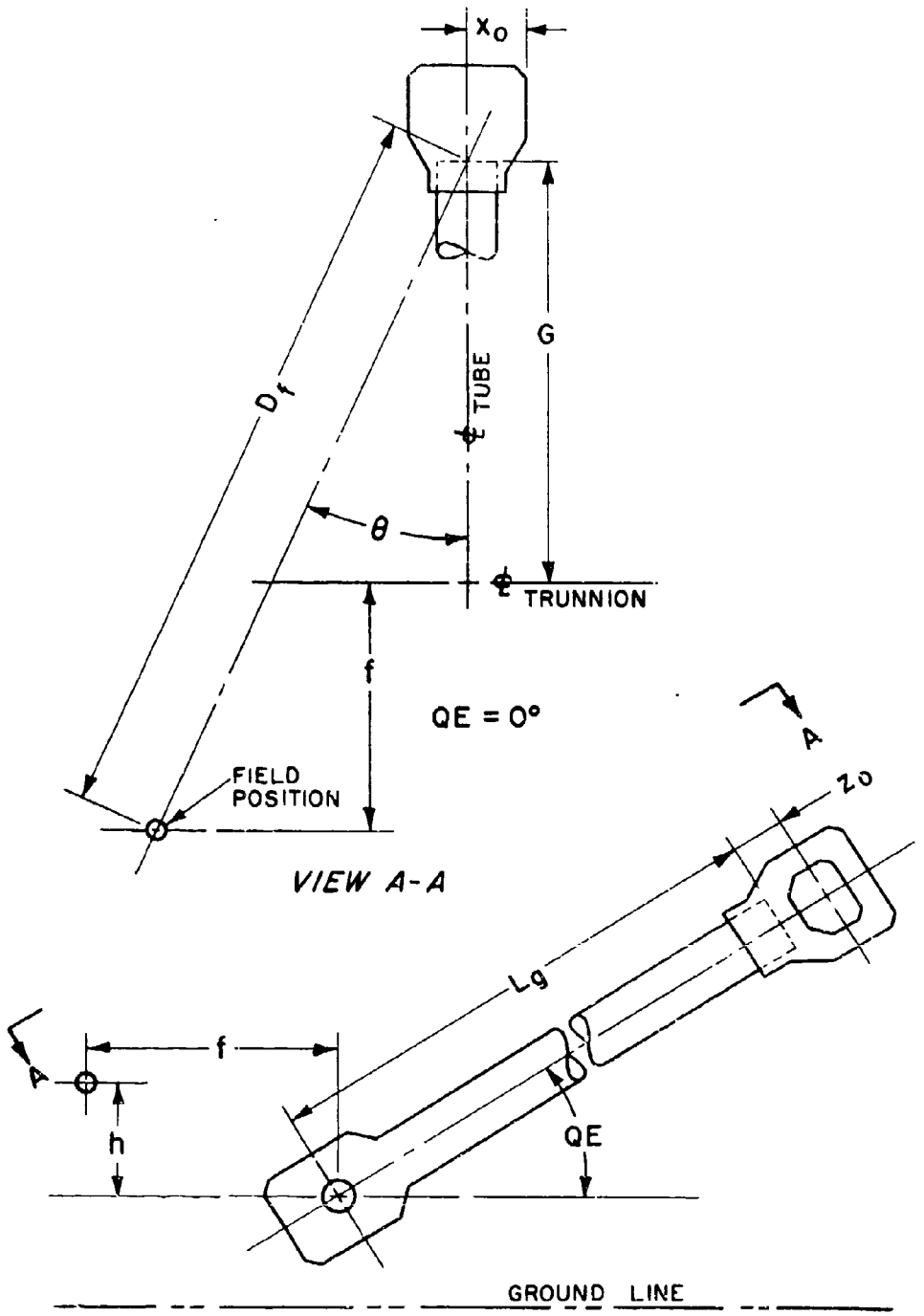

FIGURE 4-1. GEOMETRY OF BLAST AREA POSITIONS

4—2.1.2 Equations of the Analysis

The equations below are those used to direct the digital computer program:

$$W_T = W_c + W_{ig} \qquad (4—1)$$

$$\alpha = W_c / W_T \qquad (4—2)$$

$$R_x = 1545 n_x^* \qquad (4—3)$$

$$T_x\ (°R) \quad 1.8\ T_x\ (°K) \qquad (4—4)$$

$$H_x\ (BTU/lb\ ) = 1.8\ H_x\ (cal/gm) \qquad (4—5)$$

$$F_x = R_x T_x \qquad (4—6)$$

$$\Sigma = \frac{\alpha F_c}{\gamma_c - 1} + \frac{(1-\alpha) F_{ig}}{\gamma_{ig} - 1} \qquad (4—7)$$

$$R = \alpha R_c + (1-\alpha) R_{ig} \qquad (4—8)$$

$$\gamma = 1 + R / \left[\alpha R_c / (\gamma_c - 1) + (1-\alpha) R_{ig} / (\gamma_{ig} - 1) \right] \qquad (4—9)$$

$$T = (\gamma - 1) \Sigma / R \qquad (4—10)$$

$$H_T = H_c W_c + H_{ig} W_{ig} \qquad (4—11)$$

$$E_p = \left[W_p + 3.10^{-5} (V_T - V_p) \right] v_o^2 / 50030 \quad (2gJ = 50030) \qquad (4—12)$$

$$v_r / v_o = (W_1 / 2 + W_p) / (W_1 / 2 + W_r) \qquad (4—13)$$

$$K_v = (1/3)\ (1 + v_r / v_o)^2 - v_r / v_o \qquad (4—14)$$

$$E_g = \frac{W_T v_o^2 K_v}{50030} \qquad (4—15)$$

$$E_r = \frac{W_r v_o^2}{50030} (v_r / v_o)^2 \qquad (4—16)$$

$$E_f = 0.05 E_p \qquad (4—17)$$

$$E_h = \frac{0.597 (A/\pi)^{0.75} (V_T / A) (T - 530)}{777.5 \left\{ 1 + \left[2.7096 (A/\pi)^{1.0875} \right] / W_T^{0.8375} \right\}} \qquad (4—18)$$

$$E_{re} = H_T - E_p - E_g - E_r - E_f - E_h \qquad (4—19)$$

$$\varepsilon_e = 0.145 (1 + B + B^2) \qquad (4—20)$$

$$\sigma_s = (0.18\ \varepsilon_e \cdot E_{re})^{1/3} \qquad (4—21)$$

$$d_1 = \frac{\gamma V_1}{30 A} - x_b \qquad (4—22)$$

$$z_1 = d_1 (1-b) \qquad (4—23)$$

$$x_1 = (d_1^2 - z_1^2)^{1/2} \qquad (4—24)$$

$$x = x_o + x_1 \qquad (4—25)$$

*In this and subsequent equations, subscript x refers in turn to subscript c for charge and to subscript ig for igniter.

$$z = z_o + z_1 \qquad (4\text{--}26)$$

$$D_f = (L_g + f)/\cos\theta \qquad (4\text{--}27)$$

$$COM = \left[(L_g + z) \sin (QE) - h \right]^2 + \left[(L_g + z) \cos (QE) + f \right]^2 \qquad (4\text{--}28)$$

$$N = \left[(D_f \sin\theta - x)^2 + COM \right]^{1/2} \qquad (4\text{--}29)$$

$$\phi = \left[(D_f \sin\theta + x)^2 + COM \right]^{1/2} \qquad (4\text{--}30)$$

$$F_{ct} = \exp \left[2(N-\phi)/N \right] \qquad (4\text{--}31)$$

$$A_1 = \ln(N/\alpha) \qquad (4\text{--}32)$$

$$A_2 = \ln(\phi/\alpha) \qquad (4\text{--}33)$$

$$x_p = (0.60920384 - 0.20572855\, A_1)^{-1} \qquad (4\text{--}34)$$

$$\phi_{1,2} = \exp (-0.77394019 - 1.8989116\, A_{1,2} + 0.30859282\, A_{1,2}^2) \qquad (4\text{--}35)$$

$$p_3 = 14.7(\phi_1^{x_p} + F_{ct}\, \phi_2^{x_p})^{1/x_p} \qquad (4\text{--}36)$$

In iterating through Eqs. 4—27 to 4—36, choose an initial estimate for f for a pressure isobar $p_s = 7$. Call this initial estimate f_7. Then,

$$f_7 = \cos (QE) \left[\alpha \cos\theta - (L_g + z) \right] . \qquad (4\text{--}37)$$

The recursive procedure is defined by relating the $(i+1)st$ iterate for f to the i^{th}.

$$f^{(i+1)} = f^{(i)} + (2/3)\cos\theta\left[f^{(i)} + (L_R + z)\cos(QE)\right] \cdot$$

$$(p_3{}^{(i)} - p_s)/p_s \quad , \text{ for} \qquad (4\text{--}38)$$

$$f^{(i)} + (L_R + z)\cos(QE) > 0.1\,\alpha \quad .$$

Iteration continues until

$$\left| p_s - p_3{}^{(i)} \right| \leq .005\, p_s$$

If $f^{(i)} + (L_R + z)\cos(QE) > 0.1\alpha$, the value of p_s cannot be found for the current value of h. If this happens, the program will direct the computer to print "no isobar in this plane" and step to the next lower value of p_s.

4—2.2 DIGITAL COMPUTER ROUTINE FOR OVERPRESSURE ANALYSIS

The computer program is written specifically for the IBM-1620, but may be used on other systems by merely changing the control cards to be recognized by the particular equipment. The program permits three parameters to be varied: the height above the trunnion h; the elevation of the tube QE; and the muzzle brake data indicated by b, x_o, z_o, and x_b. Table 4—1 lists the symbols in the general text and the corresponding FORTRAN code. They are shown in order of appearance from Eqs. 4--1 to 4—38. Samples of input and output data are shown in Table 4—2 and 4—3 respectively, while Fig. 4—2 illustrates the isobars of one set of conditions. The program listing is found in Appendix A—1.

TABLE 4-1

SYMBOL-CODE CORRELATION FOR ISOBAR PROGRAM

Symbol	Code	Symbol	Code
W_t	EMI	W_p	EMP
W_c	EMC	V_t	VT
W_{ig}	EMIG	V_p	VP
α	ALPHA	v_o	VO
R_c	RC	v_r/v_o	VRVO
R_{ig}	RIG	K_v	CONST
T_c	TVC	E_g	EKEG
T_{ig}	TVIG	E_r	EKER
n_c	GMC	W_r	EMR
n_{ig}	GMIG	E_f	KEB
H_c	EC	E_h	EKEH
H_{ig}	EIG	A	AREA
F_c	FC	E_{re}	EGAS
F_{ig}	FIG	L_g	G
Σ	SIGMA	ϵ_e	EFC
γ_c	GAMMAC	B	BFLAT
γ_{ig}	GAMIG	α_s	ALSTR
R	R	d_1	DONE
γ	GAMMA	z_1	ZONE
T	TV	x_1	XONE
H_T	HTOT	$\hat{}$	X
E_p	EKEP	z	Z
x_o	XO	N	EN
z_o	ZO	ϕ	O
D_f	DSTAR	F_{ct}	FACT
f	F	A_1	A1
θ	THETA	A_2	A2
COM	COM	xp	XP
L_g	G	ϕ_1	PHI1
QE	QE	ϕ_2	PHI2
x_b	Zeta	P_s	PS

TABLE 4 - 2 SAMPLE INPUT

XM103 CANNON W/T36 CHARGE ZONE 8 TEST RUN FOR PHASE STUDY JUNE 1965

1.2385	1.2385	3040.	3040.	.04308	.04308	974.	974.
13.71	1710.	414.	4.35	.04	28.5	1430.	2200.
2	2	3	128.				
30.	42.	2.	45.				
1.35	5.	3.	11.				
.95	5.	3.	11.				
0.	0.	0.	0.				

TABLE 4 - 3 SAMPLE OUTPUT

ISOBAR IV G.SCHLENKER-S.OLSON AWC-OR JUNE 1965
XM103 CANNON W/T36 CHARGE ZONE 8 TEST RUN FOR PHASE STUDY JUNE 1965

GAMMA C	GAMMA IG	TV C, DEG K	TV IG, DEG K	NC, GM MOL
1.2385	1.2385	3040.0	3040.0	.04308

NIG, GM MOL	EC, CAL/GM	EIG, CAL/GM	AREA, SQ IN
.043080	974.0	974.0	13.71

VT, CU IN	VP, CU IN	MC, LBM	MIG, LBM	MP, LBM
1710.0	414.0	4.350	.040	28.500

MR, LBM	VO, FT/SEC
1430.0	2200.

ENERGIES	BTU
TOTAL	7696.55
PROJECTILE	2760.91
GAS, KINETIC	138.60
RECOILING MASS	63.55
ENGRAVING	138.05
HEAT LOSS TO GUN	291.83
GAS, THERMAL	4303.62

B-FLAT	G, IN	XO, IN	ZO, IN
1.35	128.00	5.000	3.000
QE, DEG	H, IN	PS, PSI	ZETA, IN
2.0	30.0	7.000	11.000

THETA STAR, DEG	D STAR, FT	F, FT
.00	9.314	-1.352
10.00	9.151	-1.655
20.00	9.513	-1.727
30.00	10.111	-1.910
40.00	10.738	-2.441
50.00	11.329	-3.385

TABLE 4 - 3 CONTINUED

B-FLAT	G, IN	XO, IN	ZO, IN
1.35	128.00	5.000	3.000
QE, DEG	H, IN	PS, PSI	ZETA, IN
2.0	30.0	6.000	11.000
THETA STAR, DEG	D STAR, FT	F, FT	
.00	10.234	-.433	
10.00	10.068	-.751	
20.00	10.355	-.936	
30.00	10.884	-1.241	
40.00	11.529	-1.835	
50.00	12.019	-2.941	

B-FLAT	G, IN	XO, IN	ZO, IN
1.35	128.00	5.000	3.000
QE, DEG	H, IN	PS, PSI	ZETA, IN
2.0	30.0	5.000	11.000
THETA STAR, DEG	D STAR, FT	F, FT	
.00	11.462	.795	
10.00	11.245	.407	
20.00	11.478	.119	
30.00	11.937	-.329	
40.00	12.529	-1.069	
50.00	12.986	-2.319	

B-FLAT	G, IN	XO, IN	ZO, IN
1.35	128.00	5.000	3.000
QE, DEG	H, IN	PS, PSI	ZETA, IN
2.0	30.0	4.000	11.000
THETA STAR, DEG	D STAR, FT	F, FT	
.00	13.161	2.495	
10.00	12.919	2.056	
20.00	13.053	1.599	
30.00	13.433	.966	
40.00	13.948	.018	
50.00	14.394	-1.414	

B-FLAT	G, IN	XO, IN	ZO, IN
1.35	128.00	5.000	3.000
QE, DEG	H, IN	PS, PSI	ZETA, IN
2.0	30.0	3.000	11.000
THETA STAR, DEG	D STAR, FT	F, FT	
.00	15.692	5.025	
10.00	15.485	4.583	
20.00	15.516	3.913	
30.00	15.797	3.014	
40.00	16.155	1.708	
50.00	16.564	-.020	

TABLE 4 - 3 CONTINUED

B-FLAT	G, IN	XO, IN	ZO, IN
1.35	128.00	5.000	3.000
QE, DEG	H, IN	PS, PSI	ZETA, IN
2.0	30.0	2.500	11.000
THETA STAR, DEG	D STAR, FT	F, FT	
.00	17.617	6.950	
10.00	17.334	6.404	
20.00	17.407	5.690	
30.00	17.625	4.597	
40.00	17.939	3.075	
50.00	18.244	1.060	

B-FLAT	G, IN	XO, IN	ZO, IN
1.35	128.00	5.000	3.000
QE, DEG	H, IN	PS, PSI	ZETA, IN
2.0	30.0	2.000	11.000
THETA STAR, DEG	D STAR, FT	F, FT	
.00	20.457	9.790	
10.00	20.184	9.211	
20.00	20.154	8.272	
30.00	20.324	6.935	
40.00	20.553	5.078	
50.00	20.800	2.703	

B-FLAT	G, IN	XO, IN	ZO, IN
1.35	128.00	5.000	3.000
QE, DEG	H, IN	PS, PSI	ZETA, IN
2.0	30.0	1.500	11.000
THETA STAR, DEG	D STAR, FT	F, FT	
.00	25.057	14.391	
10.00	24.769	13.726	
20.00	24.678	12.523	
30.00	24.748	10.766	
40.00	24.905	8.412	
50.00	25.073	5.450	

B-FLAT	G, IN	XO, IN	ZO, IN
1.35	128.00	5.000	3.000
QE, DEG	H, IN	PS, PSI	ZETA, IN
2.0	30.0	1.000	11.000
THETA STAR, DEG	D STAR, FT	F, FT	
.00	34.618	23.952	
10.00	34.331	23.143	
20.00	34.170	21.442	
30.00	34.117	18.880	
40.00	34.134	15.481	
50.00	34.170	11.297	

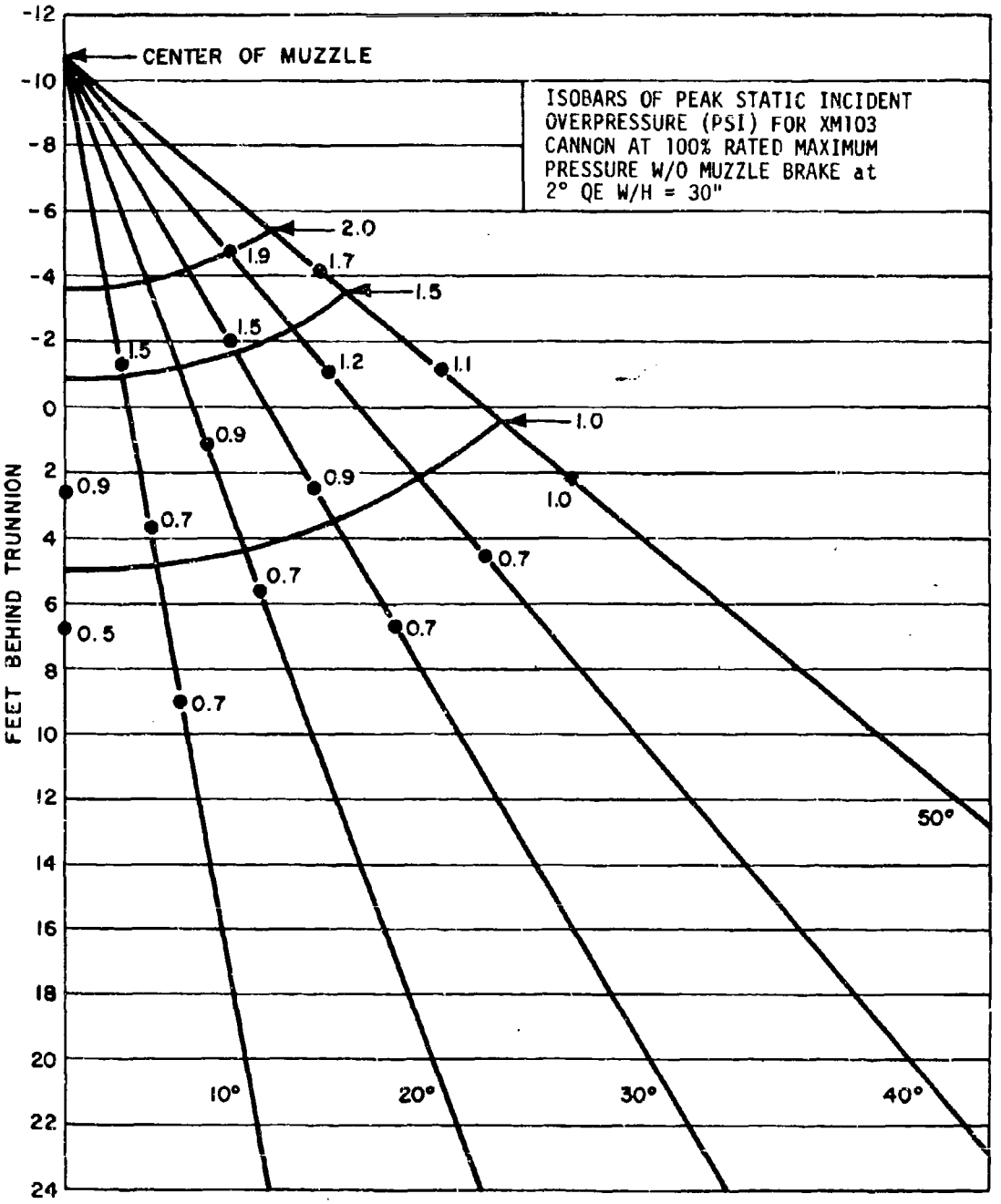

FIGURE 4-2. OVERPRESSURE ISOBARS

CHAPTER 5
FLASH SUPPRESSORS

5—1 PERFORMANCE REQUIREMENTS

Flash, the radiation of visible light from propellant gases as they emerge from the muzzle of the gun, is both physical and chemical in nature; physical in the sense that the gases are hot enough to become luminous, and chemical through the process of combustion. Suppression of flash therefore may be achieved by removing or deterring the influence of these phenomena. Low muzzle gas temperatures reduce flash tendencies and may be achieved by increasing the efficiency of the gun [12]. Two methods are immediately available for increasing the efficiency although their practical application may be questioned. Each involves inducing optimum burning rates and affiliated pressure development rates by controlling the propellant grain size or shape. One involves a higher muzzle velocity with the same charge; the other, the same muzzle velocity at reduced charge. In either case, a larger portion of the available energy is transmitted to the projectile rather than retained as heat in the gas and the gun becomes ballistically more efficient with a subsequent reduction in critical temperatures that may be below the flash-inducing range.

The flow pattern of uninhibited gases as they issue from the muzzle is shown in Fig. 5—1. The pattern is divided into eight regions designated by the corresponding numeral. Each region has unique characteristics.

Enumerating

Region

1 = surrounding air at atmospheric pressure, $p = p_a$

2 = all muzzle gas at $p = p_a$

3 = 1 + 2, mixture at $p = p_a$

4 = 3, after passing through shock wave, $p > p_a$

5 = 4, after reducing to atmospheric pressure, $p = p_a$

6 = 2, after passing through shock wave, $p > p_a$

7 = 6, after reducing to atmospheric pressure, $p = p_a$

8 = 7 + 1, mixture at $p = p_a$

Preflash and primary flash originate at the muzzle. No attachment has been devised to prevent their occurrence but some type of shielding can obscure them from all observers except those directly in front of the gun. Muzzle glow occupies Region 2 while intermediate flash occurs in Regions 4 and 7. Any mechanical device that precludes the formation of the shock bottle will destroy the formation of both phenomena. Secondary flash occurs in Regions 3, 5, and 8, provided that ignition temperatures and sufficient time prevail for any given air-to-muzzle gas ratio. Secondary

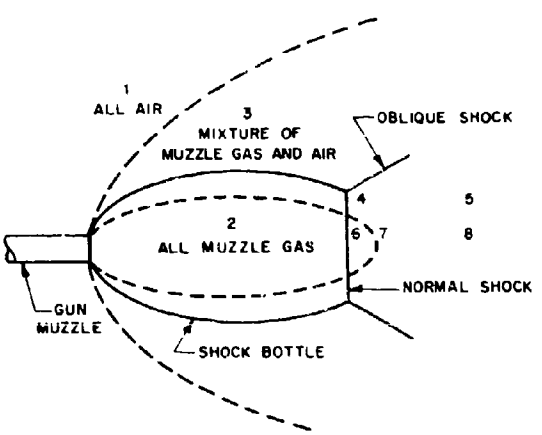

FIGURE 5-1. FLOW PATTERN AT A GUN MUZZLE

flash will be eliminated when the temperature of the gas-air mixture is lower than the ignition temperature of that particular mixture. Fig. 5—2 illustrates the susceptibility of various muzzle gas-air mixtures at atmospheric pressure to secondary flash. Curves T_a, T_b, and T_c are ignition temperature curves of three hypothetical propellants. T_3, T_5, and T_8 are the computed temperatures of the muzzle gas in Regions 3, 5, and 8, respectively, of Fig. 5—1. If the ignition temperature curve intersects the actual temperature curve in any region, secondary flash will occur. Thus, the muzzle gas of the T_a curve will not ignite, that of the T_b curve will ignite for any mixture from $r = 0.15$ to $r = 0.55$ in Region 5, whereas all three regions are susceptible for the propellant represented by the T_c curve.

The ideal suppressor contains the muzzle gases until pressures reduce to atmospheric levels. Once released, no further control can be exercised. The temperature of the gas-air mixture throughout the richness range and the corresponding ignition temperature become the criteria for determining the feasibility of installing a mechanical flash suppressor. The ignition temperatures for any given propellant are found experimentally for the range of muzzle gas-air mixtures. Some of these are plotted in Fig. 5—3. Equal or overlapping of the two temperatures renders as useless any further attempt to control secondary flash mechanically. Unfortunately, if the ideal suppressor is feasible theoretically, its geometric proportions may not be reasonable and only trials of modified versions can determine its practical application.

5—1.1 COMPUTED TEMPERATURES OF MUZZLE GAS-AIR MIXTURES

Equations are available for computing the temperatures of muzzle gas-air mixtures for any degree of richness and for any propellant having known parameters [13]. These temperatures are for the mixtures at atmospheric pressure, i.e., for an ideal flash suppressor. The specific heat at constant pressure of the mixture in Region 3

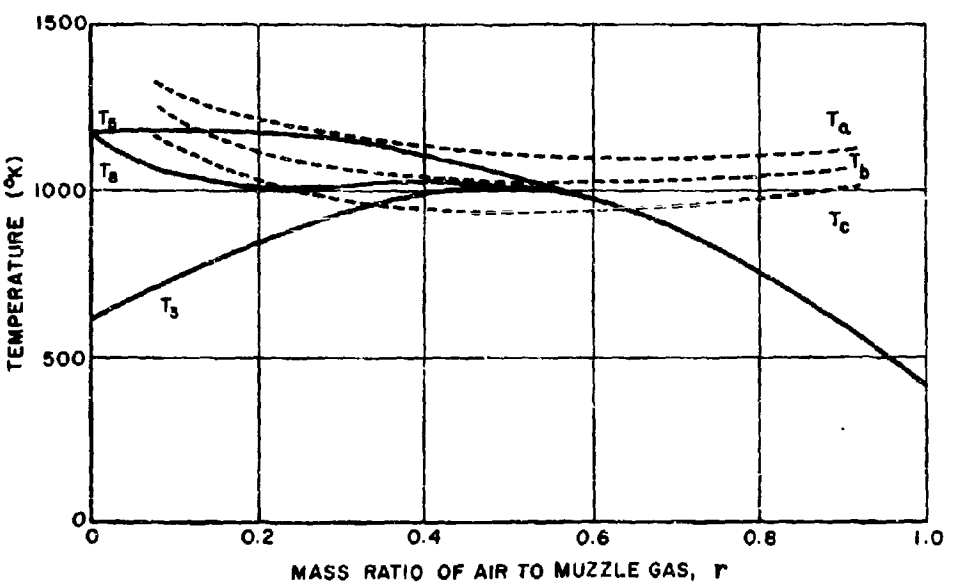

FIGURE 5-2. GAS STATE-IGNITION CURVES

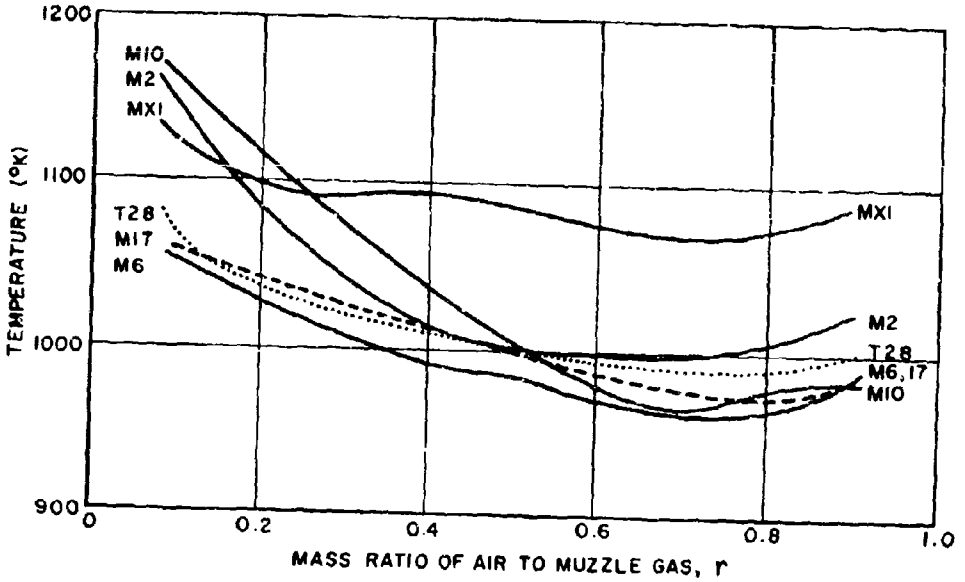

FIGURE 5-3. IGNITION BOUNDARIES OF VARIOUS PROPELLANTS

$$C_{p3} = rC_{pa} + (1-r)\,C_{pg} \qquad (5-1)$$

where

C_{pa} = specific heat of air at constant pressure

C_{pg} = specific heat of muzzle gas at constant pressure

r = ratio of air to total air-gas mixture

The ratio of specific heats of mixture in Region 3 is

$$\gamma_3 = \frac{C_{p3}}{r\,C_{va} + (1-r)\,C_{vg}} \qquad (5-2)$$

where C_{va} and C_{vg} are the specific heats at constant volume of air and muzzle gas, respectively. The absolute temperature of the mixture in Region 3 is

$$T_3 = \frac{S_1 + S_2}{F_c\,C_{p3}} \qquad (5-3)$$

where

$$S_1 = F_c r C_{pa} T_a + r(1-r)\gamma \left[F - \frac{v_m^2}{2g} \left(\frac{W_p}{W_c} + \frac{1}{3} - \frac{1}{\gamma} \right) \right] \qquad (5-4)$$

$$S_2 = (1-r)^2 \gamma \left[F - \frac{v_m^2}{2g} \left(\frac{W_p}{W_c} + \frac{1}{3} \right) \right]^{1/\gamma} \left[\frac{p_a V_t}{(\gamma-1) W_c} \right]^{(\gamma-1)/\gamma} \qquad (5-5)$$

C_{pa} = specific heat at constant pressure of air, BTU/lb/°R

F = $RT/(\gamma - 1)$, propellant potential (usually ft-lb/lb)

F_c = 1400 ft-lb/BTU/°K · (Conversion factor to make dimensions consistent)

g = acceleration of gravity, ft/sec^2

p_a = atmospheric pressure, psi

T_a = absolute temperature of ambient air, °K

V_t = total volume of gun tube, in.^{3}

v_o = muzzle velocity, ft/sec

W_c = weight of propellant charge, lb

W_p = weight of projectile, lb

γ = ratio of specific heats of propellant gas

Caution should be exercised to maintain dimensional homogeneity.

The conversion factor to compute the temperature of other mixture regions is

$$C_f = \frac{\frac{4\gamma_3}{C_{pa} T_3} \left\{ r C_{pa} T_a + (1-r) C_{pg} T_f \left[1 - \frac{v_o^2}{2gF} \left(\frac{W_p}{W_c} + \frac{1}{3} - \frac{1}{\gamma} \right) \right] \right\} - (\gamma_3 - 1)^2}{\gamma_3^2 - 1} \qquad (5-6)$$

where C_{pg} is the specific heat at constant pressure of muzzle gas and T_f is flame temperature of the propellant.

The temperature in Region 5 is

$$T_5 = C_f^{\frac{1}{\gamma_3}} \left[\frac{(\gamma_3 - 1)C_f + (\gamma_3 + 1)}{(\gamma_3 + 1)C_f + (\gamma_3 - 1)} \right] T_3 \quad (5\text{—}7)$$

The temperature in Region 8

$$T_8 = \frac{S_1 + S_2 C_f^{\frac{1}{\gamma}} \left[\frac{(\gamma - 1)C_f + (\gamma + 1)}{(\gamma + 1)C_f + (\gamma - 1)} \right]}{F_c\, C_{p3}} \quad (5\text{—}8)$$

5—1.2 DIGITAL COMPUTER ROUTINES FOR MUZZLE GAS TEMPERATURE

A digital computer routine has been programmed for computing the three temperatures T_3, T_5, and T_8, of the air-propellant gas mixtures. Table 5—1 lists the symbols in the general text and the corresponding FORTRAN code*. They are shown in order of appearence from Eqs. 5—1 to 5—5. This program may be used in any system, provided that the control cards are revised to be recognized by the particular system.

The constants that appear in the calculations are

C_{pa} = 0.24 BTU/lb/°R,

g = 32.2 ft/sec^2

C_{va} = 0.171 BTU/lb/°R

F_c = 1400 ft-lb/BTU/°K

Temperatures are computed for 8 guns having the input data listed in Table 5—2.

5—1.3 LENGTH OF BAR-TYPE

The length of the ideal bar flash suppressor is based on the physical proportions of the gun and the muzzle gas properties. Fig. 5—4 is a schematic of a bar suppressor attached to a gun muzzle. Since the transition of bore area to the circumscribed bar area should not be abrupt, an internal

TABLE 5-1. SYMBOL-CODE CORRELATION FOR TEMPERATURE PROGRAM

Symbol	Code	Symbol	Code
C_{p3}	CP3	γ	GAMMA
r	R	F	PSI
C_{pa}	CPA	v_o	VM
C_{pg}	CPG	g	G
γ_3	GAMMA3	W_p	WP
C_{va}	CVA	W_c	WC
C_{vg}	CVG	P_a	PA
T_3	T3	V_t	VT
C_{t1}	CT1	C_f	CF
C_{t2}	CT2	T_f	TF
F_c	FC	T_5	T5
T_a	TA	T_8	T8

*Appendix A—2 is the flow chart and Appendix A—3 is the source program listing.

TABLE 5-2. INPUT DATA FOR TEMPERATURE CALCULATIONS

Gun mm	Propellant	C_{pg} BTU/lb/°R	C_{vg} BTU/lb/°R	γ	T_a °K	T_f °K
1.57	IMR	0.426	0.346	1.231	295	3,105
37	T28	0.429	0.347	1.238	295	3,080
75	M6	0.434	0.346	1.254	295	2,574
90	M17	0.446	0.360	1.239	295	3,017
105	M17	0.446	0.360	1.239	295	3,017
120	M17	0.446	0.360	1.239	295	3,017
155	M6	0.434	0.346	1.254	295	2,574
175	M6	0.434	0.346	1.254	295	2,574

Gun mm	v_o ft/sec	V_t in.^{3}	W_c lb	W_p lb	F ft·lb/lb
1.57	3,250	9.5	0.0322	0.0932	1,504,000
37	3,000	183.5	0.50	1.61	1,496,000
75	2,800	1,219.8	3.385	12.21	1,249,000
90	3,000	1,854	8.24	24.1	1,523,000
105	3,950	2,900	11.74	21.6	1,523,000
120	3,500	5,374	29.43	50.85	1,523,000
155	2,800	6,566	30.86	95.0	1,249,000
175	3,000	16,030	55.1	147.0	1,249,000

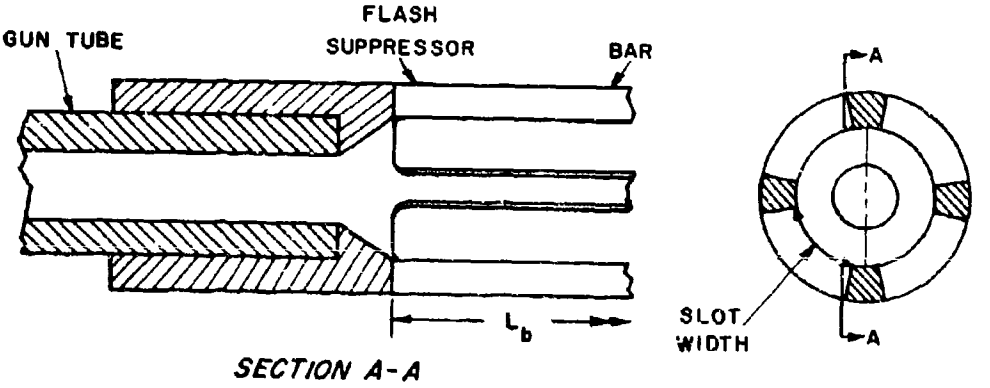

FIGURE 5-4. SCHEMATIC OF BAR SUPPRESSOR

TABLE 5-3

OUTPUT DATA FOR TEMPERATURE CALCULATIONS

MUZZLE GAS TEMPERATURES FOR VARIOUS MIXTURE RATIOS OF 1.57MM GUN

I	R	CP3	GAMMA3	T3(DEG K)	T5(DEG K)	T8(DEG K)
1	0.0	0.426	1.231	601.	1997.	1996.
2	0.1	0.407	1.240	742.	1901.	1530.
3	0.2	0.389	1.250	859.	1780.	1301.
4	0.3	0.370	1.261	949.	1641.	1107.
5	0.4	0.352	1.274	1008.	1490.	1126.
6	0.5	0.333	1.288	1030.	1329.	1081.
7	0.6	0.314	1.305	1009.	1161.	1027.
8	0.7	0.296	1.323	937.	987.	941.
9	0.8	0.277	1.346	804.	806.	804.
10	0.9	0.259	1.372	595.	571.	595.
11	1.0	0.240	1.404	295.	295.	295.

MUZZLE GAS TEMPERATURES FOR VARIOUS MIXTURE RATIOS OF 37-MM GUN

I	R	CP3	GAMMA3	T3(DEG K)	T5(DEG K)	T8(DEG K)
1	0.0	0.429	1.236	617.	1986.	1988.
2	0.1	0.410	1.245	756.	1892.	1536.
3	0.2	0.391	1.255	872.	1774.	1312.
4	0.3	0.372	1.265	960.	1638.	1198.
5	0.4	0.353	1.278	1018.	1489.	1136.
6	0.5	0.335	1.292	1039.	1331.	1090.
7	0.6	0.316	1.307	1017.	1164.	1034.
8	0.7	0.297	1.326	944.	991.	947.
9	0.8	0.278	1.347	809.	811.	809.
10	0.9	0.259	1.373	598.	570.	598.
11	1.0	0.240	1.404	295.	295.	295.

TABLE 5-3 (CONT.)

MUZZLE GAS TEMPERATURES
FOR VARIOUS MIXTURE RATIOS OF 75-MM GUN

I	R	CP3	GAMMA3	T3(DEG K)	T5(DEG K)	T8(DEG K)
1	0.0	0.434	1.254	462.	1496.	1496.
2	0.1	0.415	1.262	577.	1441.	1160.
3	0.2	0.395	1.271	675.	1364.	1001.
4	0.3	0.376	1.280	752.	1271.	927.
5	0.4	0.356	1.291	805.	1166.	892.
6	0.5	0.337	1.304	830.	1052.	867.
7	0.6	0.318	1.318	821.	932.	834.
8	0.7	0.298	1.334	773.	807.	776.
9	0.8	0.279	1.353	677.	679.	677.
10	0.9	0.259	1.376	523.	480.	522.
11	1.0	0.240	1.404	295.	295.	295.

MUZZLE GAS TEMPERATURES
FOR VARIOUS MIXTURE RATIOS OF 90-MM GUN

I	R	CP3	GAMMA3	T3(DEG K)	T5(DEG K)	T8(DEG K)
1	0.0	0.446	1.239	567.	2000.	2000.
2	0.1	0.425	1.247	719.	1921.	1518.
3	0.2	0.405	1.256	848.	1811.	1294.
4	0.3	0.384	1.267	949.	1679.	1189.
5	0.4	0.364	1.278	1018.	1531.	1138.
6	0.5	0.343	1.292	1049.	1371.	1102.
7	0.6	0.322	1.307	1035.	1201.	1053.
8	0.7	0.302	1.325	967.	1022.	970.
9	0.8	0.281	1.347	832.	836.	832.
10	0.9	0.261	1.372	615.	594.	615.
11	1.0	0.240	1.404	295.	295.	295.

TABLE 5-3 (CONT.)

MUZZLE GAS TEMPERATURES
FOR VARIOUS MIXTURE RATIOS OF 105-MM GUN

I	R	CP3	GAMMA3	T3(DEG K)	T5(DEG K)	T8(DEG K)
1	0.0	0.446	1.239	546.	2010.	2010.
2	0.1	0.425	1.247	704.	1935.	1510.
3	0.2	0.405	1.256	837.	1826.	1284.
4	0.3	0.384	1.267	943.	1694.	1183.
5	0.4	0.364	1.278	1015.	1545.	1135.
6	0.5	0.343	1.292	1050.	1383.	1102.
7	0.6	0.322	1.307	1038.	1211.	1056.
8	0.7	0.302	1.325	971.	1030.	975.
9	0.8	0.281	1.347	836.	841.	836.
10	0.9	0.261	1.372	618.	599.	618.
11	1.0	0.240	1.404	295.	295.	295.

MUZZLE GAS TEMPERATURES
FOR VARIOUS MIXTURE RATIOS OF 120-MM GUN

I	R	CP3	GAMMA3	T3(DEG K)	T5(DEG K)	T8(DEG K)
1	0.0	0.446	1.239	571.	2159.	2159.
2	0.1	0.425	1.247	742.	2081.	1610.
3	0.2	0.405	1.256	887.	1964.	1367.
4	0.3	0.384	1.267	1001.	1821.	1259.
5	0.4	0.364	1.278	1080.	1659.	1209.
6	0.5	0.343	1.292	1117.	1483.	1174.
7	0.6	0.322	1.307	1104.	1295.	1124.
8	0.7	0.302	1.325	1031.	1098.	1035.
9	0.8	0.281	1.347	884.	890.	885.
10	0.9	0.261	1.372	647.	631.	647.
11	1.0	0.240	1.404	295.	295.	295.

TABLE 5-3 (CONT.)

MUZZLE GAS TEMPERATURES
FOR VARIOUS MIXTURE RATIOS OF 155-MM GUN

I	R	CP3	GAMMA3	T3(DEG K)	T5(DEG K)	T8(DEG K)
1	0.0	0.434	1.254	467.	1597.	1597.
2	0.1	0.415	1.262	594.	1542.	1223.
3	0.2	0.395	1.271	702.	1461.	1052.
4	0.3	0.376	1.280	787.	1360.	974.
5	0.4	0.356	1.291	846.	1247.	939.
6	0.5	0.337	1.304	874.	1123.	914.
7	0.6	0.318	1.318	866.	992.	880.
8	0.7	0.298	1.334	815.	855.	817.
9	0.8	0.279	1.353	711.	713.	711.
10	0.9	0.259	1.376	543.	509.	542.
11	1.0	0.240	1.404	295.	295.	295.

MUZZLE GAS TEMPERATURES
FOR VARIOUS MIXTURE RATIOS OF 175-MM GUN

I	R	CP3	GAMMA3	T3(DEG K)	T5(DEG K)	T8(DEG K)
1	0.0	0.434	1.254	470.	1614.	1614.
2	0.1	0.415	1.262	599.	1559.	1234.
3	0.2	0.395	1.271	707.	1476.	1061.
4	0.3	0.376	1.280	794.	1375.	983.
5	0.4	0.356	1.291	853.	1260.	947.
6	0.5	0.337	1.304	882.	1134.	923.
7	0.6	0.318	1.318	873.	1001.	887.
8	0.7	0.298	1.334	821.	862.	824.
9	0.8	0.279	1.353	716.	718.	716.
10	0.9	0.259	1.376	546.	514.	546.
11	1.0	0.240	1.404	295.	295.	295.

conical surface joins the bore to the inner surface of the bar. The axial length of the conical surface is somewhat arbitrary and the optimum distance can best be obtained empirically. A series of equations have been developed to compute the various parameters that affect the ideal bar length. The stagnation temperature from Eq. 18 of Reference 13 is

$$T_s = T_f \left[1 - \frac{v_o^2}{2gF} \left(\frac{W_p}{W_c} + \frac{1}{3} - \frac{1}{\gamma} \right) \right] \qquad (5\text{—}9)$$

where T_f is the given flame temperature.

From Eq. 16 of Reference 13, the stagnation pressure

$$P_s = \frac{(\gamma - 1)F W_c}{V_t} \frac{T_s}{T_f} \qquad (5\text{—}10)$$

The pressure at the origin of the slots between the bars of the suppressor is computed from the expression [13]

$$\left(\frac{A_o}{A}\right)^2 = \left(\frac{\gamma-1}{2}\right) \frac{\left(\frac{2}{\gamma+1}\right)^{(\gamma+1)/(\gamma-1)}}{\left(\frac{P_o}{P_s}\right)^{2/\gamma} \left[1 - \left(\frac{P_o}{P_s}\right)^{(\gamma-1)/\gamma}\right]} \qquad (5\text{—}11)$$

where

A = area of gun bore

A_o = area of flash suppressor at origin of slots

P_o = pressure at origin of slots

All other values being given or assumed, P_o can be obtained through iterative computation. The length of the bars of an ideal flash suppressor according to Eq. 2 of Reference 15 is

$$L_b = \frac{\frac{2}{\gamma-1}\left(\sqrt{\frac{1-y}{y}} - \sqrt{\frac{1-y_o}{y_o}}\right) + \frac{\gamma+1}{2(\gamma-1)} \left[\sin^{-1}(2y-1) - \sin^{-1}(2y_o - 1)\right]}{\frac{W_s}{A_o}\sqrt{\frac{\gamma-1}{2}\left(\frac{2}{\gamma+1}\right)^{(\gamma+1)/(\gamma-1)}}} \qquad (5\text{—}12)$$

where $y = P_s/P_s$

$y_o = P_o/P_s$

w_s = total width of slots around periphery

The length of the gun tube, therefore total gun volume, for any given propellant charge and projectile has a decided effect on this length of the flash suppressor bar. For instance, large bore guns, the total volume-to-propellant charge ratio of which is much smaller than that for small bore guns, will need relatively much longer bars, in fact, far out of proportion to the length of gun tubes. Sample calculations will demonstrate this peculiarity. One fortunate discovery during experimentation with suppressors of theoretical proportions was their retention of effectiveness after the bars were shortened.

Another favorable aspect of the bar flash suppressor is its ability to function satisfactorily without resorting to theoretical variations of discharge area along its length. After computing the total length (L_b of Eq. 5—12), the theoretical discharge area at any intermediate distance would have to be evaluated for a short incremental distance of discharge. Fig. 5—5 gives a qualitative description of this activity. Assume that the various gas pressures are known at a distance L_{b1} from the slot origin and over an axial distance ΔL. In Eq. 5—11, let $A = w_s \Delta L$, $P_o = P_s$, and $A_o = A_e$. The exit area A_e can now be computed, from which the column length or actual bar thickness t_b can be found from geometric proportions. This theory has not been tested experimentally but, as mentioned above, verification may not be necessary.

5—2 CONE-TYPE SUPPRESSOR

The design of cone-type suppressor configuration follows approximately the same procedure as that of the bar-type. Where slot width and number of bars are selected somewhat arbitrarily and the length computed to conform to these selections, the exit area of the cone is computed and a reasonable length selected to conform with the conventional practice of having the included angle of about 20° to 25° [18]. After stagnation temperature and pressure (Eqs. 5—9 and 5—10) are computed, the exit area of the cone is found according to Eq. 5—11

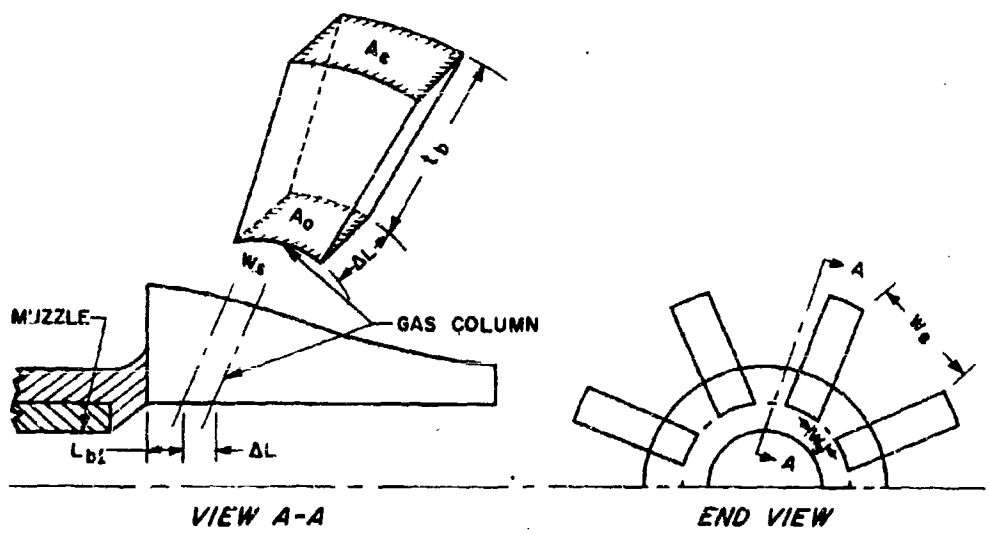

FIGURE 5-5. BAR CONTOUR FOR THEORETICAL GAS DISCHARGE

$$A_e = \frac{A\sqrt{f(\gamma)}}{\left(\frac{p_a}{p_s}\right)^{1/\gamma}\sqrt{1-y}} \qquad (5\text{—}13)$$

where $f(\gamma) = \frac{\gamma-1}{2}\left(\frac{2}{\gamma+1}\right)^{(\gamma+1)/(\gamma-1)}$

$$y = \left(\frac{p_a}{p_s}\right)^{(\gamma-1)/\gamma}$$

The exit diameter

$$D_e = \sqrt{4A_e/\pi} \qquad (5\text{—}14)$$

The length of the cone

$$L_c = \tfrac{1}{2} D_e/\tan\theta \qquad (5\text{—}15)$$

where θ = the included angle of the cone.

5—3 DIGITAL COMPUTER ROUTINES FOR FLASH SUPPRESSOR CONFIGURATION

For convenience, particularly for the iterative solution of p_o, Eq. 5—11 may be written

$$p_s^{(\gamma-1)/\gamma} p_o^{2/\gamma} - p_o^{(\gamma+1)/\gamma} - f(\gamma) p_s^{(\gamma+1)/\gamma}\left(\frac{A_b}{A_o}\right)^2 = 0 \qquad (5\text{—}16)$$

The solution of p_o is available by applying the Newton-Raphson method of approximations where

$$x_n = x_{n-1} - \frac{F(x_{n-1})}{F'(x_{n-1})} \qquad (5\text{—}17)$$

and where F' is the first derivative of Eq. 5—16.

$$F'(p_o) = \frac{2}{\gamma} p_s^{(\gamma-1)/\gamma} p_o^{(2-\gamma)/\gamma} - \frac{\gamma+1}{\gamma} p_o^{1/\gamma} \qquad (5\text{—}18)$$

Letting $F'(p_o) = 0$ and $p_o = p_{os}$, solve Eq. 5—18

$$p_{os} = p_a \left(\frac{2}{\gamma+1}\right)^{\gamma/(\gamma-1)} \qquad (5—19)$$

This value is the limit of p_o for, when substituted in the denominator of Eq. 5—17, x_n becomes infinite and therefore meaningless. For a rational beginning of the iterative computation to solve for the correct value of p_o, choose its initial value to be

$$p_{o1} = \frac{p_o}{3} \qquad (5—20)$$

Table 5—4 lists the symbols used in the text with their FORTRAN coded counterparts in the computer program*. They are arranged in order from Eqs. 5—9 to 5—20.

Some of the input data are natural constants such as atmospheric pressure p_a = 14.7 psi and gravitational acceleration g = 32.2 ft/sec^2. The inside diameter of the bar suppressor at the origin of the slot equals the O.D. of the tube at the muzzle, and the total slot width equals half the inner circumference of the suppressor. These choices are arbitrary and may be varied to suit the required performance. Three guns are included in the sample calculations: one 90 mm and 2 cal. .50, one with a 20-inch and the other with a 41-inch barrel. For the 90 mm gun (with outer diameter of 5.6 in.)

$$A_o = \frac{\pi}{4} D_o^2 = \frac{\pi}{4}(5.6)^2 = 24.63 \text{ in.}^2$$

$$w_s = \frac{\pi}{2} D_o = \frac{\pi}{2}(5.6) = 8.8 \text{ in.}$$

TABLE 5—4. SYMBOL-CODE CORRELATION FOR FLASH SUPPRESSOR COMPUTATIONS

Symbol	Code	Symbol	Code
T_s	TS	L_b	LB
T_f	TF	y	Y
v_o	VM	y_o	YO
g	G	p_a	PA
F	PSI	w_s	WS
w_c	WC	A_e	AE
W_p	WP	$f(\gamma)$	GF
γ	GAMMA	D_e	DE
p_s	PS	L_c	LC
V_t	VT	θ	THETA
A_o	AO	$F(x_{n-1})$	FXN
A_b	AB	$F'(x_{n-1})$	FPRXN
p_o	PO	p_{os}	POA

*Appendix A—4 is the flow chart and Appendix A—5 is the source program listing.

For the cal. .50 guns (with outer diameter of 0.875 in.)

$$A_o = \frac{\pi}{4} D_o^2 = \frac{\pi}{4} 0.875^2 = 0.601 \text{ in.}^2$$

$$w_e = \frac{\pi}{2} D_o = \frac{\pi}{2} 0.875 = 1.37 \text{ in.}$$

The remaining input data are listed in Table 5–5.

TABLE 5–5. INPUT DATA FOR FLASH SUPPRESSOR

Gun	90 mm	Cal. .50, 20-in. barrel	Cal. .50, 41-in. barrel
A_b, in.^{2}	9.8423	0.1964	0.1964
T_f, °K	3,017	3,105	3,105
v_o, ft/sec	3,000	2,600	3,252
V_t, in.^{3}	1,842	5.184	9.5
W_c, lb	8.24	0.0322	0.0322
W_p, lb	241	0.0932	0.0932
γ	1.24	1.23	1.23
F, ft-lb/lb	1,517,000	1,510,000	1,510,000

TABLE 5–6. BAR AND CONE TYPE FLASH SUPPRESSOR DATA

TYPE GUN	STAGNATION PRESSURE (PSIA)	PRESSURE AT ORIGIN (PSIA)	BAR LENGTH (IN.)	CONE EXIT DIAMETER (IN.)	CONE LENGTH (IN.)
90MM GUN	15,130.0	13,348.2	61.8	28.28	80.20
CAL.50 20-IN BBL	21,541.3	19,240.5	10.7	4.66	13.22
CAL 50 41-IN BBL	10,416.4	9,229.1	8.7	3.52	9.97

CHAPTER 6

SMOKE SUPPRESSORS OR ELIMINATORS

6—1 SUPPRESSOR COMPONENTS

A mechanical eliminator or smoke suppressor has been developed to filter muzzle gases by the impingement process [17] The operational characteristics of this process are discussed in par. 1—3.4. The suppressor has three major components: the diverter, the filter chamber, and the filter medium. Fig. 6—1 is a cross-sectional view of the device. The diverter is a cylindrical structure with perforated walls that attaches to and extends beyond the gun muzzle. The perforations permit the radially expanding propellant gas to pass into the filter chamber and later to return to the projectile passageway. A larger cylindrical structure attached to both ends of the diverter forms the filter chamber. Neither outer wall nor end attachments are perforated. A porous medium fills the chamber to absorb the smoke. Present practice strives to eliminate smoke from 80 percent of the muzzle gas.

6—1.1 DIVERTER DESIGN PROCEDURE

Definite design parameters or data have not been established for smoke suppressors, either for the complete assembly or for any of the individual components. Whatever information is available is empirical and still somewhat nebulous. Design data of two types of diverter are included, the even flow type and the evenly spaced port type. Both follow similar design procedures. Dimensions are usually based on those of predecessors. The diverter of an experimental suppressor for a 40 mm gun has perforations extending over a 12-inch length, or approximately 7.5 times the bore diameter. On the other hand, a cal. .30 suppressor is 5.0 inches long, or almost 17 times the bore diameter. The required length-bore ratio appears to be somewhat arbitrary and at this stage may be assumed to be a length that is most appropriate to provide the required port area from both functional and structural view-

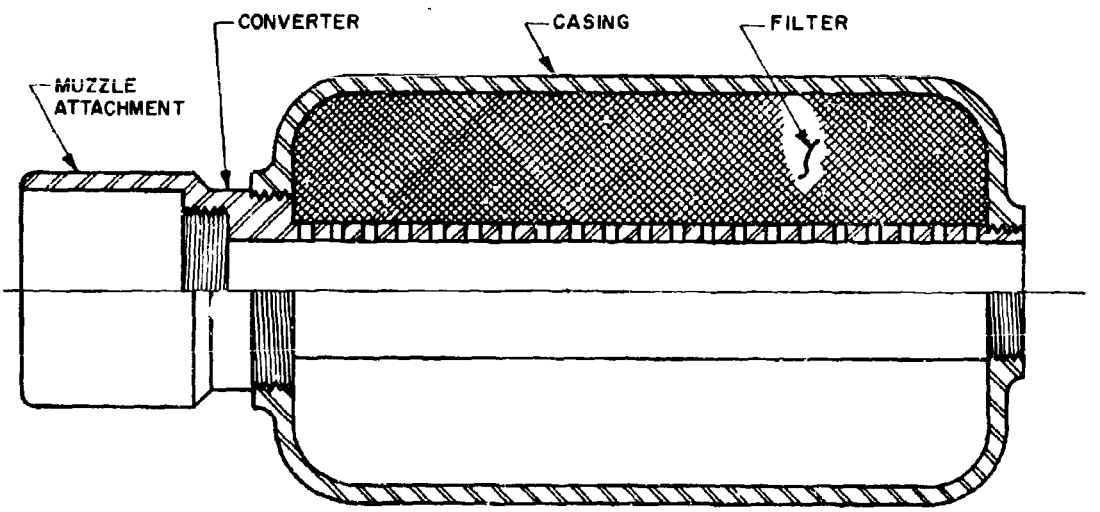

FIGURE 6-1. SMOKE SUPPRESSOR SHOWING MAJOR COMPONENTS

points. The inside diameter of the projectile passageway (diverter bore diameter) is about 10% larger than the gun bore diameter. After computing this value, the dimension is rounded to the nearest convenient fraction. For example, the diverter bore diameter

$$D_b \approx 1.1D \qquad (6—1)$$

where D = gun bore diameter

An experimental suppressor for a cal. .30 gun

$D_b = 1.1 \times 0.30 = 0.33$ in.

This dimension was rounded to $D_b = 0.375$ in.

For the 40 mm diverter

$D_b = 1.1 \times 1.575 = 1.733$ in.

The actual diameter $D_b = 1.75$ in.

The wall thickness of the diverter was based on a design pressure of 7000 psi but strain gage measurements indicated stresses that were not always compatible with the computed stresses. Discrepancies varied widely enough to indicate that not only were design pressures questionable but that pressures seemed to vary considerably along the axis. However, the amount of test data was limited. Also too few areas were investigated to determine where and how theory was found wanting, and what were the actual quantitative properties of the gas.

The designer is on firmer ground when he determines the distribution of the port area in the diverter wall. An even flow diverter has the port area so arranged along its length that the same quantity of gas flows into the filter chamber for each equal distance along the diverter. The desired port area, increased from the muzzle, at any distance along the diverter is computed as

$$A_p = \frac{\rho A_b}{1-\rho} \qquad (6—2)$$

where A_b = area of projectile passageway.

$$\rho = \frac{A_p}{A_b + A_p} \qquad (6—3)$$

where $A_b + A_p$ = open area

The ratio ρ is read from the curve in Fig. 6—2[17] This curve is based on firing test data from a cal. .30 gun and shows the relation between the quantity of gas diverted and the port area. By selecting any position along the diverter in terms of the percentage of total diverter length (ordinate), the open area may be found on the abscissa in terms of a fractional part of the open area. Although Fig. 6—2 indicates that 100 percent of the propellant gas can pass through this smoke suppressor, Eq. 6—2 proves this condition attainable only for an infinite port area. Hence, some ratio less than 1.0 becomes a practical limit. Present practice has this limit at 0.80.

The total port area can be determined from Fig. 6—2 and Eq. 6—2. For 80 percent of propellant gas received by the smoke suppressor the required open area corresponds to 0.9 of the total open area. Substituting this value of ρ in Eq. 6—2, the total port area is

$$A_{pt} = 9A_b \qquad (6—4)$$

The port area is distributed along the diverter by small holes spaced axially at equal increments. The length of the increments is generally about twice the hole diameter. Based on the 40 mm experimental suppressor[17], the cylindrical surface of the diverter is approximately 3 times the total port area. With $A(cyl) \approx 3\ A_{pt} \approx 27\ A_b$, the substitution of $\frac{\pi}{4}D_b^2$ for A_b and $\pi D_b L_d$ for A(cyl) puts the first approximation of the diverter length at

$$L_d \approx 6.75D_b \qquad (6—5)$$

Later this length may change in order to compensate for the limit imposed by the available peripheral area, i.e., the computed port area may be larger than that

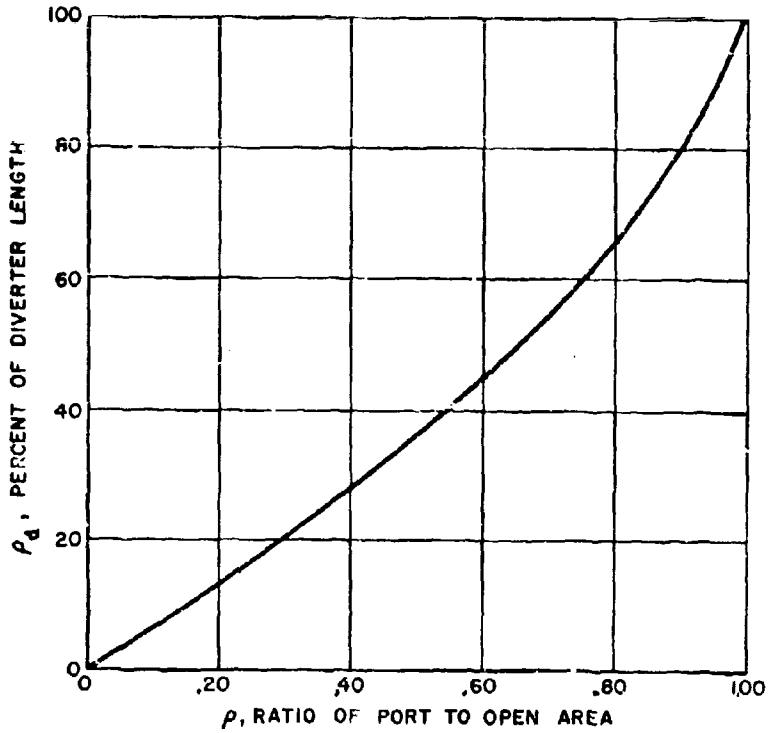

FIGURE 6-2. AREA FUNCTION OF EVEN FLOW DIVERTER FOR A CAL. .30 GUN

available for a particular segment of the diverter. Thus, the structure itself imposes geometric limits on the port area distribution.

6—1.1.1 Example Problem

Determine the size of a smoke suppressor diverter for a 20 mm gun.

According to Eq. 6—1, the inside diameter of the diverter is

$$D_b \approx 1.1D = 1.1 \times 0.787 = 0.866,$$

say 7/8 in.

$$A_b = \pi/4\, D_b^2 = 0.601 \text{ in.}^2$$

From Eq. 6—5, the length of the diverter

$$L_d \approx 6.75 D_b = 6.75 \times 0.875 = 5.9, \text{ say } 6 \text{ in.}$$

The total port area for 80 percent gas intake is, from Eq. 6—4,

$$A_p = 9A_b = 5.409 \text{ in.}^2$$

On the assumption that 1/8-in. holes are drilled in the diverter walls, the maximum number of holes around the periphery at each increment of diverter length

$$N_m = \frac{\pi D_b}{D_h} = \pi(7/8) \Big/ (1/8) = 22 \text{ holes}$$

where D_h = diameter of each hole or perforation. Because these holes would overlap slightly on the inner periphery, the number is reduced to $N_m = 20$. The required number of peripheral groups of holes

$$i = \frac{A_p}{N_m A_h} = \frac{5.409}{20 \times 0.01227} = 22$$

where $A_h = 0.01227$ in.^{2}, the area of a 1/8 diameter hole.

By spacing the peripheral groups at 1/4-inch increments, the length of 6 inches provides space for 24 groups ($i=24$) which should be adequate. Table 6—1 lists the given and computed data of the required port area at each increment which represents 0.80/24 of propellant gas intake.

To illustrate the computed results listed in Table 6—1, the seventh increment ($i=7$) is selected for the purpose. The percentage of propellant gas entering the filter chamber is equivalent to the ratio of the perforation position to the diverter length which can be expressed in terms of the increment of travel. Since the effects are cumulative the desired ratio of propellant gas entering the chamber at increment $i = 7$ to the 80 percent that eventually enters the chamber is

$$\rho_d = \frac{7}{24}\ (0.80) = 0.233 \text{ or } 23.3\%$$

This ratio may be considered to be the theoretical design ratio.

The corresponding initial port area ratio from the chart in Fig. 6—2, $\rho = 0.348$.

Insert this value in Eq. 6—2 and solve for the initial port area.

$$A_{pd} = \frac{\rho A_b}{1-\rho} = \frac{0.348 \times 0.601}{1-0.348} = 0.3208 \text{ in.}^2$$

The total number of perforations including those at 7 is

$$\Sigma N_7 = \frac{A_{pd}}{A_h} = \frac{0.3208}{0.01227} = 26.1, \text{ say } 26$$

The number at 7, $N_7 = \Sigma N_7 - \Sigma N_6 = 26 - 21 = 5$

The actual port area at 7

$$A_p = \Sigma N_7 A_h = 26 \times 0.01227 = 0.3190 \text{ in.}^2$$

The total open area

$$A_t = A_p + A_b = 0.3190 + 0.6010 = 0.920 \text{ in.}^2$$

The actual ratio of port area to open area is

$$\rho_a = \frac{A_p}{A_t} = \frac{0.319}{0.920} = 0.347$$

and the corresponding percent of gas entering the filter in the first 1.75 in. of diverter length is read from Fig. 6—2.

$$\rho_g = 23\ 5 \text{ (read on } \rho_d \text{ axis)}$$

Note that ρ_g equals or nearly equals ρ_d. The difference is caused by the fixed diameter of the perforations which cannot be converted into a whole number and still furnish the precise port area. Generally, ρ_g shows the amount of gas escaping the diverter is evenly distributed through increment 18 ($4\frac{1}{2}$ inches). After this, only 20 holes can be drilled around the periphery, and since more are needed for even flow, the actual flow begins to decrease over this last part of the diverter. If the original length of 6 inches is maintained, only 72.2% of the propellant gas will enter the filter chamber. If 80% is still desired, a 2-inch length must be added to the diverter to provide the 441 holes needed to reach the 80% capacity.

The last portion of the diverter length represents a rapid rate of diminishing returns. Whether the additional unfiltered smoke can be tolerated is a matter of trial and observation. In terms of total propellant gas, the increase amounts to only 8% which seems low enough. But in terms of the 20% unfiltered smoke, the increase becomes 40%, which is considerably more significant. More holes at the beginning would absorb the 8% although the increased flow at this location may prove undesirable. Any of these approaches, or any others that seem feasible, may be used. However, only experiments will determine the logical choice.

6—1.1.2 Diverter With Uniformly Distributed Port Area

Except for the distribution of the holes in the diverter walls, the design procedures

TABLE 6-1. COMPUTED PORT AREA AT REGULAR INTERVALS

i	ρ_d	ρ	A_{pd}	ΣN	A_p	A_t	ρ_a	ρ_g
1	0.033	0.050	0.0321	3	0.0368	0.6378	0.058	0.038
2	0.067	0.100	0.0644	6	0.0736	0.6746	0.096	0.064
3	0.100	0.155	0.1035	9	0.1104	0.7114	0.155	0.100
4	0.133	0.205	0.1550	13	0.1595	0.7605	0.210	0.138
5	0.167	0.252	0.2025	17	0.2086	0.8096	0.258	0.170
6	0.200	0.300	0.2576	21	0.2577	0.8587	0.300	0.200
7	0.233	0.348	0.3208	26	0.3190	0.9200	0.347	0.235
8	0.267	0.390	0.3842	32	0.3926	0.9936	0.395	0.270
9	0.300	0.435	0.4627	38	0.4663	1.0673	0.437	0.300
10	0.333	0.475	0.5436	44	0.5399	1.1409	0.473	0.333
11	0.367	0.515	0.6382	52	0.6380	1.2390	0.515	0.367
12	0.400	0.550	0.7346	60	0.7362	1.3372	0.551	0.400
13	0.433	0.585	0.8472	69	0.8466	1.4476	0.583	0.433
14	0.467	0.622	0.9889	81	0.9939	1.5949	0.623	0.467
15	0.500	0.655	1.1410	93	1.1411	1.7421	0.655	0.500
16	0.533	0.690	1.3377	109	1.3374	1.9384	0.690	0.533
17	0.567	0.720	1.5454	126	1.5460	2.1470	0.720	0.567
18	0.600	0.750	1.8030	147	1.8037	2.4047	0.750	0.600
19	0.633	0.780	2.1308	169	2.0736	2.6746	0.775	0.630
20	0.667	0.805	2.4610	191	2.3436	2.9446	0.796	0.652
21	0.700	0.833	2.9978	213	2.6135	3.2145	0.813	0.673
22	0.733	0.860	3.6918	235	2.8835	3.4845	0.828	0.690
23	0.767	0.880	4.4073	257	3.1534	3.7544	0.840	0.706
24	0.800	0.900	5.4090	279	3.4233	4.0243	0.851	0.722

for the evenly distributed perforation type are the same as for those of the even flow type. The evenly distributed perforation type permits more gases to enter the filter chamber near the muzzle than at positions farther away. Computations based on the same general data as those for the even flow diverter will demonstrate the difference in performance for the two types. Thus,

A_b = 0.601 $in.^2$, area of projectile passageway

A_h = 0.01227 $in.^2$, area of each perforation

D_b = 7/8 in., diameter of projectile passageway

D_h = 1/8 in., diameter of each perforation

i_t = 24, total number of peripheral groups of perforations

L_d = 6 in., length of diverter

N_m = 20, number of perforations on periphery at each increment

$A_p = i\, N_m\, A_h \approx 20 \times 0.01227\, i = 0.2454\, i$, $in.^2$, cumulated port area at any given increment.

The solutions for ρ from Eq. 6—3 gives the ratio of the quantity of gas diverted to the total quantity of gas.

$$\rho = \frac{A_p}{A_b + A_p}$$

TABLE 6-2. DIVERTED GAS RATIOS FOR UNIFORMLY DISTRIBUTED PORT AREA

i	A_p	$A_b + A_p$	ρ	i	A_p	$A_b + A_p$	ρ
1	.2454	.8464	.290	13	3.1902	3.7912	.842
2	.4908	1.0918	.450	14	3.4356	4.0366	.851
3	.7362	1.3372	.551	15	3.6810	4.2820	.860
4	.9816	1.5826	.620	16	3.9264	4.5274	.867
5	1.2270	1.8280	.671	17	4.1718	4.7728	.874
6	1.4724	2.0734	.710	18	4.4172	5.0182	.880
7	1.7178	2.3188	.741	19	4.6626	5.2636	.886
8	1.9632	2.5642	.766	20	4.9080	5.5090	.891
9	2.2086	2.8096	.787	21	5.1534	5.7544	.896
10	2.4540	3.0550	.803	22	5.3988	5.9998	.900
11	2.6994	3.3004	.818	23	5.6442	6.2452	.904
12	2.9448	3.5458	.830	24	5.8896	6.4906	.907

6—1.2 CASING DESIGN

The casing is the outer cover of the smoke suppressor. Its length is determined by the length of the diverter whereas its inside diameter is determined by the size of the filter packing. Pressures are generally low, subsequently, the casing wall will be relatively thin. Unless the radius-to-wall-thickness ratio is less than 10, the method for computing hoop stresses in a thin-walled cylinder will apply. If less than 10, Lame's Equation for hoop stress will be adequate. For the experimental models, this stress was computed for a pressure of 1,500 psi although the actual pressure for the 40 mm Automatic Gun M1 used in the test was not measured. Strain gage data showed stresses well below the critical.

6—1.3 FILTER PACKING MATERIAL

The optimum form of filter media has not been found because of the need for further investigation but the assumption persists that the efficiency of particle removal is a function of surface area and asymmetry of the matrix. There must be sufficient surface area to remove all of the smoke that enters the chamber. The material that provides the area must also resist the erosion of the high velocity hot propellant gas. Tests have shown that some stainless steels and other high-temperature alloys show promise. Three types of filter packing were tested in a 40 mm model. Table 6—3 lists the data.

A total of 38 rounds was fired for the steel shavings filter. The No. 6 shavings are equivalent to the coarsest commercial steel wool available. This filter material maintained its shape but some erosion occurred in the first few inches in the rear. Some erosion also occurred at the perforations near the rear. Although structurally acceptable, the steel shavings are inferior material with respect to erosion.

A total of 34 rounds was fired for the 1.75-in. thick stainless steel mesh and 27 rounds were fired for the thinner variety that had a 1-inch gap between it and the casing. Both showed good filtration properties and survived the erosion test. The thick-walled filter was compressed forward to almost half its length. The thin-walled filter maintained its outside diameter despite the lack of radial support and decreased in length by only one inch. From the point of view of erosion and filtering ability, the stainless steel wire mesh shows much promise as a filtering material. Further investigation is needed to improve on structural strength, and to determine the optimum size and structure of the mesh.

TABLE 6-3. FILTER PACKING DATA

Material	Radial Thickness, in.	Weight, lb	Density, lb/ft^3	Specific Surface, ft^2/lb	Total Surface, ft^2
Steel Shavings No. 6 Mild Carbon	1.75	10.0	71.5	7.3	73.0
Wire Mesh 304 Stainless	1.75	6.0	40.0	21.0	126.0
Wire Mesh 304 Stainless	0.75	2.5	40.0	21.0	52.5

CHAPTER 7

BORE EVACUATORS

7—1 GENERAL DESIGN PARAMETERS

A design procedure is available to compute various parameters of a bore evacuator from available data[18]. However, these parameters, although basically correct, must be considered as preliminary inasmuch as several other factors may later exert their influence on the design. Some of these factors are newly acquired performance data, limiting geometric proportions, and available material. Meanwhile the theoretical approach establishes the general concept of the designs by following a well-defined format.

Given V_t the total gun volume which is bore volume plus chamber volume, p_o the muzzle pressure at shot ejection, A the bore area, and W_c the weight of the propellant charge; the time can be computed for the pressure to drop to 0.06% or $6\times10^{-4}\,p_o$ on the assumption that all gases are immediately discharged from the muzzle into a vacuum. This time interval is

$$\theta = \frac{2}{Ak(\gamma-1)}\sqrt{\frac{W_c V_t}{g p_o}} \qquad (7—1)$$

where g = acceleration of gravity

$$k = \sqrt{\gamma}\left(\frac{2}{\gamma+1}\right)^{(\gamma+1)/2(\gamma-1)} \qquad (7—2)$$

γ = ratio of specific heats

Breech opening normally should be delayed until the bore pressure has subsided to atmospheric levels in order to preclude copious gas discharge rearward. The minimum breech opening time is the time of this delay.

$$\theta_m = \theta\left[R_p^{\left(\frac{1-\gamma}{2\gamma}\right)} - 1\right] \qquad (7—3)$$

where $R_p = \frac{p_a}{p_o}$, the ratio of ambient to muzzle pressure at shot ejection.

Another parameter needed for computing design data is the equivalent length

$$L_e = \frac{V_t}{A} \qquad (7—4)$$

All the above computed values are independent of reservoir location and geometry but are needed to compute some of the actual design details. Other design parameters are dependent on data, empirical in nature, that are based on the performance of earlier designs. Nozzle location, angle of inclination, and the velocity of head wind are so designated. The nozzles should be far enough to the rear of the muzzle to insure that both the charging and discharging functions of the evacuator perform efficiently, i.e., allow sufficient time for the reservoir to be filled to capacity and then for jet action to purge the tube of propellant gases. Mechanical limitations may disturb the ideal location, however, a strong attempt should be made to limit the nozzle location distance L_n to the muzzle to

$$0.1L_e \leq L_n \leq 0.2L \qquad (7—5)$$

The best results are achieved with those nozzles that are inclined at very small angles with respect to the bore axis. But, nozzles inclined less than 30° offer fabrication difficulites, thus a nozzle angle of ϕ = 30° is recommended and becomes the lower limit.

The presence of headwinds at the muzzle is deleterious to the performance of an evacuator. Some compensatory measures must be taken to neutralize the strongest anticipated wind. A wind velocity of v_w = 75 ft/sec is generally accepted as practical. A ratio of dynamic pressure to static pressure may be expressed as

$$W_w = \frac{\rho_a v_w^2}{2p_n} \qquad (7-6)$$

where $\rho_a = \frac{\delta}{g}$, the mass density of air

δ = density of air

7—2 FIXED NOZZLE DESIGN PARAMETERS

Since fixed nozzles have the same flow area in either direction, no distinction need be made between charge and discharge parameters. The ratio of nozzle area to bore area may be expressed in terms of W_w, γ, and ϕ such that

$$\omega = \frac{W_w}{(\gamma+1)\cos\phi} \qquad (7-7)$$

The required total nozzle area

$$A_n = \omega A \qquad (7-8)$$

The value of ω is solely dependent on the assigned head wind velocity which varies to fit prevailing climatic conditions.

The computed value of ω is necessary for computing the reservoir volume. The ratio of reservoir volume to gun volume is identified as

$$\lambda = \frac{V_r}{V_t} \qquad (7-9)$$

where V_r is the reservoir volume.

Nozzle area is associated with reservoir area through the ratio ω/λ. For the evacuator to operate over a period of time that is a theoretical maximum

$$\omega/\gamma = \frac{2.5\,R_p}{\chi^{1.46}} \qquad (7-10)$$

where χ is the heat transfer factor. To introduce a measure of assurance to the computed design data, the ratio of Eq. 7—10 is arbitrarily doubled so that the ratio used for design purposes

$$(\omega/\gamma)_d = 2(\omega/\gamma) = \frac{5R_p}{\chi^{1.46}} \qquad (7-11)$$

Later ω_d and λ_d are introduced as the practical design equivalents of the theoretical ratios of nozzle area to bore area and reservoir volume to bore volume, respectively.

Present practice has $\chi = 0.5$, therefore

$$\omega/\gamma = \frac{2.5\,R_p}{0.364} = 6.87\,R_p \qquad (7-12)$$

Nozzles may be fixed or check valve types. The fixed type, Fig. 7—1(A), has no moving parts and usually is merely a hole drilled through the tube wall. The check valve type, Fig. 7—1(B), has a moving part that regulates the flow; a relatively large opening while the evacuator is being charged, a smaller opening during discharge. Valves that close completely after charging are also used. This type relies on other nozzles that remain partially or totally open for discharging purposes. Required jet duration time usually dictates the type nozzle. If charging and discharging activities are compatible for the same nozzle area, then a fixed nozzle becomes the logical choice. It is simple, has no moving parts and is therefore more reliable, and costs less. If charging and discharging are not compatible for the same nozzle area, then check valves or a combination of check valves and fixed nozzles are indicated.

The maximum theoretical operating pressure in the reservoir is based on a 50% heat loss, i.e., $\chi = 0.5$, and is computed from the equation

$$P_r = P_o\,\chi(\omega/\gamma)_d = \frac{1}{2}\,P_o\,(\omega/\gamma)_d \qquad (7-13)$$

The operating pressure should always be at least 80 psi. This pressure is reasonable when compared to firing test results with the XP-3 Evacuator. In these tests, a p_r of 70 psi for Zone 5 resulted in marginal evacuation.

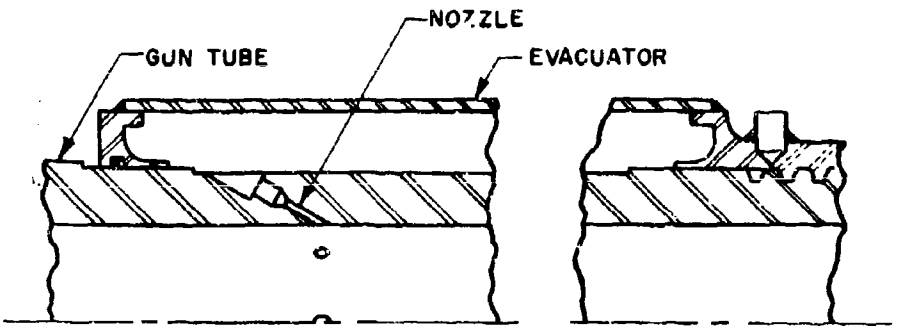

(A) Fixed Nozzle Type

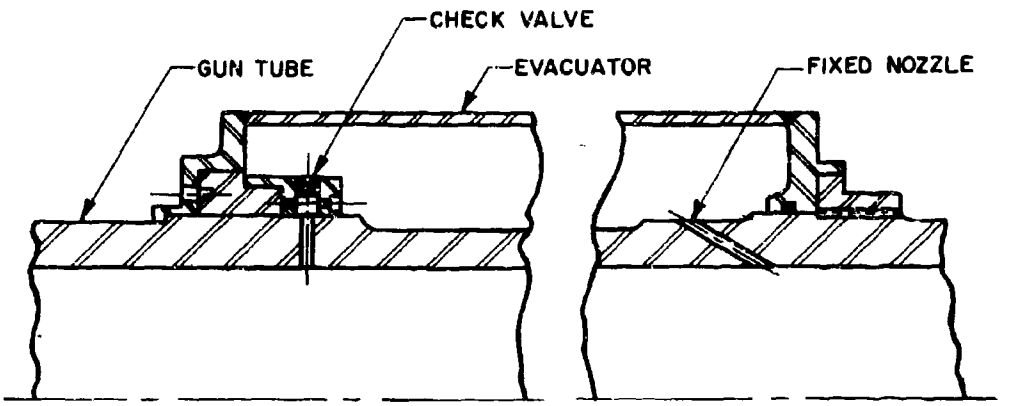

(B) Check Valve Type

FIGURE 7-1. BORE EVACUATORS SHOWING NOZZLES

Test data on the XP-3 ball-type experimental bore evacuator agree closely with the theoretical pressure p_r, i.e.:

Zone	Computed p_r, psi	Actual p_r, psi	No. of Tests
5	65	70	3
7	294	293	18

On the other hand, test pressure on the M126E1 Evacuator did not compare as favorably with the computed pressures, i.e.:

Zone	Computed p_r, psi	Actual p_r, psi	Modified p_r, psi
7	352	200	176
8	560	300	280

A possible explanation of this discrepancy may be that $\phi = 30°$, the inclination of the charging nozzles toward the muzzle. If the computed pressure were modified by multiplying the expression for pressure in Eq. 7—13 by $\sin \phi$, the new value would

approach the actual value more closely. A word of caution should be interjected here to emphasize that practice does not always precisely follow theory. According to the data below, the actual pressures obtained in the firing tests were for evacuators that differed to some extent from computed design parameters.

Evacuator	M126E1		XP-3	
Parameter	Computed	Actual	Computed	Actual
Nozzle Location, in.	14-19	22	24-48	53
Nozzle area, in.^{2}	0.0468	0.188	0.0468	0.0689
Evac. Volume in.^{3}	845	1,100	760	1,980

The XP-3 Evacuator is still in the experimental stage but the M126E1 Evacuator is standard equipment for its assigned weapon. The discharge area of the latter is 4 times larger and its volume 23 percent larger than their theoretical counterparts. Since the standard evacuator performs adequately, indications are that the theoretical design approach should be modified to conform more closely to the practical approach and that more development work is needed to modify the theory. Until this criterion is realized, the designer can use the present theory as a guide and rely on experience and experiments to design an acceptable bore evacuator. The wall of the reservoir must be strong enough to sustain the pressure if gases were accumulated with no heat loss, thus, $\chi = 1.0$ and the design pressure becomes

$$p_d = 2p_r \qquad (7—14)$$

One of the most critical parameters involving the design of bore evacuators is that of jet duration time T_j which is the time required to discharge the gas from the reservoir. The discharge time must exceed the breech opening time by a margin great enough to give the induced air flow adequate time to purge the tube effectively. As a precautionary measure, the jet duration time is increased 25 percent above the breech opening time. Intricate and tedious computations are avoided by obtaining the jet duration factor $\Delta\tau$ that corresponds with $(\omega/\lambda)/R_p$ on the appropriate curve of Fig. 7—2 if $(\omega/\lambda)/R_p$ is assigned the readily computable value of $(\omega/\lambda)_d/R_p$. The jet duration time can now be computed after θ is found from Eq. 7—1.

$$T_j = \frac{\Delta\tau\,\theta}{R_p} \qquad (7—15)$$

If a departure from the theoretical minimum nozzle size appears advisable, new values of the various parameters must be computed. The ratio of nozzle area to bore area becomes

$$\omega_d = \frac{n\pi D_n^2}{4A} \qquad (7—16)$$

where D_n = nozzle diameter

n = number of nozzles

$$\lambda_d = \frac{\omega_d}{(\omega/\lambda)_d} \qquad (7—17)$$

The reservoir volume is

$$V_r = \lambda_d V_t \qquad (7—18)$$

Reservoir volumes should be kept reasonably small; therefore, nozzles should be kept reasonably small since reservoir volume varies directly with nozzle area.

7—3 CHECK VALVE DESIGN PARAMETERS

If conditions are such that the breech opening time exceeds the initial fixed nozzle jet duration time, a check valve type nozzle must be used. A longer discharge time can be had by using a smaller discharge nozzle or by retaining the discharge nozzle and using a larger charging nozzle

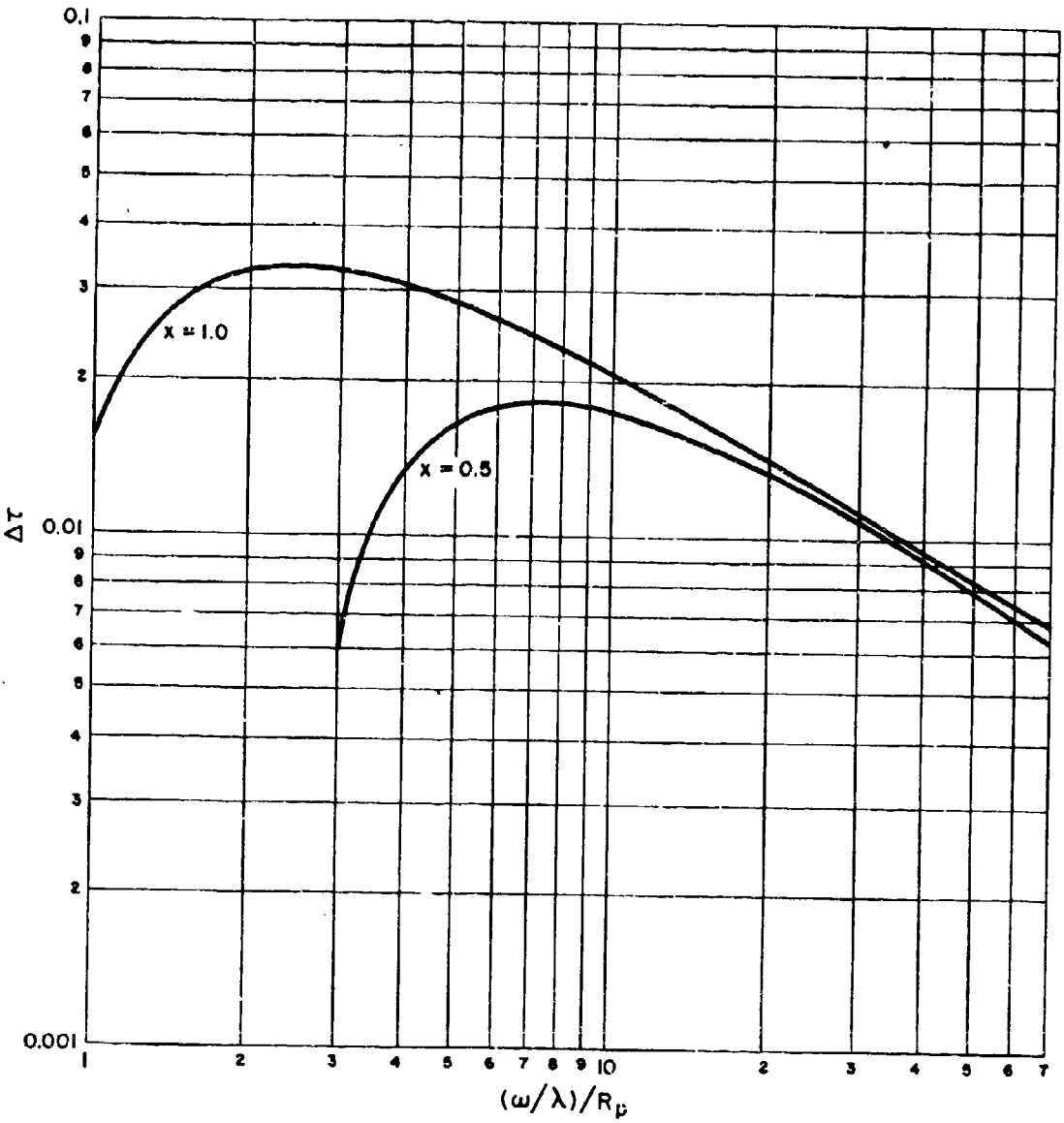

FIGURE 7-2. JET DURATION FACTORS

which leads to a larger reservoir. Since smaller discharge nozzles cannot compensate for anticipated strong headwinds, the logical choice is the larger charging nozzle with correspondingly larger reservoir. This approach is aided by the expression

$$\frac{\omega_c}{\omega_{dc}} = \frac{T_{jc}}{T_j} \qquad (7\text{—}19)$$

where T_j = jet duration time of a fixed nozzle

T_{jc} = jet duration time of a check valve nozzle

ω_c = ratio of charging nozzle area to bore area

ω_{dc} = ratio of discharging nozzle area to bore area

The minimum values of ω_{dc} and ω_c/λ are equated to their counterparts in fixed nozzle design

$$\omega_{dc} = \omega \qquad (7\text{—}20)$$

$$\omega_c/\lambda = (\omega/\lambda)_d \qquad (7\text{—}21)$$

If the breech opens T_b seconds after shot ejection, the jet duration time is set at

$$T_{jc} = 1.25\, T_b \qquad (7\text{—}22)$$

The ratio of the charging nozzle area to bore area becomes

$$\omega_c = \omega_{dc}\,\frac{T_{jc}}{T_j} \qquad (7\text{—}23)$$

and the ratio of reservoir volume to tube volume

$$\lambda = \frac{\omega_c}{(\omega_c/\lambda)} \qquad (7\text{—}24)$$

The total charging nozzle area and the reservoir volume are computed according to Eqs. 7—8 and 7—18.

The final step of the general design procedure is the efficient distribution of the reservoir volume in order to minimize heat losses. Two variables are known, the volume V_r and the inside radius R_i of the gas cell. This radius is usually that of the outer gun tube surface. By computing the ratio V_r/R_i^3, and obtaining the corresponding ratio of R_o/R_i from Fig. 7—3, both the outer radius of the gas cell R_o and its length L may be computed.

$$R_o = R_i(R_o/R_i) \qquad (7\text{—}25)$$

$$L = \frac{V_r}{\pi(R_o^2 - R_i^2)} \qquad (7\text{—}26)$$

Normally these computed dimensions will yield a bulky structure. However, the provision of a relatively long duration time will compensate for the additional heat losses and accompanying pressure drop that occur when the gas is exposed to the larger cooling surfaces of the slimmer reservoir.

7—4 SAMPLE PROBLEMS

7—4.1 FIXED NOZZLE

Determine the size of reservoir and three fixed nozzles for a gun having the following characteristics:

A = 13.42 in.^{2}, bore area

p_o = 12,000 psi, muzzle pressure

V_t = 3858 in.^{3}, total gun volume

v_o = 3500 ft/sec, muzzle velocity

W_c = 17.3 lb, weight of propellant charge

γ = 1.23 ratio of specific heats of propellant gas

$$k=\sqrt{\gamma}\left(\frac{2}{\gamma+1}\right)^{(\gamma+1)/2(\gamma-1)}=\sqrt{1.23}\left(\frac{2}{2.23}\right)^{2.23/0.46}=0.65$$

From Eq. 7—1

$$\theta=\frac{2}{Ak(\gamma-1)}\sqrt{\frac{W_c V_t}{gp_o}}=\frac{2}{13.42\times0.65\times0.23}\sqrt{\frac{17.3\times3858}{386.4\times12000}}=0.1183\text{ sec}$$

From Eq. 7—3, the minimum breech opening time

$$\theta_m=\theta\left(R_p\frac{1-\gamma}{2\gamma}-1\right)=\theta\left[\left(\frac{1000}{1.225}\right)^{0.0935}-1\right]=0.1183\times0.878=0.104\text{ sec}$$

where

$$R_p=\frac{p_a}{p_o}=\frac{14.7}{12000}=0.001225$$

The equivalent length of the gun tube (Eq. 7—4)

$$L_e=\frac{V_t}{A}=\frac{3858}{13.42}=287\text{ in.}$$

According to Eq. 7—6, the ratio of dynamic pressure to static pressure

$$W_w = \frac{\rho_a v_w^2}{2p_a} = \frac{0.00236 \times (75)^2}{2 \times 14.7 \times 144} = 0.00312$$

where v_w = 75 ft, sec, velocity of head wind

$$\rho_a = \frac{\delta}{g} = \frac{0.076}{32.2} = 0.00236 \ \frac{lb}{ft^3} \cdot \frac{sec^2}{ft},$$

mass density of air

The ratio of nozzle area to bore area (Eq. 7—7)

$$\omega = \frac{W_w}{(\gamma+1)\cos\phi} = \frac{0.00312}{2.23 \times 0.866} = 0.00161$$

where ϕ = 30°, the inclination angle between nozzle and bore. The total nozzle area required (Eq. 7—8)

$$A_n = \omega A = 0.00161 \times 13.42 = 0.02165 \text{ in.}^2$$

The diameter of each of 3 nozzles

$$D_n = \sqrt{\frac{4A_n}{3\pi}} = \sqrt{0.009193} = 0.0959 \text{ in.}$$

From Eqs. 7—12 and 7—11

$$\omega/\lambda = 6.87 \ R_p = 6.87 \times 0.001225 = 0.0084$$

$$\left(\frac{\omega}{\lambda}\right)_d = 2\left(\frac{\omega}{\lambda}\right) = 0.0168$$

The operating and design reservoir pressures are obtained from Eqs. 7—13 and 7—14

$$p_r = \frac{1}{2} p_o \left(\frac{\omega}{\lambda}\right)_d = \frac{1}{2} \times 12000 \times 0.0168 = 100 \text{ psi}$$

$$p_{rd} = 2p_r = 200 \text{ psi}$$

$$(\omega/\lambda)_d/R_p = \frac{0.0168}{0.001225} = 13.7$$

From Fig. 7—2, the jet duration factor $\Delta\tau$ = 0.0157

Eq. 7—15 provides the fixed nozzle jet duration time

$$T_j = \frac{\Delta\tau\theta}{R_p} = \frac{0.0157 \times 0.1183}{0.001225} = 1.52 \text{ sec}$$

This time is adequate provided that the breech opening time is somewhat less, say $\frac{1.52}{1.25}$ = 1.2 sec.

For manufacturing convenience, increase the nozzle diameter to 1/8 in. The total nozzle area

$$A_n = 3 \times \frac{\pi}{4} \times 0.125^2 = 0.0368 \text{ in.}^2$$

$$\omega_d = \frac{A_n}{A} = \frac{0.0368}{13.42} = 0.00274 \text{ (Eq. 7—16)}$$

$$\lambda_d = \frac{\omega_d}{(\omega/\lambda)_d} = \frac{0.00274}{0.0168} = 0.1631 \text{ (Eq. 7—17)}$$

The required reservoir volume (Eq. 7—18)

$$V_r = \lambda_d V_t = 0.1621 \times 3858 = 629 \text{ in.}^3$$

7—4.2 CHECK VALVE

Should the fixed nozzle jet duration time of T_j = 1.52 sec be too short because circumstances dictate that the breech opens at T_b = 2.5 sec after shot ejection, a check valve type charging nozzle is needed. The jet duration time

$$T_{jc} = 1.25 \ T_b = 1.25 \times 2.5 = 3.125 \text{ sec (Eq. 7—22)}$$

According to Eqs. 7—20, 7—21, and 7—22, ω_{dc} = 0.00161, ω_c/λ = 0.0168, and

$$\omega_c = \omega_{dc} \frac{T_{jc}}{T_j} = 0.00161 \ \frac{3.125}{1.52} = 0.00331$$

From Eq. 7—24

$$\lambda = \frac{\omega_c}{(\omega_c/\lambda)} = \frac{0.00331}{0.0168} = 0.197$$

The three nozzles would have a total area of

$$A_n = \omega_c A = 0.00331 \times 13.42 = 0.0445 \text{ in.}^2$$

which is equivalent of a nozzle diameter of $d_c = 0.137$ in.

The reservoir volume (Eq. 7—18)

$$V_r = \lambda V_t = 0.197 \times 3858 = 760 \text{ in.}^3$$

The nozzles would be located, according to Eq. 7—5, between 28.7 and 55.4 inches from the muzzle. Assume a gun tube O.D. of 7 in., then $R_i = 3.5$ in. and

$$\frac{V_r}{R_i^3} = \frac{760}{42.875} = 17.7$$

From Fig. 7—3, $\frac{R_o}{R_i} = 2.15$, and $R_o = 2.15$ $R_i = 7.525$, say 7.5. The length of the gas cell (Eq. 7—26)

$$L = \frac{V_r}{\pi (R_o^2 - R_i^2)} = \frac{760}{(56.25-12.25)\pi} = \frac{760}{138.23}$$

$$= 5.5 \text{ in.}$$

This shape is somewhat of a monstrosity. A cell having a gap of one inch and a corresponding length of 30 inches would be more palatable. However, design layouts are needed to conduct a more thorough study before an acceptable compromise design is realized.

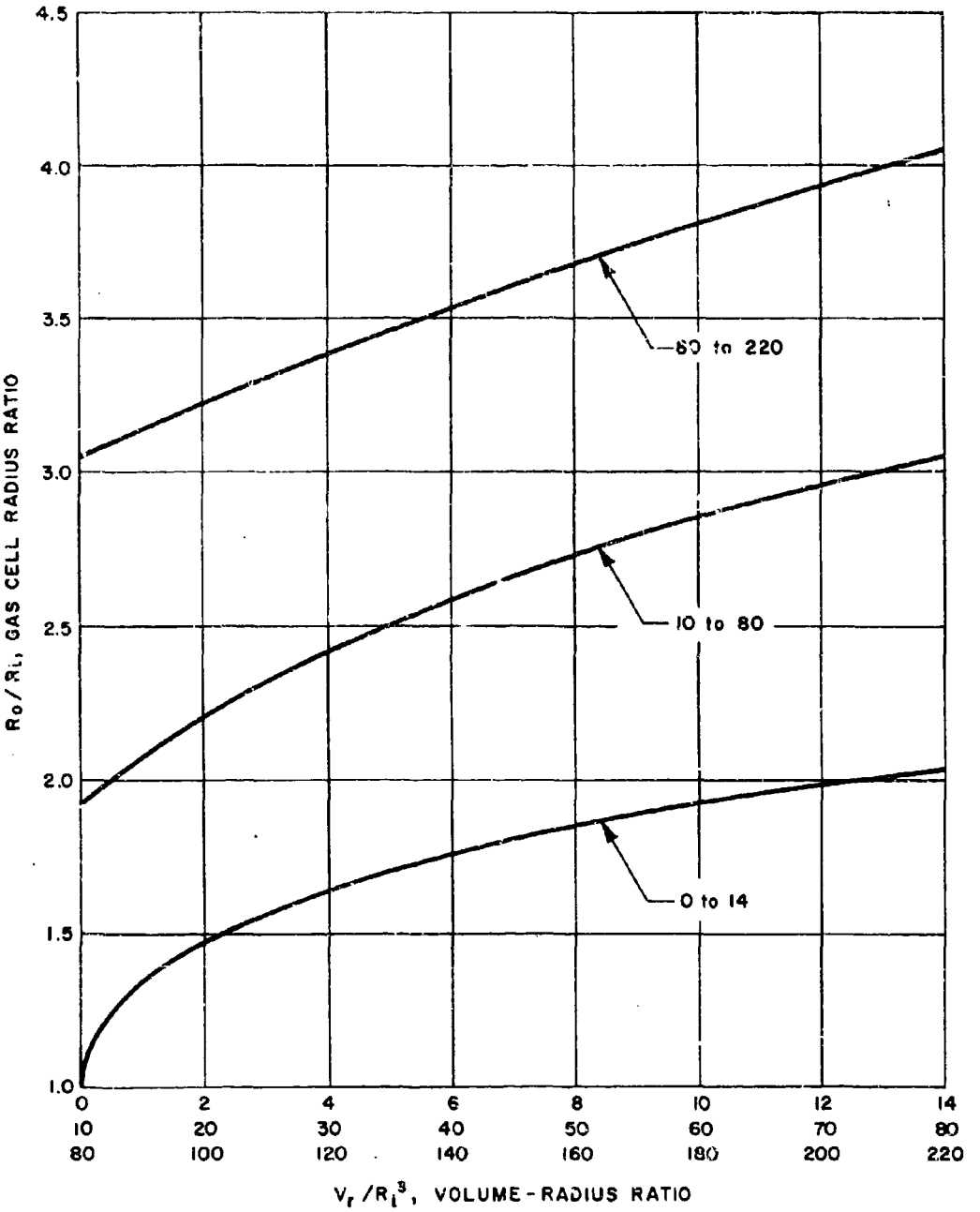

FIGURE 7-3. GAS CELL MINIMUM SURFACE

CHAPTER 8

NOISE SUPPRESSORS

8—1 GENERAL REQUIREMENTS

Noise is an inherent characteristic of a gun and is usually associated with three main producers: the projectile, the muzzle, and the gun components other than the muzzle. The noises produced by the gun components are mostly mechanical such as the sounds of moving parts, impact, and vibration. The projectile noises are mainly those caused by air turbulence following the projectile and the supersonic shock wave or ballistic crack generated by the projectile nose. Muzzle noises are produced by the air pressure build-up in the tube ahead of the projectile and by the propellant gases issuing from the muzzle after the projectile passage.

The most intense noise of a firing gun is caused by the rapidly decaying shock wave that continues to travel at sonic velocity as an impulse wave or sound wave. A crude but effective experiment was conducted by firing a 7.62 mm rifle through a metal container 10 inches long by 8 inches diameter[19]. One end was attached to, and supported by, the muzzle. The other end had a bullet exit hole of 7/16-inch diameter in its center. When the gun was fired, the sound level of the report was drastically reduced. This sound level was not measured but seemed equivalent to that of a cal. .22 rimfire cartridge. The sound reduction may be rationalized by computing the gas pressure in the can. Based on Corner's theory for space mean pressure and the characteristics of NATO 7.62 mm round, adiabatic expansion will yield a computed gas pressure of 31.5 psia for one round. The resulting critical gas pressure ratio of 0.47 indicates the gas exit velocity to be subsonic; therefore, the sound heard is that of the projectile.

Four operations determine the effectiveness of a noise suppressor:

1. It should cool the muzzle gases to the temperature that would quench the burning gases and later prevent reignition.
2. It should mix muzzle gases with air gradually to prevent atmospheric oxygen from supporting combustion.
3. It should decelerate the muzzle gases to prevent shock-front formation.
4. It should retain the gases until they become relatively cool through expansion thus preventing shock-front temperature increases.

Operations 1, 2, and 4 prevent secondary flash and thus the noise associated with it. Operation 3 has inherent noise producing capabilities. To be successful, any one or a combination of the four operations must be incorporated in a suppressor. Cooling will occur if the gas flow is checked long enough at a heat sink for heat to transfer by convection and conduction, or by adiabatic expansion in a changing area flow passage. Gradual mixing can be arranged by progressive venting downstream. Deceleration and retention are to be had by changing the cross-sectional area of the directed flow passage.

8—2 SOUND SUPPRESSOR EXPERIMENTS

No specific procedures or data now exist for designing a sound suppressor for any given gun but work is currently being done in this area. However, experiments have been made to determine the feasibility of such muzzle devices. One type was based on the practice of bleeding off the gases before normal acceleration of the projectile is complete. This method was effective to a large degree, but at the expense of a greatly reduced muzzle velocity that generally cannot be tolerated. Other tests were

performed with two conventional silencer types and two divergent-convergent flow passage types. These four are shown schematically in Fig. 8—1. Type (A) is the conventional baffle type. Type (B) has vents that permit access to a chamber filled with absorbent material, such as glass wool or metal screening. Type (C) has two diverging passageways connected by a converging one, whereas Type (D) adds another converging-diverging section. Types (C) and (D) are effective flash suppressors. These models were tested by firing cal. .45 M1911 ammunition. The sound was measured at 10 meters to the right of the muzzle. The measured intensities are shown below to be compared with the 141 decibels having no suppressor attached.

Suppressor	(A)	(B)	(C)	(D)
Decibels	124	119	136	132

The above data indicate that the divergent-convergent passage does suppress sound but still not as effectively as the baffle or absorbent material type silencers. However, when based on energy levels, Type (D), in attenuating the sound from 141 dB to 132 dB, reduces the energy level by 87 percent. Although there is a paucity of technical information with respect to designing sound suppressors, the known characteristics indicate that this muzzle device is feasible. Many attempts throughout the years have been made to prove this feasibility particularly for hand guns although considerable effort has been devoted to the larger small arms guns. Many patents, both foreign and domestic, attest to this activity. Appendix A-6 is a partial list of these patents.

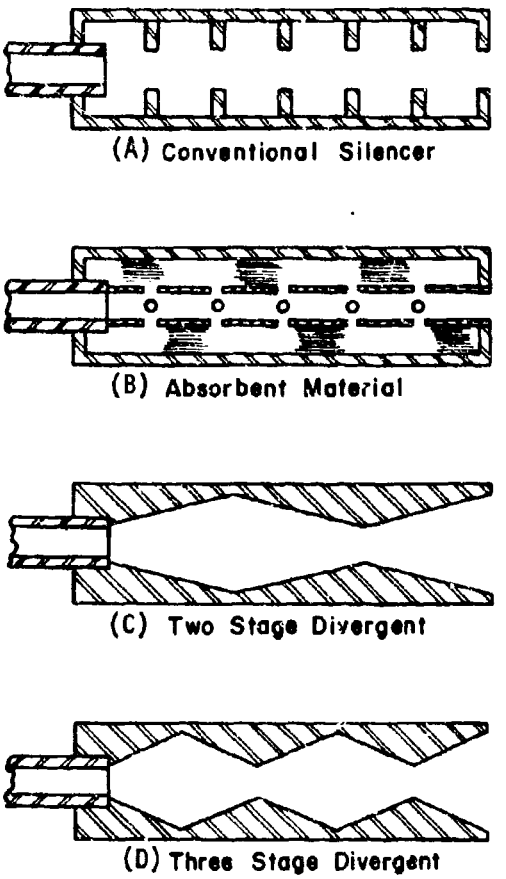

FIGURE 8–1. SOUND SUPPRESSORS (SCHEMATICS)

CHAPTER 9

HUMAN FACTORS*

9—1 INTRODUCTION

The two-fold purpose of the muzzle device is to give added protection to gun and crew from the effects of the muzzle gases and to hinder the enemy in locating the gun emplacement. Muzzle brakes and blast deflectors aid the gun by reducing recoil forces. Flash, noise, and smoke suppressors reduce the probability of being detected by the enemy. These muzzle devices plus the bore evacuator also affect personnel in the immediate vicinity of the gun. The effectiveness of the muzzle devices with respect to physical characteristics can be measured almost precisely but the limits of personnel tolerance to light, dust, and noise -- at and near the muzzle -- cover a large range. The effects of these muzzle phenomena on personnel are being studied, the emphasis being put on noise since it appears to be the most damaging.

9—2 EFFECTS OF BLAST AND OVERPRESSURE

Recent trends in weapon-system development have made these weapons psychologically unpleasant and physiologically dangerous to our own forces. Three major changes are responsible. First, weapons must be as light as possible for air mobility. To decrease weight, tubes are shortened, thereby placing the origin of the impluse noise closer to the gun crew. Corresponding decreases in weight of other components, particularly of the recoiling parts, tend to increase recoil energy and therefore recoil forces unless these increases are compensated for by muzzle brakes. But a muzzle brake deflects the impulse noise back toward the crew. Second, nuclear and other sophisticated ammunition require greater ranges than conventional projectiles. The larger propellant charges needed to reach the increased distances develop higher pressures and cause an increase in noise level. Third, increased firepower increases the number of impulse noise insults to the operator's ears. Thus, increased firepower, increased pressures, and shorter tubes, collectively expose the gun crew to dangerous impulses.

When weapons – such as rifles, mortars, or cannons -- are fired, the spherical shock wave, developed by the propellant gases just beyond the muzzle, continues to move outward, producing an abrupt increase in pressure called a shock wave. As the shock wave continues outward, it begins to lose energy and several changes occur:

1. Velocity decreases
2. Peak pressure decreases
3. "Impulse" decreases
4. Duration increases

When it slows to sonic velocity, the shock wave becomes simply an impulse sound wave. Both are transient in nature and may be damaging to personnel. Amplitude and rate of pressure increase and decay distinguish shock waves from impulse sound waves for physical measurement purposes. The shock wave has greater peak-to-rms ratio than an impulse sound wave, and requires a shorter time interval to reach its maximum pressure and then to decay. Because personnel are generally located in areas where pressure waves are of lower intensity and of longer duration than in the proximity of the muzzle – and may include both shock waves and impulse sound waves – all transient pressure waves will be referred to as impulse noises. Also, the maximum pressure reached will be referred to as the peak pressure level. Fig. 9—1 represents a typical impulse noise created by small arms.

*Most of Chapter 9 is based on the contents of Ref. 20.

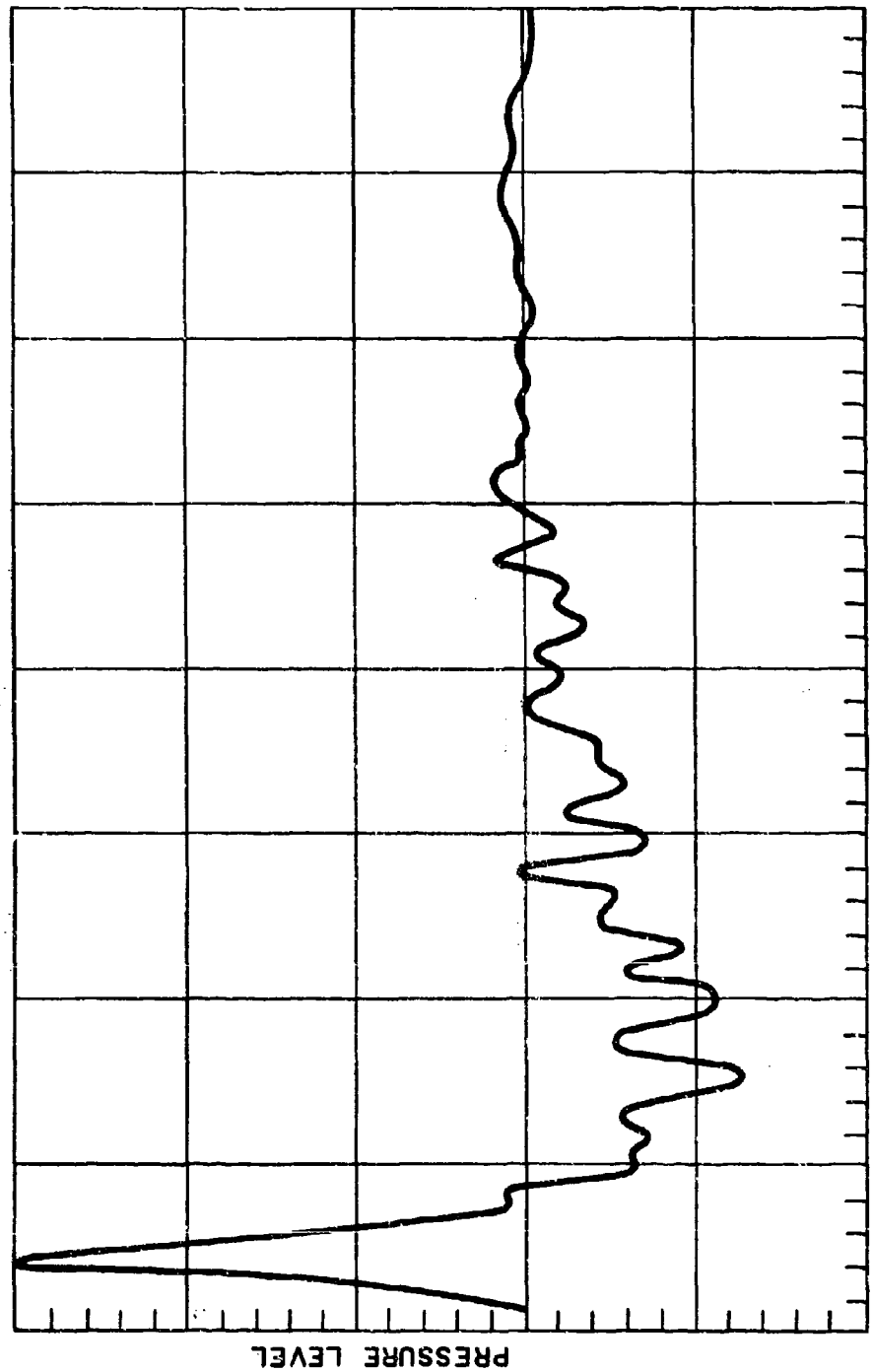

FIGURE 9-1. A TYPICAL IMPULSE NOISE WAVE FORM

9—2.1 PHYSIOLOGICAL EFFECTS

Repeated impulses produced by guns have their greatest effect upon the ears. By the time the pressure level becomes so great that other organs are noticeably affected, the unprotected ear will usually have been irreparably damaged. Even if the long-term hearing-loss were to be disregarded, field commanders still have to consider the short-term lowered efficiency of partially deafened gun crewmen when these crewmen are assigned to other duties, e.g., night perimeter guard. The development of a hearing-damage-risk criterion is basic to the entire impulse-noise problem. Until the hearing-loss effects that impulse noises have on man are determined accurately, the degree to which these parameters should be reduced cannot be precisely specified.

Many physical parameters are involved in a damage-risk criterion. Among these are the following:

1. Peak pressure
2. Sound frequency-energy spectrum
3. Rise time
4. Total duration
5. Repetition rate
6. Total number of exposures

Physiological parameters include:

1. Amount of temporary hearing loss which can be tolerated without degrading performance of personnel.
2. Percentage of personnel to be protected by the damage-risk criterion.
3. Relationship between temporary hearing loss and permanent hearing loss.

The noises produced by many small arms and artillery are sufficiently intense to rupture the human eardrum. Some new guns under development produce impulse noise levels substantially greater than some of the older models. The new developments add to the burden of finding methods of attenuating the pressure waves.

Peak pressure levels are defined quantitatively in pounds per square inch (psi) or in decibels (dB) above a reference point of 0.0002 dynes per square centimeter. Fig. 9—2 depicts the relationship between these two measures. Converting to decibels:

when p is in dyn/cm^2

$$dB = 20 \log (5000p)$$

when p is in psi

$$dB = 20 \log (34475p \times 10^4)$$

Four methods predominate in attempts to reduce exposure to high impulse noise levels:

1. The noise may be reduced at its source.

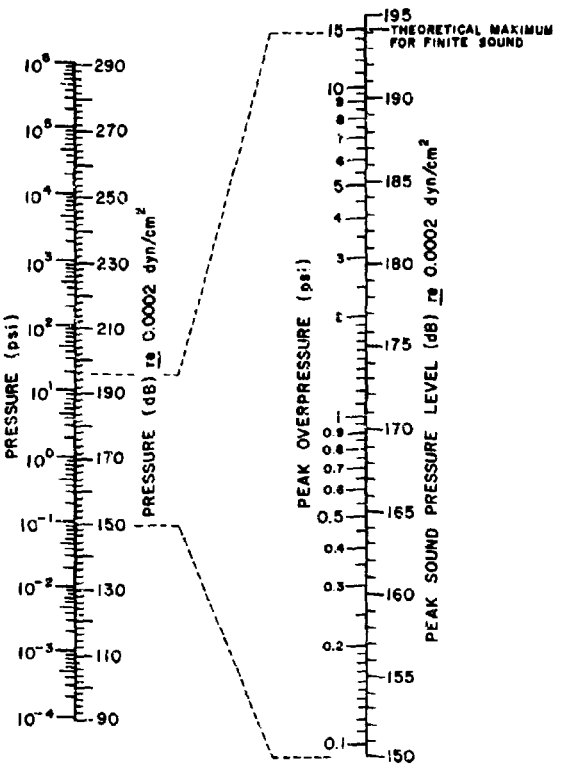

FIGURE 9-2. RELATIONSHIP BETWEEN PRESSURE IN PSI AND SOUND PRESSURE LEVEL IN dB

2. The operator may be isolated from the impulse-noise source by either distance or a barrier.
3. Protective devices, such as earplugs or earmuffs may be worn by the crew.
4. The ear may be conditioned so that it becomes less sensitive to noise.

The first method is a difficult one, but the most desirable if practical. Propellants may be developed that maintain or increase projectile range while keeping muzzle pressure at a minimum. This means a high chamber pressure with a rapid pressure-travel decay. A mechanical method of attenuating the impulse noise may be substituted. Mechanical attenuators are attached to the muzzle either to deflect the excessive impulse noise from the crew or to reduce the intensity, or both. If a muzzle brake is needed to reduce recoil forces, the pressures may be intensified due to the induced action by the conventional brake on the discharging muzzle gas. Therefore, some devices must be used to eliminate this undesirable influence. One such device is a muzzle brake-silencer. A muzzle brake-silencer traps most of the exiting gases, then cools, expands, diffuses, and expels these trapped gases over an extended time interval. Trapping these gases also reduced the recoil impulse. The U.S. Army Human Engineering Laboratories at Aberdeen Proving Ground recently applied this principle to increase firing stability of two light automatic rifles, the M16 and the Stoner Assault rifle. The standard M16 rifle's peak pressure level is 154 dB at the right-handed gunner's left ear. A conventional muzzle-brake, although effective in the reduction of recoil impulse, increased the peak sound-pressure level (SPL) to over 160 dB. An attempt to attenuate the noise while taking advantage of the recoil reduction was made with a single-baffle combination brake-compensator which reduced the peak level to 152 dB. A later design featured a double baffle with smaller-diameter outlet holes than earlier designs. This arrangement gave the lowest peak level 148 dB, 6 dB less than the standard M16 rifle, yet it provided excellent stability. Fig. 9—3, the latest design, shows the twin baffles and gas-collection area.

The second method involves placing a barrier between the source and the crew. The obvious means is the gun shield itself. For a tank, the very massiveness of the hull and turret provides an effective shield for a crew inside, but this mass provides little if any protection to the infantryman

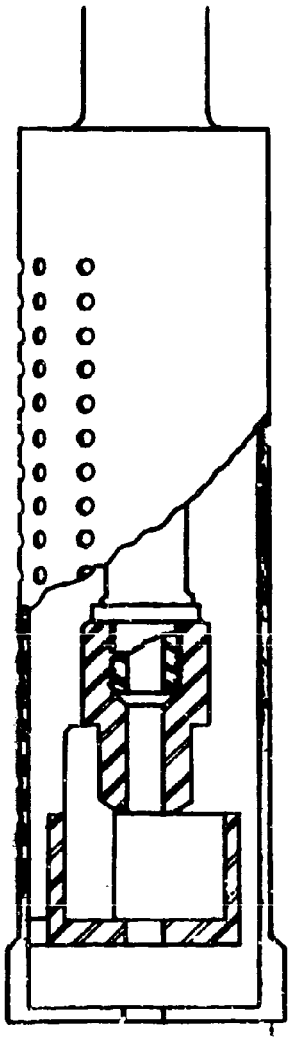

FIGURE 9-3. DOUBLE-BAFFLE COMBINATION BRAKE-SILENCER

walking alongside, or to the tank commander whose head may be outside the cupola, at the time of firing. Shields on artillery have very minimal blast-deflecting properties. Firing test results of the M102, 105 mm Howitzer support this contention. When fired with and without a shield, without or with one of three different muzzle brakes, at elevations of 0°, 45°, and 68°, and with charges of 85 percent and 100 percent, the shield did not significantly reduce the peak pressure level in the crew area. Fig. 9—4 shows a few representative equal-pressure contour lines measured in three of the many tests. The firings depicted were with a 100 percent charge at 45° angle of elevation. Placing the crew farther from the impulse noise source would increase operating time and therefore reduce the weapon's effectiveness. Resorting to remote controls and automatic ammunition handling systems seems too costly and not conclusively superior to a relatively simple structure as a sound attenuator.

The third method involves using protective devices applied directly to the ear. There are two possibilities: (1) placing a device in the ear; (2) placing a device over the ear. There is no highly accurate information about the *impulse*-noise-attenuating characteristics of the various types of ear protectors. (Most evaluations of ear protectors have been done with *steady* noises or tones.) Personnel can wear several types of pressure-attenuating devices. The most common and practical are: (a) the earplug, an extremely effective but often uncomfortable device, (b) the earmuff, several types are available, and (c) the helmet which is used in tanks and self-propelled howitzers but provides very little attenuation. Typical ear-protective devices provide good attenuation of steady-state sound at high frequencies (above 1000 cycles per second), but relatively poor protection at lower frequencies. Fig. 9—5 shows attenuation of steady-state sound as a function of frequency for an average earmuff, for the standard Army-issue V-51R earplug, for the CVC helmet, and for the combination of earplugs and earmuffs. Note that a combination of earmuff and earplug was not as effective as the earmuff alone for frequencies around 1200-2400 cps.

Existing standard earplugs have a number of major deficiencies. Three follow:

1. They must be selected to fit the individual and inserted properly to achieve the desired attenuation.
2. Although properly inserted originally, they may work loose because of movement of facial muscles.
3. Faint sounds cannot penetrate. Voices must be raised to be heard. This is especially objectionable since, in many combat situations, the perception of faint auditory cues is vitally important; therefore, loud talk cannot be tolerated.

Certain experimental types have eliminated the first and third deficiencies.

The fourth method involves conditioning the ear so that it becomes less sensitive to noise. One method of conditioning the ear appears to have promise. It has proved effective in some instances and may afford almost as much protection as an earplug. This method complements a natural physiological protective mechanism of the ear by eliciting, before firing, the contraction of certain middle-ear muscles, thereby blocking to a certain extent the transmission channel of impulse noise. The muscle stimulant is introduced over an intercommunication system and consists of sharp pulses of sound during a 0.1-second interval prior to firing the weapon. This device would be of greatest value to tank and self-propelled artillery crews. Infantrymen firing their individual weapons would be more difficult to protect with this conditioning method.

9—2.2 TOLERANCE LIMITS

The Atomic Energy Commision has determined the effects that high-intensity shock waves, from actual and simulated nuclear explosions, have on animals and on men. Its research has established tentative lethality limits and thresholds of injury for

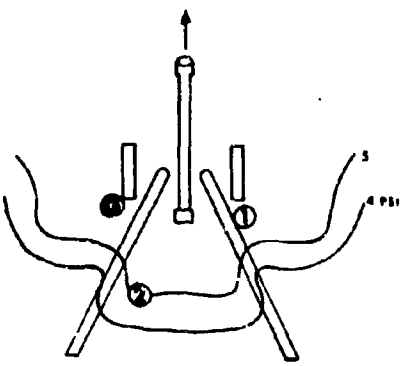

(A) No Blast Shield, WTV-F8241 Brake

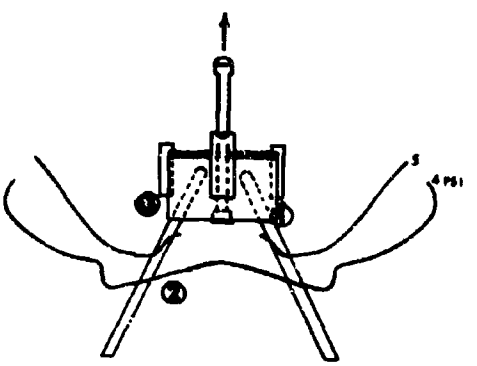

(B) With Blast Shield, WTV-F8241 Brake

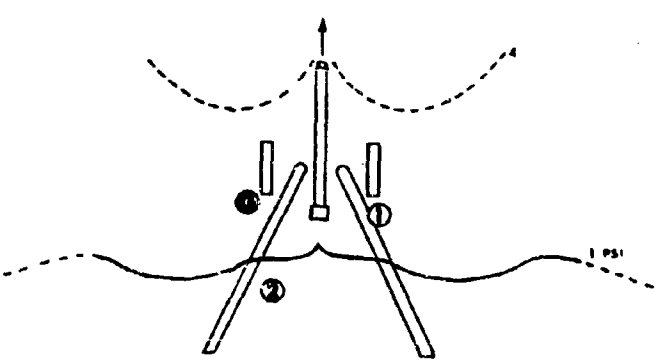

(C) No Blast Shield, No Brake

NOTE:
Positions 1, 2, and G are normally occupied by personnel during firing

FIGURE 9-4. OVERPRESSURE CONTOURS

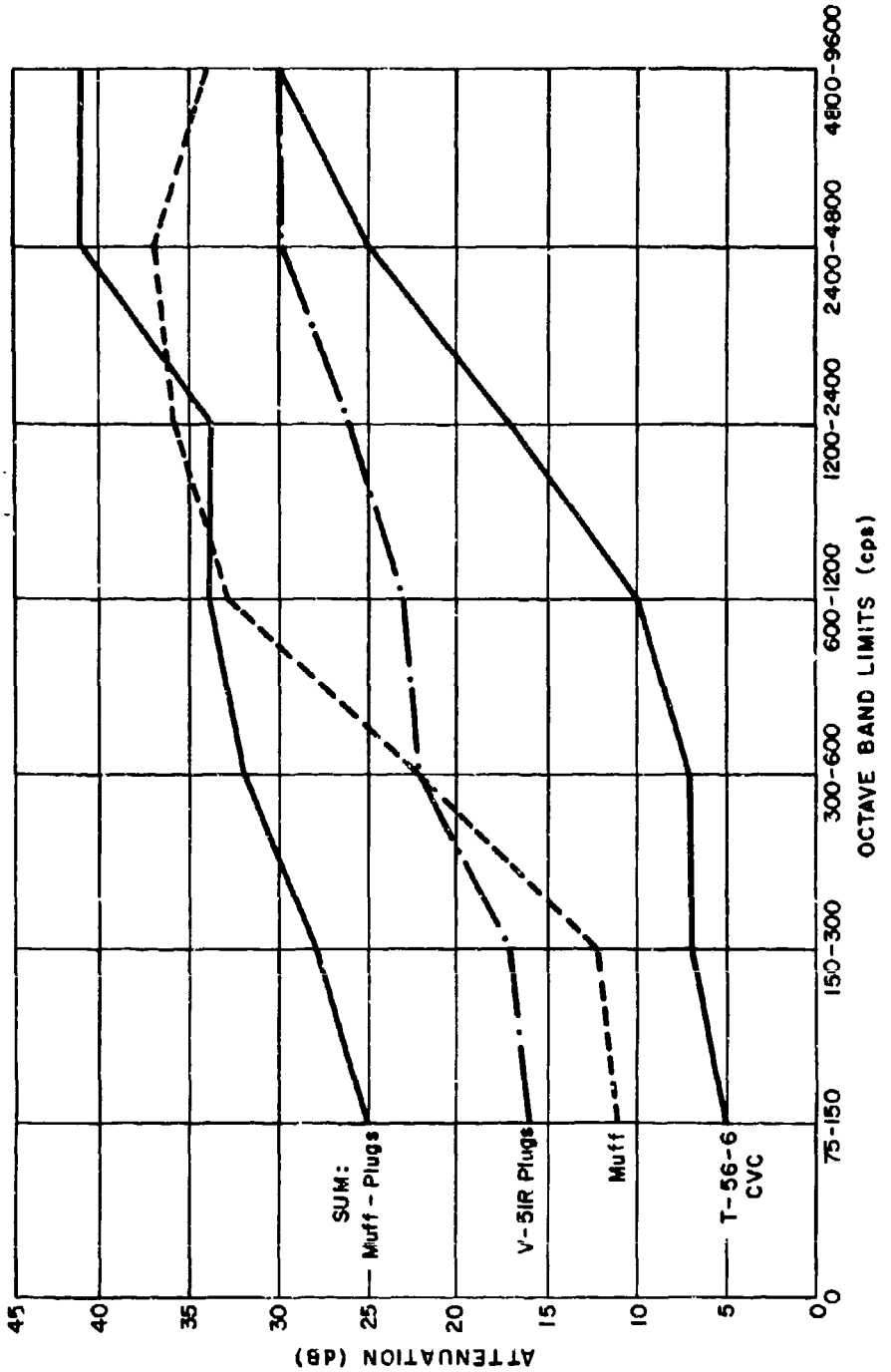

FIGURE 9-5. CHARACTERISTICS OF EAR PROTECTIVE DEVICES

various bodily organs. But man's hearing mechanism can be temporarily or permanently damaged by exposure to shock waves or impulse-noise conditions that are far below the threshold for damage to the lungs or other organs. Thus the noise and shock-wave phenomena that prevail in muzzle blast may cause temporary or permanent damage to hearing, or decrements in human performance, or lesser physiological harm to other organs of the body, but which are not sufficiently intense to threaten death. The sites of hearing damage are identified in Fig. 9–6 which shows a cross-section of the human hearing mechanism, including the external, middle, and inner ear. Impulse-noise of high intensity (above 180 dB) may rupture the eardrum or damage the chain of three tiny bones or ossicles of the middle ear. But most temporary and permanent changes in hearing are believed to be due to damage inside the inner ear, or cochlea, and usually occur at levels below 180 dB. Airborne acoustic energy is transmitted to the eardrum, through the middle ear, and through the fluid inside the inner ear. Histological studies of animals exposed to high level noises have shown that damage to the hair cells inside the cochlea is characteristic, and this damage is at least partly responsible for permanent hearing loss. The underlying bases of temporary hearing losses are not yet well understood.

Our knowledge about the effects of impulse sound-pressure levels on hearing is at best sketchy. The first systematic studies had Australian enlisted men exposed to a variety of small arms and artillery noises. Fig. 9–7 shows some of the results. Note that ten-round exposures at a peak pressure level of about 188 dB, comparable to noise in the crew area of a 105 mm Howitzer, produced temporary hearing losses of 85 dB.

Many researchers have found the use of firearms as noise sources impractical and, therefore, have had to use other sources to generate impulses. A number of impulse-noise generators have been constructed, but all have the same limitation: the acoustic pulses are so unlike those produced by Army weapons that doubt exists on the usefulness of their quantitative value. However, the qualitative results of various exposures are probably valid.

Several conclusions may be reached based on the assumption that the qualitative relationships are valid. There are very large individual differences in susceptibility to impulse-noise effects, both in Army and in civilian populations. Fig. 9–8 illustrates this wide variation. The subject represented by the upper curve sustained a temporary hearing change, i.e., temporary threshold shift *(TTS)* of 41 dB from exposure to 20 impulses at a peak level of 156 dB, while another subject, represented by the lower curve, sustained a *TTS* of only about 2 dB after exposure to 40 impulses (twice as many) with a peak level of 168 dB. The impulses in this study were generated by an impulse-noise source other than a gun, but similar variation in susceptibility has been reported for an M14 rifle as a noise source. Other conditions being equal, the higher the peak pressure level, the greater the resulting *TTS*. This relationship has already been illustrated with data in Fig. 9–8. However, the lowest peak level which will cause a measurable *TTS* in the average person, remains an unknown quantity. Recent research by the British Royal Navy has shown that to describe an impulse noise solely in terms of peak pressure level is no longer defensible. The time during which potentially hazardous energy is present must also be considered. Impulse durations vary from 100 microseconds for some small arms to several milliseconds for artillery. Fig. 9–9 shows a measurable *TTS* by exposure to 75 impulses with a peak pressure level of only 132 dB, 12 dB of *TTS* at 141 dB, and 24 dB of *TTS* at 144 dB. These data were gathered from a sound source other than a gun. On the other hand, experiments at the Human Engineering Laboratories, Aberdeen Proving Ground, have shown negligible *TTS* after exposure to 100 gunfire impulses with a controlled peak level of 140 dB. Thus, while it is logical to assume some relationship between peak level and amount of *TTS* produced, existing data are

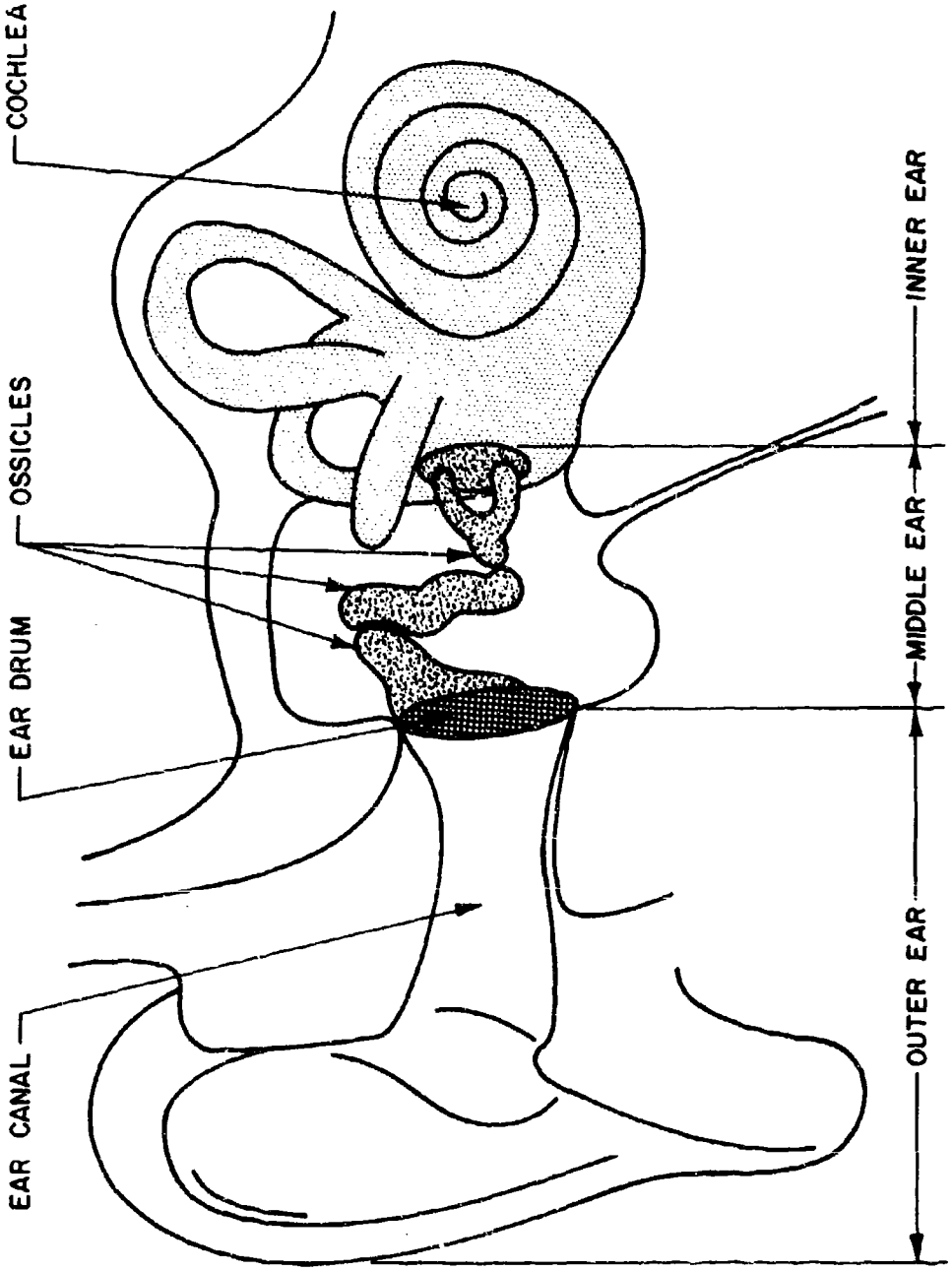

FIGURE 9-6. DIAGRAM OF THE EAR

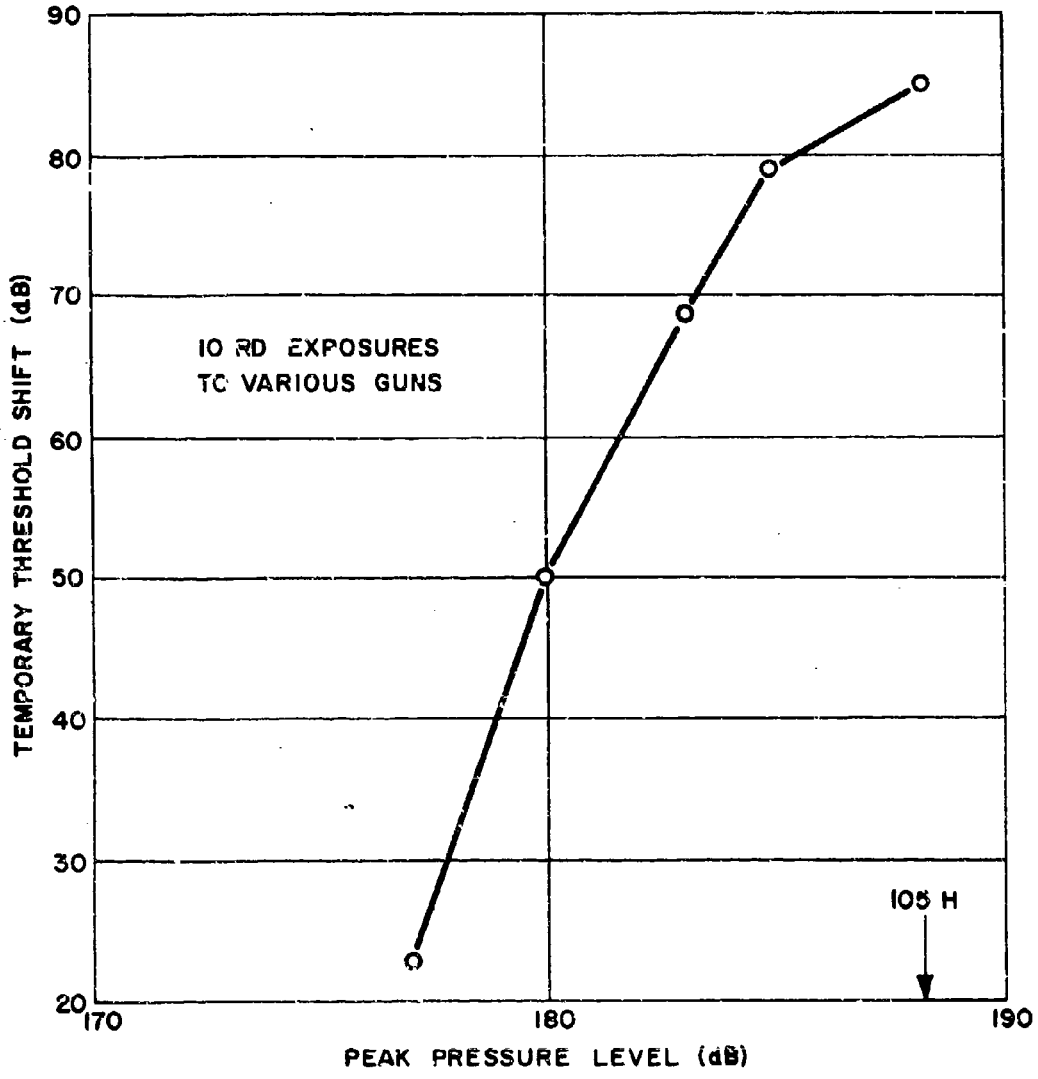

FIGURE 9–7. TEMPORARY THRESHOLD SHIFT VS PEAK PRESSURE LEVEL

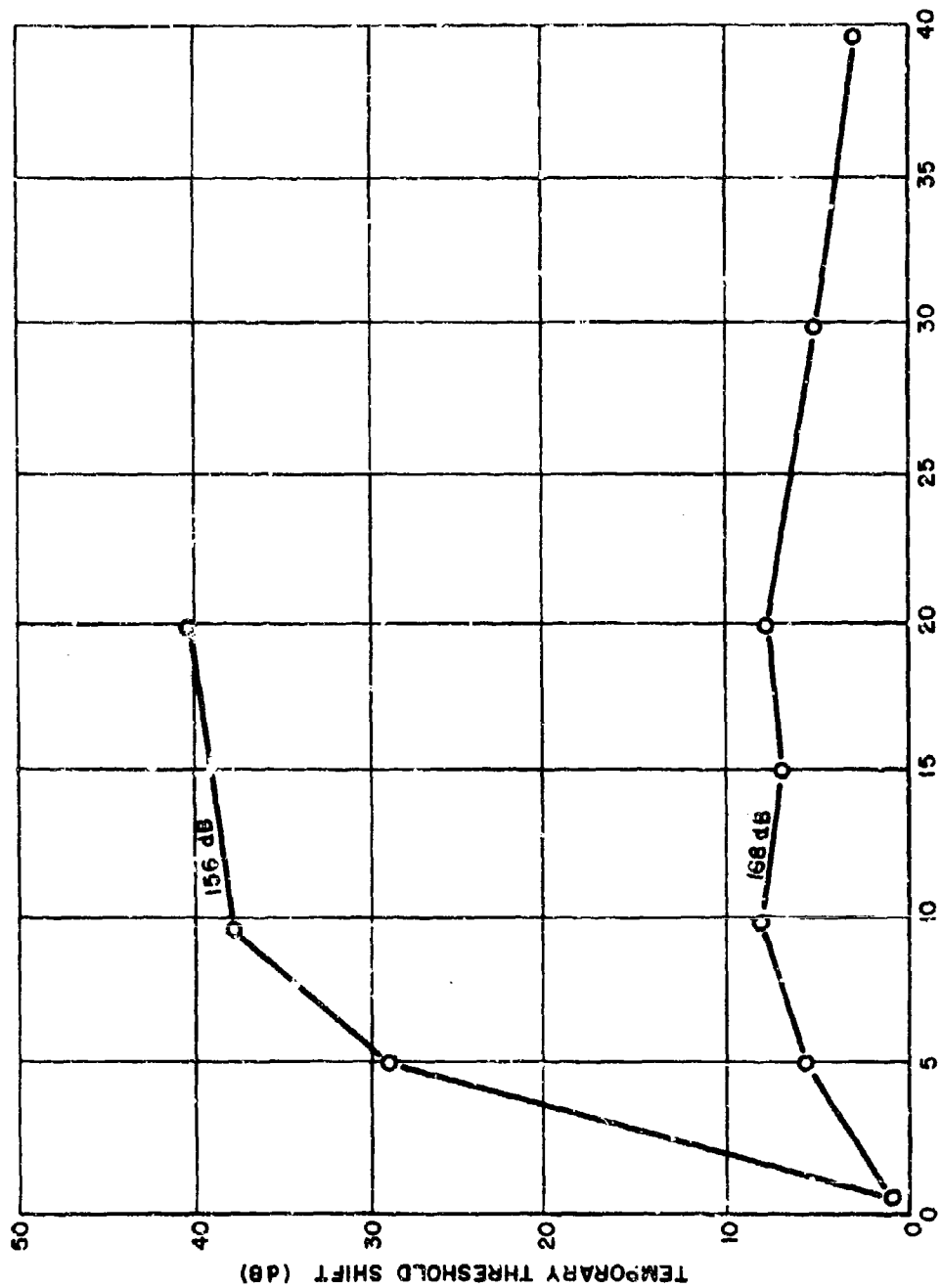

FIGURE 9-8. INDIVIDUAL DIFFERENCES IN SUSCEPTIBILITY TO TEMPORARY THRESHOLD SHIFTS

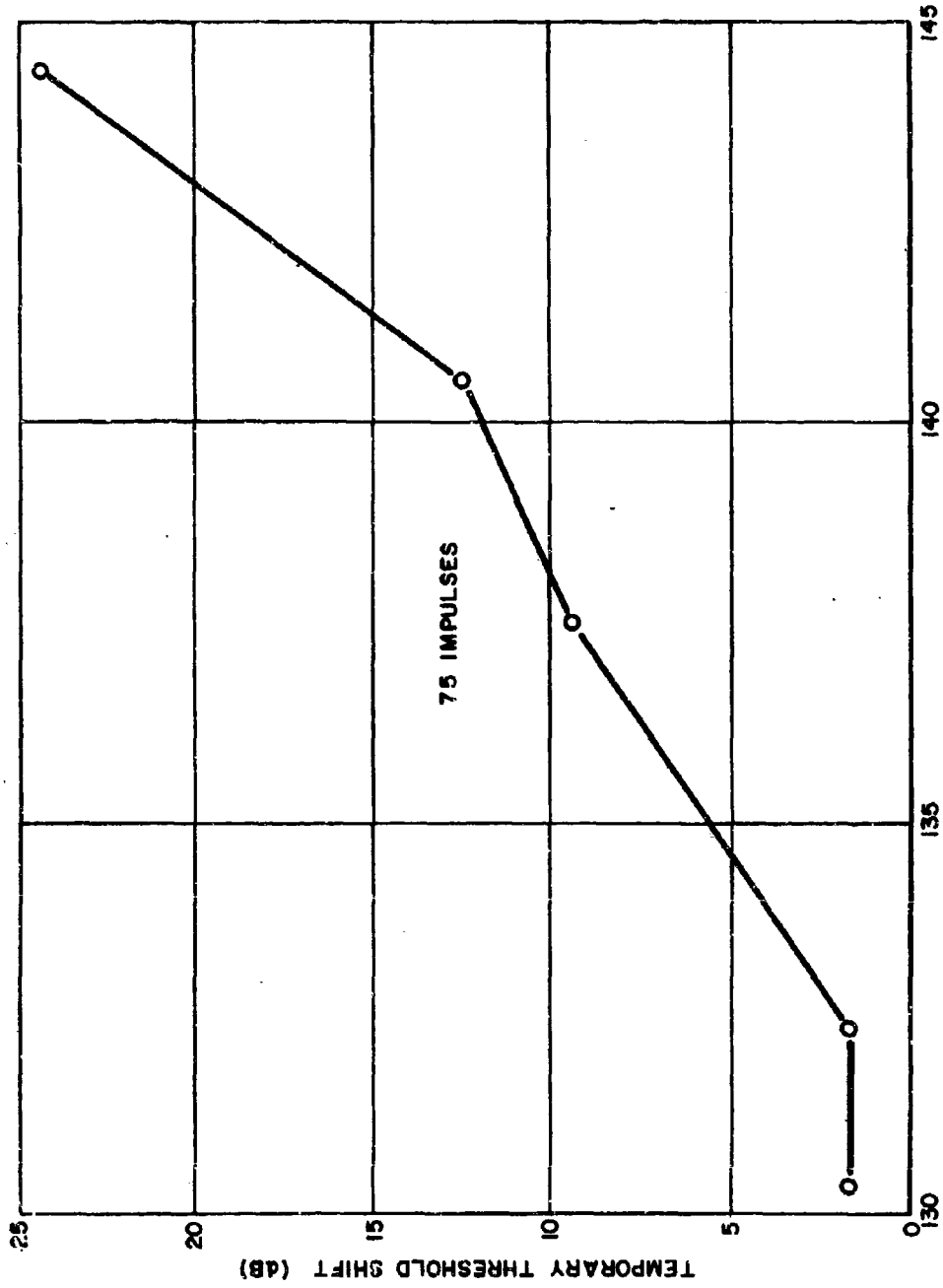

FIGURE 9-2. MEAN TEMPORARY THRESHOLD SHIFTS (TTS) VS PEAK LEVEL

neither sufficient nor adequate to establish the critical peak pressure level or duration where hearing damage is imminent.

The rate of exposure is an important variable. When the rate of exposure falls between one impulse per second and one impulse each nine seconds, there is no significant difference in the amount of *TTS* produced. However, when the rate decreases to one impulse each 30 seconds, the *TTS* is considerably less, indicating that some recovery occurs in the 30 seconds between successive impulses. A number of studies by the Army Medical Research Laboratory, Ft. Knox, have shown that, as the rate increases to more than one impulse per second, the *TTS* decreases. This and other evidence indicate that acoustical disturbances excite reflex action of the middle ear muscles to provide a certain amount of protection and maintain this protection for subsequent impulse noises.

Other evidence indicates that the more impulses a person is subjected to, for a given peak level and rate of exposure, the larger the *TTS* will be, but this relationship has not been fully substantiated.

The available information on tolerance limits may be summarized as follows:

1. There are large individual differences in susceptibility to impulse-noise effects.
2. Higher peak pressure levels mean more hazard to hearing.
3. Rate of fire has an appreciable effect.
4. Number of impulses has an appreciable effect.

There are few data to indicate how these variables influence each other, whether the effects of impulse-noise parameters are augmentative or compensatory. Also, there is little information about the effects of rise time or duration of individual impulses because no means has been developed to generate the type of acoustic impulses needed without firing guns. Existing instrumentation confines research to (1) sound generators which while giving some control over rise time, duration, peak level, and repetition rate, generate impulses which are unlike gunfire, or (2) small arms and artillery whose impulse sound-pressure characteristics are, in general, invariant and can be modified only by placing the subject at various distances from the muzzle. In the former case only qualitative data can be obtained, in the latter only hazards associated with specific weapons can be established. Interpolation of data to intermediate noise conditions is difficult, and similarly difficult is obtaining data on the relative value of rise time and duration. Duration, incidentally, was a very significant variable in the high-intensity, shock-wave studies carried out by the Atomic Energy Commission. Research by the British Royal Navy confirms this significance.

Until considerably more research has been completed, the nearest approach to a damage-risk criterion is that recommended by the National Research Council's Committee on Hearing, Bio-Acoustics and Bio-Mechanics (CHABA). This committee recommended that the unprotected ear should not be subjected to peak sound-pressure levels above 140 dB (.03 psi). Every standard weapon that the Army uses, including small arms, exceeds this level. Therefore, the armed services are faced with the problem of determining how hazardous to the user are the various weapons, how much must the pressure level of these weapons be reduced, and how can this reduction be accomplished.

APPENDIX A-1

ISOBAR SOURCE PROGRAM LISTING IBM-1620

```
C    ISOBAR IV G.SCHLENKER,S.OLSON AWC-OR JUNE 1965
     DIMENSION BFLAT(6),XO(6),ZO(6),  ZETA(6),QE(16),H(16),PS(9),
    1 TITLE(16),F7(6)
     PS(1)=7.
     PS(2)=6.
     PS(3)=5.
     PS(4)=4.
     PS(5)=3.
     PS(6)=2.5
     PS(7)=2.
     PS(8)=1.5
     PS(9)=1.
 49  READ 1,TITLE,GAMAC,GAMIG,TVC,TVIG,GMC,GMIG,EC,EIG,AREA,VT,
    1 VP,EMC,EMIG,EMP,EMR,VO,NH,NQE,NMZB,G,H,QE,(BFLAT(I),XO(I),
    2 ZO(I),ZETA(I),I=1,NMZB)
  1  FORMAT (16A5,2(/8F10.0)/3I2,F14.0,2(/16F5.0)/(4F10.0))
     IF (SENSE SWITCH 2)70,71
 70  PAUSE 1111
 71  CONTINUE
     IF (SENSE SWITCH 1)5,4
  4  PRINT 2,TITLE
     PRINT 3,GAMAC,GAMIG,TVC,TVIG,GMC,GMIG,EC,EIG,AREA,VT,VP,EMC,
    1 EMIG,EMP,EMR,VO
     GO TO 6
  5  PUNCH 2,TITLE
     PUNCH 3,GAMAC,GAMIG,TVC,TVIG,GMC,GMIG,EC,EIG,AREA,VT,VP,EMC,
    1 EMIG,EMP,EMR,VO
  2  FORMAT (48H ISOBAR IV G.SCHLENKER-S.OLSON AWC-OR JUNE 1965  //
    1     16A5 //8X 7HGAMMA C 7X  8HGAMMA IG 4X 11HTV C, DEG K 3X
    2 12HTV IG, DEG K 5X 10HNC, GM MOL )
  3  FORMAT (2F15.4,2F15.1,F15.6// 4X 11HNIG, GM MOL 5X 10HEC, CAL/GM
    1 4X 11HEIG, CAL/GM  19X 11HAREA, SQ IN /F15.6,
    2 2F15.1, F30.2//6X 9HVT, CU IN 6X 9HVP, CU IN 8X 7HMC, LBM 7X
    3 8HMIG, LBM 8X 7HMP, LBM /2F15.1,3F15.3//8X 7HMR, LBM 5X
    4 10HVO, FT/SEC / F15.1,F15.0 / )
  6  EMT = EMC+EMIG
     EC=1.8*EC
     EIG=1.8*EIG
     HTOT=EIG*EMIG+EC*EMC
     ALPHA=EMC/EMT
     RC=1545.*GMC
     RIG=1545.*GMIG
     TVC=1.8*TVC
     TVIG=1.8*TVIG
     FC=RC*TVC
     FIG=RIG*TVIG
```

APPENDIX A-1 (CONT)

```
      SIGMA=ALPHA*FC/(GAMAC-1.)+(1.-ALPHA)*FIG/(GAMIG-1.)
      R=ALPHA*RC+(1.-ALPHA)*RIG
      GAMMA=1.+R/(ALPHA*RC/(GAMAC-1.)+(1.-ALPHA)*RIG/(GAMIG-1.))
      TV=SIGMA*(GAMMA-1.)/R
      EKEP=VO*VO*(EMP+3.E-5*(VT-VP))/50030.
      VRVO=EMT/2.
      VRVO=(VRVO+EMP)/(VRVO+EMR)
      CONST=1.+VRVO
      CONST=CONST*CONST/3.-VRVO
      EKEG=EMT*VO*VO*CONST/50030.
      EKER=EMR*VO*VO*VRVO*VRVO/50030.
      EKEB=EKEP*.05
      CALIB=AREA/3.1415926
      EKEH=.597*CALIB**.75*VT/AREA*(TV-530.)/
     1 (777.5*(1.+ .7096*CALIB**1.0875/EMT**.8375))
      EGAS=HTOT-EKEB-EKEG-EKEH-EKEP-EKER
      GF=G/12.
      IF (SENSE SWITCH 1)7,8
    8 PRINT 68,HTOT,EKEP,EKEG,EKER,EKEB,EKEH,EGAS
      GO TO 9
    7 PUNCH 68,HTOT,EKEP,EKEG,EKER,EKEB,EKEH,EGAS
   68 FORMAT(/16H E N E R G I E S 15X 5HB T U / 6H TOTAL 15X F15.2 /
     1 11H PROJECTILE 10X F15.2 / 13H GAS, KINETIC 8X F15.2 /
     215H RECOILING MASS 6X F15.2 / 10H ENGRAVING 11X F15.2 /
     3 17H HEAT LOSS TO GUN 4X F15.2 / 13H GAS, THERMAL 8X F15.2 /)
    9 DO 10 IBFLT=1,  ZB
      EFC = (1.+BFLAT(IBFLT)*(1.+BFLAT(IBFLT)))*.145
      ALSTR=(EFC*.18*EGAS)**.33333333
      TEST=ALSTR*.1
      DONE=GAMMA*VT/AREA/30.-ZETA(IBFLT)/12.
      ZONE=DONE*(1.-BFLAT(IBFLT))
      XONE=SQRTF(DONE*DONE-ZONE*ZONE)
      X=XONE+XO(IBFLT)/12.
      Z=ZONE+ZO(IBFLT)/12.
      GPZ=GF+Z
      DO 10 IQE=1,NQE
      COSQE=QE(IQE)/57.29578
      SINQE=GPZ*SINF(COSQE)
      COSQE=GPZ*COSF(COSQE)
      DO 10 IH=1,NH
      COMA=(SINQE-H(IH)/12.)**2
      ISW=1
      DO 10 IPS=1,9
      ERROR=PS(IPS)*.005
      IF (SENSE SWITCH 1)12,11
   11 PRINT 13, BFLAT(IBFLT),G ,XO(IBFLT),ZO(IBFLT),ZETA(IBFLT),
     1 QE(IQE),H(IH),PS(IPS)
      GO TO 14
   12 PUNCH 13, BFLAT(IBFLT),G ,XO(IBFLT),ZO(IBFLT),ZETA(IBFLT),
     1 QE(IQE),H(IH),PS(IPS)
```

APPENDIX A-1 (CONT)

```
13 FORMAT (/9X 6HB-FLAT 10X 5HG, IN 9X 6HXO, IN 9X 6HZO, IN 7X
  1 8HZETA, IN / 2F15.2,3F15.3/ 8X 7HQE, DEG 10X 5HH, IN 8X
  2 7HPS, PSI / 2F15.1, F15.3/15H THETA STAR,DEG 5X 10HD STAR, FT
  3 10X 5HF, FT )
14 THETA=0.
   DO 15 ITHTA=1,8
   COSTH=THETA/57.29578
   SINTH=SINF(COSTH)
   COSTH=COSF(COSTH)
   GO TO (26,27),ISW
26 F=COSQE*(ALSTR*COSTH/GPZ-1.)
   GO TO 28
27 F=F7(ITHTA)
28 DO 17 ITER=1,20
   DSTAR=(GF+F)/COSTH
   COM=COMA+(COSQE+F)**2
   O=DSTAR*SINTH
   EN=SQRTF((O-X)**2+COM)
   O=SQRTF((O+X)**2+COM)
   A1=LOGF(EN/ALSTR)
   A2=LOGF(O/ALSTR)
   PHI1=EXPF(-.77394019-1.8989116*A1+.30859282*A1*A1)
   PHI2=EXPF(-.77394019-1.8989116*A2+.30859282*A2*A2)
   FACT=EXPF(2.*(EN-O)/EN)
65 XP=1./(.60920384-.20572855*A1)
64 PS3=14.7*(PHI1**XP+PHI2**XP*FACT)**(1./XP)
   IF (ABSF(PS3-PS(IPS))-ERROR)18,18,19
19 FPC=F+COSQE
   IF(FPC-TEST)16,16,17
16 CONTINUE
   IF (SENSE SWITCH 1)52,20
20 PRINT 47,THETA
   GO TO 53
52 PUNCH 47,THETA
47 FORMAT( F15.1,5X 23HNO ISOBAR IN THIS PLANE )
53 F=COSQE*(ALSTR*COSTH/GPZ-1.)
   GO TO 46
17 F=F+2.*FPC*(PS3-PS(IPS))/PS(IPS)/3.*COSTH
   GO TO 16
18 CONTINUE
   IF (SENSE SWITCH 1)21,23
23 PRINT 22, THETA,DSTAR,F
   GO TO 46
21 PUNCH 22, THETA,DSTAR,F
16 F7(ITHTA)=F
22 FORMAT(F15.2,2F15.3)
15 THETA=THETA+10.
   ISW=2
10 CONTINUE
   CALL DUMP
   END
```

APPENDIX A-2

FLOW CHART - MUZZLE GAS TEMPERATURES

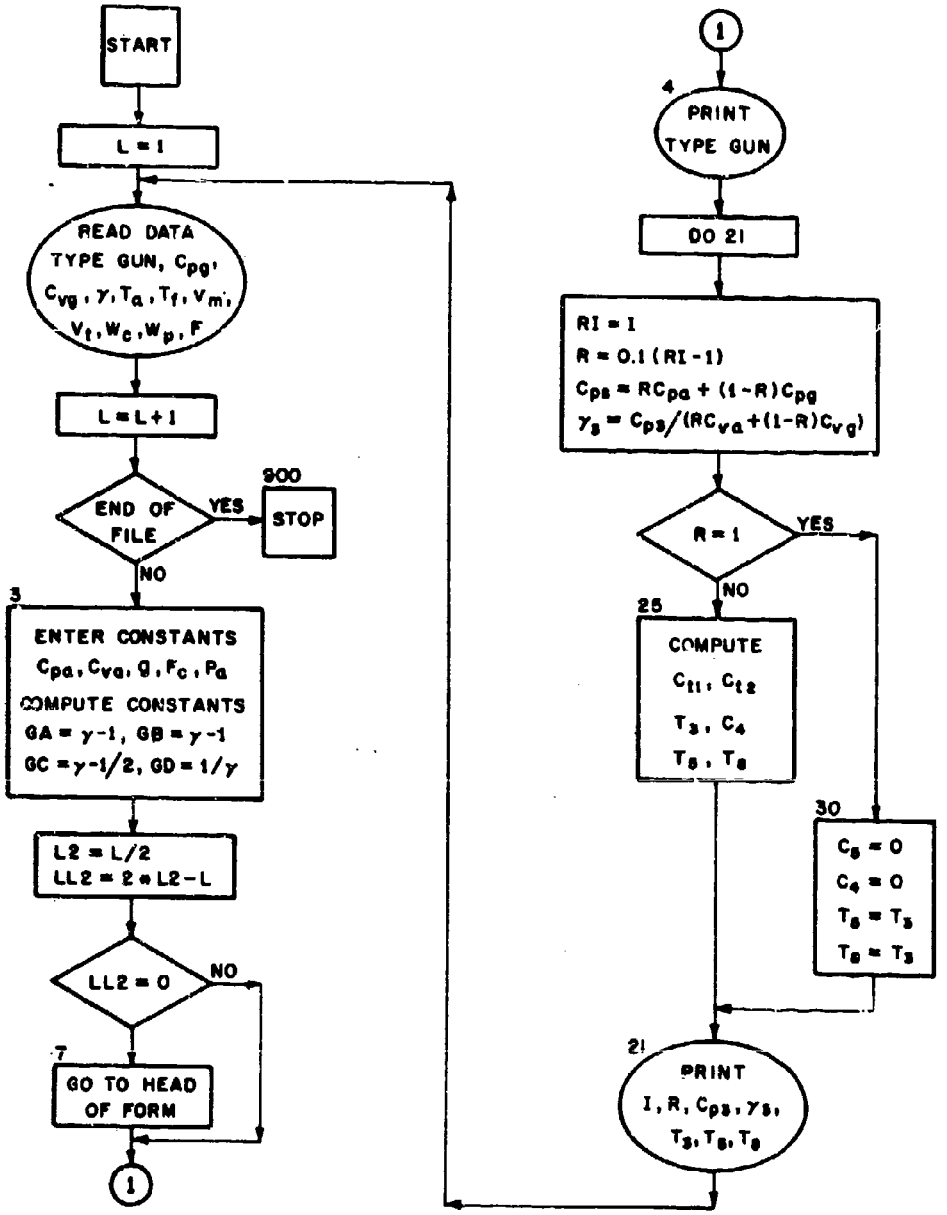

APPENDIX A-3

MUZZLE TEMPERATURE SOURCE PROGRAM LISTING

AUTOMATH SYSTEM H-1400 - MOD I

```
TITLEMUZTMP                                                          2
     L = 1                                                          2A
   1 READ 2,ATITLE, CPG, CVG, GAMMA, TA, TF, VM, VT, WC, WP, PSI     4
     L = L+1                                                        4A
   2 FORMAT ( A8/ 5F12.0 / 5F12.0 )                                 5
     IF END OF FILE 900, 3                                          6
   3 CPA = 0.24                                                     7
     CVA = 0.171                                                    8
     PA = 14.7                                                      8A
     G = 32.2                                                       9
     FC = 1400.0                                                    10
     GA = GAMMA - 1.0                                               11
     GB = GAMMA + 1.0                                               12
     GC = GA/GAMMA                                                  13
     GD = 1.0/GAMMA                                                 14
     L2 = L/2                                                       15A
     LL2 = 2*L2 - L                                                 15B
     IF(LL2)4,7,4                                                   15C
   7 PRINT 5                                                        15D
   4 PRINT 6,ATITLE                                                 15E
     DO 21 I = 1,11                                                 16
     RI = I                                                         17
     R = 0.1*(RI -1.0)                                              18
     CP3 = R*CPA + (1.0 - R)*CPG                                    19
     GAMMA3 = CP3/(R*CVA + (1.0-R)*CVG)                             20
     GM3 = GAMMA3                                                   21
     GMA   GM3-1.0                                                  22
     GMB = GM3+1.0                                                  23
     GMC = 1.0/GM3                                                  24
     VMSQ = VM**2/(2.0*G)                                           25
     FVM1 =VMSQ*((WP/WC)+(1.0/3.0)-GD)                              26
     FVM2 = VMSQ*((WP/WC)+(1.0/3.0))                                27
     RCT = R*CPA*TA                                                 28
     CT1 = FC*RCT +R*(1.0-R)*GAMMA*(PSI-FVM1)                       29
     CT2 = (1.0-R)**2*GAMMA*(PSI-FVM2)**GD*(PA*VT/(12.0*GA*WC))**GC 30
     T3 = (CT1 + CT2)/(FC*CP3)                                      31
     IF(R-1.0)25,30,25                                              31A
  30 C5=0.0                                                         31B
     C4=0.0                                                         31C
     T5=T3                                                          31D
     T8=T3                                                          31E
     GO TO 21                                                       31F
  25 C5 = (1.0-R)*CPG*TF*(1.0 - FVM1/PSI)                           32
     C4 = (4.0*GM3*(RCT-C5)/(CP3*T3) - GMB**2)/GMA                  33
     T5 = C4**GMC*((GMA*C4 + GMB)/(GMB*C4 + GMA))*T3                34
     T8 = (CT1 + CT2*C4**GD*((GA*C4 + GB)/(GB*C4 + GA)))/(FC*CP3)   35
  21 PRINT 66,        I,R,CP3,GM3,T3,T5,T8                          41
   5 FORMAT (1H1)                                                   42
  60FORMAT (///47B,23HMUZZLE GAS TEMPERATURES/38B,29HFOR VARIOUS MIXTU 43
    1RE RATIOS OF,1A8,4H GUN//29B,59HI     R      CP3    GAMMA3    T3(DEG K 44
    2)   T5(DEG K)    T8(DEG K)//)                                  45
  66 FORMAT(25B,I5,F6.1,F7.3,F9.3,F10.6,2F12.0)                     45A
     GO TO 1                                                        46
 900 STOP                                                           47
     END                                                            48
```

APPENDIX A-4

FLOW CHART – FLASH SUPPRESSOR DESIGN

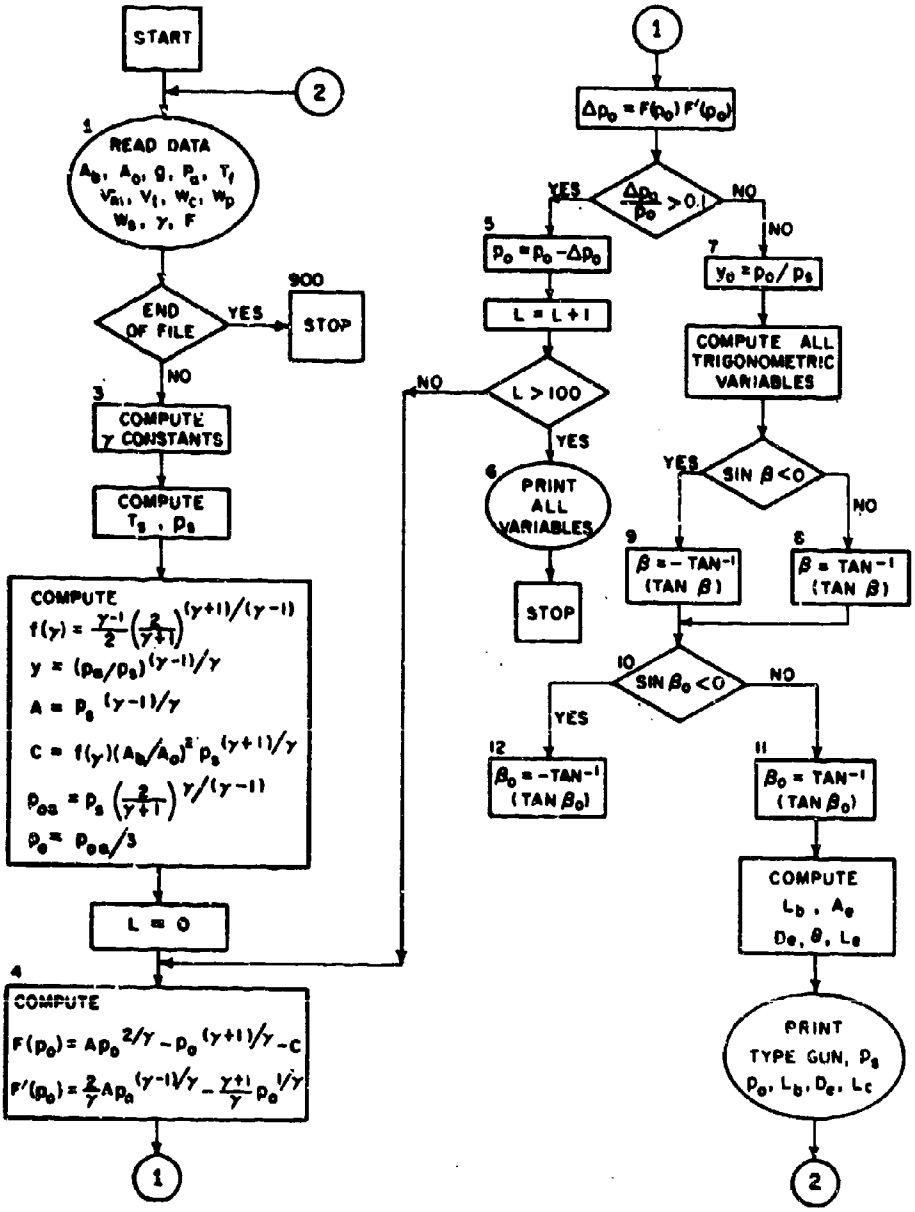

APPENDIX A-5

FLASH SOURCE PROGRAM LISTING

AUTOMATH SYSTEM H-1400 - MOD I

```
TITLEFLASH
      DIMENSION ATITLE(2)
      PRINT 21
  210FORMAT (1H1/40B,39HBAR AND CONE TYPE FLASH SUPPRESSOR DATA//39B,53
     1HSTAGNATION   PRESSURE        BAR     CONE EXIT      CONE/40B,53HPRES
     2SURE     AT ORIGIN     LENGTH     DIAMETER     LENGTH/24B69HTYPE GUN
     3        (PSIA)       (PSIA)       (INCH)      (INCH)      (INCH)//)
    1 READ 2, ATITLE,  AB, AO, G, PA, TF, VM, VT, WC, WP, WS, GAMMA, PSI
    2 FORMAT (2A8/6F12.0/6F12.0)
      IF END OF FILE 900, 3
    3 XA = (GAMMA - 1.0)
      XB = (GAMMA + 1.0)
      X1 = XA/2.0
      X2 = 2.0/XB
      X3 = XB/XA
      X4 = XA/GAMMA
      X5 = XB/GAMMA
      X6 = GAMMA/XA
      X7 = 2.0/GAMMA
      X8 = 2.0/XA
      X9 = 1.0/GAMMA
      TS =TF*(1.0-(((VM*VM)/(2.0*G*PSI)) * ((WP/WC)+(1.0/3.0)-X9)))
      PS = (12.0*XA*PSI*WC*TS)/(VT*TF)
      ARSQ = (AB/AO)**2
      GF =  X1*X2 **X3
      Y = (PA/PS)**X4
      A = PS**X4
      C = GF*ARSQ*PS**X5
      POA = PS*X2**X6
      PO = POA/3.0
      L = 1
    4 FXN =   A*PO**X7- PO**X5 -C
      FPRXN = X7*A*PO**X4 - X5*PO**X9
      DELPO = FXN/FPRXN
      IF (ABSF(DELPO/PO) - 0.01)7,7,5
    5 PO = PO - DELPO
```

APPENDIX A-5 (CONT)

```
      L = L+1
      IF (L-100)4,4,6
   60PRINT 101 , L,XA,XB,    X1,X2,X3,X4,X5,X6,X7,X8,X9,TS,PS,ARSQ,GF,Y,
     1A,C,POA,PO,FXN,FPRXN,DELPO
  101 FORMAT(//I7/8E14.6/8E14.6/8E14.6/7E14.6)
      GO TO 900
    7 YO =(PO/PS)**X4
      BSIN = 2.0*Y - 1.0
      BOSIN = 2.0*YO - 1.0
      BCOS  = SQRTF(1.0 - BSIN**2)
      BOCOS = SQRTF(1.0 - BOSIN**2)
      BTAN = ABSF(BSIN/BCOS)
      BOTAN = ABSF(BOSIN/BOCOS)
      IF (BSIN)9,8,8
    8 BETA = ATANF(BTAN)
      GO TO 10
    9 BETA = -ATANF(BTAN)
   10 IF (BOSIN)12,11,11
   11 BETAO = ATANF(BOTAN)
      GO TO 13
   12 BETAO = -ATANF(BOTAN)
   13 ZB = 0.5*X3*(BETA -BETAO)
      ZY =X8*(SQRTF((1.0-Y)/Y) - SQRTF((1.0-YO)/YO))
      ZGS = SQRTF(GF)
      ZG = ZGS*WS/AO
      ELB= (ZB + ZY)/ZG
      AE = (AB*ZGS)/(SQRTF(1.0-Y)*(PA/PS)**X9)
      DE = SQRTF(AE/0.7854)
      THETAD = 20.0
      THETA  = THETAD/57.296
      TSIN   = SINF(THETA/2.0)
      TCOS   = COSF(THETA/2.0)
      TTAN   = TSIN/TCOS
      ELC= DE/(2.0*TTAN)
      PRINT 22 ,ATITLE , PS, PO,ELB, DE,ELC
   22 FORMAT (20B,2A8,2F12.1,F10.1,F12.2,F10.2)
      GO TO 1
  900 STOP
      END
```

APPENDIX A-6 PATENTS ON SILENCERS

UNITED STATES PATENTS

Patent No.	Inventor	Date	Title
381,950	N. W. Pratt	4/1/88	Pneumatic Ordnance
692,819	T. E. Bissell	2/11/02	Noiseless Discharge
880,386	H. P. Maxim	2/25/08	Silent Firearms
951,770	J. M. Miller	3/8/10	Silencer
953,943	G. F. Childress	4/5/10	Gun Muffler
958,935	H. P. Maxim	4/24/10	Silent Firearm
984,750	H. Craven	2/21/11	Gun Silencer
1,017,003	C. H. Kenney	2/13/12	Silencer for Firearms
1,111,202	W. E. Westfall	9/22/14	Silencer Coupling
1,130,609	S. T. Jones	3/2/15	Muffler for Shotguns
1,229,675	E. W. Thompson	6/12/17	Gun Silencer
1,290,596	J. N. Lewis	1/7/19	Quick Combustion Gun
1,341,363	A. Fiala	5/25/20	Silencer and Flash Obscurer
1,497,553	J. Dickman	6/10/24	Exhaust Silencer
1,736,319	H. P. Maxim	11/19/29	Silencer
1,874,326	W. P. Mason	8/30/32	Sound Muffler
2,043,731	R. B. Bourne	6/9/36	Sound Attenuating Device
2,241,768	F. E. Deremer	5/13/41	Silencer Construction
2,449,571	B. Walker	9/21/48	Silencer for Firearms
2,868,078	W. J. Jarrett	1/3/59	Noise Reducer for Gun

APPENDIX A-6 (CONT.)

FOREIGN PATENTS

Patent No.	Inventor	Date	Title
8,453	C. A. Aeppli	3/20/94	Silencer
144,415	R. Schultz	3/3/01	Silencer
172,498	K. Haussner	9/21/05	Silencer Attachment
210,314	B. Gavriloff	4/19/08	Gun Silencer
12,850	M. R. A. Moore	11/26/10	Silencer
298,935	P. Schauer	1, 19/15	Silencer
301,229	F. Stendenbach	5/30/16	Silencer for Small Arms
74,757	E. Berthoud	9/17/17	Silencer
191,758	A. M. Low	6/2/19	Improved Silencers for Guns
35,748	T. S. Anderson	3/15/26	Silencer
47,405	Bror Witt	4/30/28	Silencer
786,895	E. G. Caron	9/11/35	Silencer
695,929	K. Rehor	2/28/39	Silencer
858,032	A. Chantreux	11/15/40	Silencer
401,021	A. B. a Torino	1/2/43	Silencer
911,148	M. Marcel	5/28/46	Silencer
918,658	J. J. Stapelle	2/14/47	Silencer
1,021,270	L. Baer	11/26/52	Silencer
1,123,835	J. M. Lefebore	6/18/56	Silencer

GLOSSARY

ballistic crack. The intense sharp noise of the shock wave that is generated by a projectile moving through the air at supersonic velocity.

blast deflector. A muzzle device that deflects the muzzle blast from its normal course.

blast deflector, baffle type. A blast deflector that has baffles to redirect the muzzle blast.

blast deflector, duct type. A blast deflector that redirects the muzzle blast through ducts or tubes.

blast deflector, perforated type. A blast deflector of tubular construction having oblique perforations in the wall.

blast deflector, T-type. A one-baffle blast deflector whose baffle is a flat plate forming the cross on the T with its muzzle attachment.

blast field. The area of a gun emplacement that is affected by the muzzle blast.

breech opening time. The time interval between firing and breech opening.

casing. The external structure of a smoke suppressor.

closed-breech gun. A gun having a breech completely sealed during firing to preclude gas leakage.

decibel. A measure of sound intensity above a reference point of 0.0002 dyn/cm^2.

discharge time. The time required for an evacuator to discharge its accumulated gas into the gun bore.

diverter. The perforated inner wall of a smoke suppressor that permits the propellant to enter and leave the filter chamber.

diverter, even flow. A diverter with perforations so distributed along its length that the same quantity of gas flows into the filter chamber for each equal distance along the diverter.

diverter, tapered bore. A diverter with conical bore and large end adjacent to the muzzle to reduce erosion of the diverter.

diverter, variable flow. A diverter having evenly spaced perforations thereby permitting more gas to pass into the filter chamber through the perforations nearest the gun muzzle.

equivalent length. The total volume of a gun tube, bore volume plus chamber volume, divided by the bore area.

evacuator. A device located near the muzzle that drains off some of the propellant gas, then discharges it toward the muzzle thereby inducing a flow of clean air to flow from the opened breech toward the muzzle to purge the bore of propellant gas.

filter chamber. The space between the diverter and casing that contains the filter of a smoke suppressor.

flash. The illumination appearing beyond the muzzle when a gun is fired.

flash hider. A muzzle device, usually having conical walls, which supposedly obscures the flash from a distant observer.

flash, intermediate. A red, or reddish-orange cone of light just outside the shock bottle with apex pointing away from the muzzle.

flash, primary. The visible light just outside the muzzle.

flash, secondary. An intense voluminous flash caused by the burning of the flammable content of the propellant gas.

flash suppressor. A muzzle device that reduces or eliminates various flash phenomena.

flash suppressor, bar type. A flash suppressor constructed of bars that destroys the flash reducing patterns of the discharged propellant gas.

flash suppressor, cone type. *See:* **flash hider.**

impingement process. The phenomenon of reducing speed or stopping a particle by having it strike a motionless object.

impulse wave. A transient pressure traveling at either sonic or supersonic velocity.

isobar. A line connecting all points of equal pressure in a given location.

jet duration factor. A value that corresponds with a given ratio of nozzle area to bore area and with the ratio of ambient to muzzle pressure. It is useful in computing jet duration time.

jet duration time. The time interval during which the evacuator discharges its gas.

Mach number. The ratio of a given velocity to sonic velocity in a particle medium.

mass rate of flow. The mass of a fluid flowing through a particular reference plane per unit of time.

mechanical eliminator. A smoke suppressor.

momentum index. The factor that determines the effective impulse of a muzzle brake.

muzzle. The end of a gun tube from which the projectile emerges.

muzzle blast. Sudden air pressure generated by the expansion of propellant gas as it emerges from the muzzle.

muzzle brake. A muzzle device that uses the propellant gas momentum to reduce the momentum of the recoiling parts.

muzzle brake, closed. A muzzle brake whose baffles are too close to the muzzle to permit free expansion of the gas.

muzzle brake, free periphery. An open muzzle brake with half the periphery open for gas discharge provided that the bottom deflector-support closes about 40 percent and the top support closes about 10 percent of the periphery.

muzzle brake, open. A muzzle brake that permits free expansion of the propellant gas before it impinges on the baffle.

muzzle device. A mechanical structure attached to the barrel at the muzzle that performs one or more useful functions to augment the gun's effectiveness.

muzzle glow. The faint visible light inside the shock bottle.

noise suppressor. A muzzle device that eliminates or reduces the report of a gun.

nozzle angle of inclination. The angle of inclination of a bore evacuator nozzle with reference to the bore axis.

nozzle, check valve type. A discharge nozzle of a bore evacuator that functions as a check valve.

nozzle, fixed. A nozzle of a bore evacuator that is merely an open port.

obscuration. Any phenomenon adjacent to a fired gun that reduces visibility.

overpressure. The transient pressure of the muzzle blast that exceeds atmospheric pressure.

preflash. The visible light of propellant gas that leaks past and precedes the projectile from the bore.

pressure decay. The relative gradual reduction of propellant gas pressure in the bore to atmosphere.

pressure level. The pressure of a sound wave.

pressure level, peak. The maximum pressure level.

propellant gas. The gas generated by the burning propellant.

propellant potential. The specific potential energy of a propellant gas usually written ft-lb/lb and includes the influence of ratio of specific heats.

recoil distance. The distance that a gun or the recoiling parts of a gun move in recoil.

recoil force. The force that resists recoil.

recoil mechanism. The component of a gun that provides recoil resistance.

silencer. *See:* **noise suppressor.**

shock. *See.* **shock wave.**

shock bottle. The central supersonic region of a muzzle blast bounded by the normal and oblique shocks.

shock, normal. The strong shock wave that forms perpendicular to the path of the projectile.

shock, oblique. The shock wave that forms oblique to the path of the projectile.

shock envelope. The boundary of the shock bottle.

shock wave. An area, not necessarily plane, of moving compressed gas.

smoke ring. The shell of turbulent gases that surrounds the shock bottle.

smoke suppressor. A muzzle device that traps, filters out the smoke, and then releases a considerable portion of the propellant gas as it emerges from the muzzle.

specific impetus. A specific energy potential of a propellant usually written ft-lb/lb. It does not include the influence of the ratio of specific heats.

speed-up factor. The ratio of exit velocity to the entrance velocity of the flow passage in a muzzle brake.

temporary threshold shift. A temporary hearing change measured in decibels after exposure to intense noises.

thrust correction factor. A factor that compensates for inaccuracies in the theory for computing muzzle brake thrust during the first and final intervals of the pressure decay period.

REFERENCES

1. H.H. Young, *Smoke and Flash in Small Arms Ammunition,* Midwest Research Institute, Contract No. DA-23-072-ORD-769, 1954.
2. E.W. Hammer, *Anti-Obscuration Devices and Muzzle Brakes,* The Franklin Institute Research Laboratories, June 1947, p. 51.
3. J. Corner, *Theory of Interior Ballistics of Guns,* John Wiley and Sons, Inc., New York, 1950, p. 175
4. *Op. cit.,* Reference 2, p. 121.
5. E.W. Hammer, *Muzzle Brake Theory, Vol II,* The Franklin Institute Research Laboratories, June, 1949, p. 320.
6. AMCP 706-340, Engineering Design Handbook, *Carriages and Mounts — General.*
7. AMCP 706-342, Engineering Design Handbook, *Recoil Systems.*
8. George Schlenker, *Contribution to the Analysis of Muzzle Brake Design,* Rock Island Arsenal Report 62-1794, May 1962.
9. George Schlenker, *Theoretical Study of the Blast Field of Artillery with Muzzle Brakes,* Rock Island Arsenal Report No. 62-4257, Dec. 1962, Appendix II.
10. Harold L. Brode, *Point Source Explosions in Air,* RM-1824-AEC, AD133030, Rand Corp., Santa Monica, Cal., Dec. 1956.
11. George Schlenker and Stuart Olsen, *A Revised Method of Computing the Overpressure Isobars in the Blast Field of Artillery,* Rock Island Arsenal Technical Note 65-2, July 1965.
12. S.P. Carfagno and G.P. Wachtell, *Research and Development on Ignition of Propellants and Muzzle Gases,* The Franklin Institute Research Laboratories Report F-A1828, June 1958, p. 27.
13. S. P. Carfagno, *Handbook on Gun Flash,* The Franklin Institute Research Laboratories, November 1961, Table 1, p. 16.
14. H.W. Lupman and A.E. Puichett, *Introduction to Aerodynamics of a Compressible Fluid,* John Wiley and Sons, Inc., N.Y., 1947, p. 34.
15. *Op. cit.,* Reference 13, Equation 2.
16. R. Landenburg, *Studies of Muzzle Flash and its Suppression,* Ballistic Research Laboratories, February 10, 1947.
17. S.F. Mathews, *Feasibility Study of a Mechanical Eliminator for Use on 40mm Artillery Weapons,* Midwest Research Institute Final Report 2199-C, March 1959.
18. J.J. Pascale, *Design Criteria for Bore Evacuators,* Watervliet Arsenal, File Misc. 141, June 1957.
19. W.H. Watling, *Investigation of Flash Suppressor for M73, 7.62mm Machine Gun,* Springfield Armory Report SA-TR3-1911.
20. R.F. Chaillet. et al, *High-Intensity Impulse Noise: A Major Problem,* Technical Note 4-64, U.S. Army Human Engineering Laboratory, Aberdeen Proving Ground, Md., Aug., 1964.
21. AMCP 706-255, Engineering Design Handbook, *Spectral Characteristics of Muzzle Flash.*

BIBLIOGRAPHY

1. J.T. Agnew, *Basic and Technical Work on Military Propellants,* Final Report No. F-2092-15, The Franklin Institute Research and Development Laboratories, Philadelphia, Pa., Dec. 1949.

2. J. Berry, *Development of UBU Muzzle Brake as Applied to the 105mm Howitzer, XM102,* Final Report, Rock Island Arsenal, August 1964.

3. J. M. Berry, P. Norausky and L. L. Frauen, *Development of UBU Muzzle Brake, The 105mm Howitzer, XM102,* Supplement to Final Report, Technical Report 64-2560, Rock Island Arsenal, August 1965.

4. H.L. Brode, *Space Plots of Pressure, Density, and Particle Velocity for the Blast Wave from a Point Source in Air,* RM-1913-AEC, Rand Corp., Santa Monica, Calif., June 1957.

5. J. L. Brown, *The Use of Colored Filtered Goggles for Protection against Flashblindness.* Aviation Medical Acceleration Laboratory, U. S. Naval Air Development Center, Johnsville, Pa., NADC-MA-5917, October 1959.

6. S.P. Carfagno, *Relationship Between Propellant Composition and Flash and Smoke Produced by Combustion Products* (U), Report No. I-A2132-1, The Franklin Institute Research Laboratories, Philadelphia, Pa., July 1958. (Confidential).

7. R. F. Chaillet and G. R. Garinther, *Maximum Noise Level for Army Materiel Command Equipment,* HEL Standard S-1-63B, U.S. Army Human Engineering Laboratory, Aberdeen Proving Ground, June 1964.

8. R. F. Chaillet, G. R. Garinther, D. C. Hodge, F.N. Newcomb, *High Intensity Impulse Noise: A Major Problem,* Technical Note 4-64, U.S. Army Engineering Laboratory, Aberdeen Proving Ground, August 1964.

9. Gloria Chisum and J.H. Hill, *Flash-blindness Recovery Times following Exposure to High-Intensity Short-Duration Flashes,* Aviation Medical Acceleration Laboratory, U.S. Naval Air Development Center, Johnsville, Pa., NADC-MA-6142, November 1961.

10. Development and Proof Service, *Evacuator Pressures and Operation 90mm Gun, M3E4,* Second Report, Project TR3 3000, Aberdeen Proving Ground, July 1949.

11. Development and Proof Service, *Proof and Recoil Energy Absorbtion Tests of Blast Deflectors for Gun, 76mm, T91E3, and for Gun, 76mm, T124,* Second Report, Project TR3-3037, Aberdeen Proving Ground, September 1952.

12. Development and Proof Service, *Second Report on the Development Tests of the Prong Type Flash Suppressor for the 75mm (AA) Gun, T83,* Project TR3-3000 B/5th, Aberdeen Proving Ground, Nov. 1953.

13. D.W. Eldredge, *The Effects of Blast Phenomena on Man: A Critical Review,* CHABA Report No. 3, Armed Forces—National Research Council, St. Louis, June 1955.

14. Walter Fagan, *Bore Scavenging Study for Case-Loaded Cannon Mounted In Closed-Cab Vehicles,* AMF Project MR1014, Mechanics Research Department, American Machine and Foundry Company, 20 September 1954.

15. Walter Fagan, *Bore Scavaging Study for Case-Loaded Cannon Mounted In Closed-Cab Vehicles,* AMF Project

MR1030, Mechanics Research Department, American Machine and Foundry Company, 15 June 1955.

16. G.A. Fry and Norma Miller, *Visual Recovery from Brief Exposure to Very High Luminance Levels*, USAF School of Aerospace Medicine, Brooks Air Force Base, Texas, SAM TDR 64-36, August 1964.

17. G. R. Garinther and J. B. Moreland, *Transducer Techniques for Measuring the Effects of Small Arms Noise on Hearing*, Tech. Memo. 11-65, U. S. Army Human Engineering Laboratory, Aberdeen Proving Ground, July 1965.

18. H.C. Graves, *Muzzle Blast Data from Firing of Howitzer 105mm, XM102*, Report No. DPS-670, Aberdeen Proving Ground, June 1962.

19. E.W. Hammer, Jr., *Muzzle Brakes, Volume I, History and Design*, The Franklin Institute Research Laboratories, Philadelphia, Pa., June 1949.

20. D.C. Hodge, R.B. McCommons and R.F. Blackmer, *Reliability of Temporary Threshold Shifts Caused by Repeated Impulse-Noise Exposures*, Technical Memorandum 3-65, U.S. Army Human Engineering Laboratory, Aberdeen Proving Ground, Md., February 1965.

21. D. C. Hodge and R. B. McCommons, *Further Studies of the Reliability of Temporary Threshold Shift from Impulse-Noise Exposure*, Tech. Memo. 3-66, U.S. Army Human Engineering Laboratory, Aberdeen Proving Ground, Md., December 1964.

22. Hugoniot, *Comptes Rendus*, Acad. Sci. Paris, Vol. 103, 1886.

23. G.F. Kinney, *Explosive Shocks in Air*, Macmillan, New York, 1962.

24. C.B. Millikan, E.E. Sechler and R.D. Buhler, *A Study of Blast Deflectors*, NDRC Report No. A-351, October 1945.

25. H.G. Noble, Jr., *Muzzle Brake Blast Attenuator (105mm Howitzer, XM102)*, Rock Island Arsenal, June 1963.

26. Pittaway, Young and Mathews, *Reduction of Smoke and Flash in Small Arms Ammunition — Historical and Technical Summary Report*, (U), Progress Report No. 12, Contract No. DA-23-072-ORD-769, Midwest Research Institute, Kansas City, Missouri, 31 October 1954.

27. A. Rateau, *Theorie des Freins de Boucke*, Memorial de l' Artillerie Francaise, Vol. XI, 1932.

28. R. Raymond and M. Salsbury, *A Discussion of the Use of the Atlantic Research Pencil Blast Gauge*, Rock Island Arsenal, August 1964.

29. R. Raymond and M. Salsbury, *Calculating the Blast Field from Artillery Weapons*, Rock Island Arsenal, June 1964.

30. E.L. Robinson, *Reduction of Smoke and Blast Obscuration Effect*, NDRC Report A-325, April 1945.

31. M.J. Salsbury, *Experimental Test of Reservoir-Type Muzzle Brake*, Tech. Report 65-1517, Rock Island Arsenal, June 1965.

32. A.H. Shapiro, *The Dynamics and Thermodynamics of Compressible Fluid Flow*, Vols. I and II, New York, The Ronald Press Co., 1953.

33. J.J. Slade, Jr., *Muzzle Blast: Its Characteristics, Effects, and Control*, NDRC Report No. A-391 (OSRD No. 6462), National Defense Research Committee, March 1946.

34. R.J. Sneed, G.G. Knight and E. Hartouni, *Flash Protection Device*, Final Report DA-19-129-QM-1965, General Dynamics, Pomona, Calif., U.S. Army Natick Labs, Natick, Mass., USA NLABS 64-1, 1963.

35. P.E. Townsend, *Development of a Gas Gun to Investigate Obscuration Effects*, Tech. Report 66-3281, Rock Island Arsenal, November 1966.

36. J.W. Wise, *Further Investigation Into the Propagation of High Pressure Waves in an Air Column*, Ordnance Dept., U.S. Army, June 1950.

37. R. R. A. Coles, G. R. Garinther, D. C. Hodge, C. G. Rice, "Hazardous Exposure to Impulse Noise", *Journal of the Acoustical Society of America*, December 1967.

INDEX

INDEX (CONT.)

INDEX (CONT.)

INDEX (CONT.)

INDEX (CONT.)

V

W

* U.S. GOVERNMENT PRINTING OFFICE : 1968 O—310-226

ENGINEERING DESIGN HANDBOOK

Listed below are the Handbooks which have been published or are currently being printed. Handbooks with publication dates prior to 1 August 1962 were published as 20-series Ordnance Corps pamphlets. AMC Circular 310-38, 19 July 1963, redesignated those publications as 706-series AMC pamphlets (i.e., ORDP 20-138 was redesignated AMCP 706-138). All new, reprinted, or revised Handbooks are being published as 706-series AMC pamphlets.

No.	Title
100	
102	
104	
106	Elements of Armament Engineering, Part One, Sources of Energy
107	Elements of Armament Engineering, Part Two, Ballistics
108	Elements of Armament Engineering, Part Three, Weapon Systems and Components
110	Experimental Statistics, Section 1, Basic Concepts and Analysis of Measurement Data
111	Experimental Statistics, Section 2, Analysis of Enumerative and Classificatory Data
112	Experimental Statistics, Section 3, Planning and Analysis of Comparative Experiments
113	Experimental Statistics, Section 4, Special Topics
114	Experimental Statistics, Section 5, Tables
115	
121	Packaging and Pack Engineering
123	
125	
127	
130	Design for Air Transport and Airdrop of Materiel
134	Maintainability Guide for Design (Revised)
135	Inventions, Patents, and Related Matters (Revised)
136	Servomechanisms, Section 1, Theory
137	Servomechanisms, Section 2, Measurement and Signal Converters
138	Servomechanisms, Section 3, Amplification
139	Servomechanisms, Section 4, Power Elements and System Design
140	Trajectories, Differential Effects, and Data for Projectiles
145	
150	Interior Ballistics of Guns
160(S)	Elements of Terminal Ballistics, Part One, Kill Mechanisms and Vulnerability (U)
161(S)	Elements of Terminal Ballistics, Part Two, Collection and Analysis of Data Concerning Targets (U)
162(S-RD)	Elements of Terminal Ballistics, Part Three, Application to Missile and Space Targets (U)
165	
170(C)	Armor and Its Application to Vehicles (U)
175	Solid Propellants, Part One
176(C)	Solid Propellants, Part Two (U)
177	Properties of Explosives of Military Interest
179	Explosive Trains
180	
185	Military Pyrotechnics, Part One, Theory and Application
186	Military Pyrotechnics, Part Two, Safety, Procedures and Glossary
187	Military Pyrotechnics, Part Three, Properties of Materials Used in Pyrotechnic Compositions
189	Military Pyrotechnics, Part Five, Bibliography
190	
205	
210	Fuzes, General and Mechanical
211(C)	Fuzes, Proximity, Electrical, Part One (U)
212(S)	Fuzes, Proximity, Electrical, Part Two (U)
213(S)	Fuzes, Proximity, Electrical, Part Three (U)
214(S)	Fuzes, Proximity, Electrical, Part Four (U)
215(C)	Fuzes, Proximity, Electrical, Part Five (U)
235	
238	
239	
240(C)	Grenades (U)
241	
242	Design for Control of Projectile Flight Characteristics
244	Ammunition, Section 1, Artillery Ammunition--General, with Table of Contents, Glossary and Index for Series
245(C)	Ammunition, Section 2, Design for Terminal Effects (U)
247	Ammunition, Section 4, Design for Projection
248	Ammunition, Section 5, Inspection Aspects of Artillery Ammunition Design
249	Ammunition, Section 6, Manufacture of Metallic Components of Artillery Ammunition
250	Guns--General
251	Muzzle Devices
252	Gun Tubes
255	Spectral Characteristics of Muzzle Flash
260	
270	Propellant Actuated Devices
280	
281(S-RD)	Weapon System Effectiveness (U)
282	Propulsion and Propellants
283	Aerodynamics
284(C)	Trajectories (U)
285	
286	Structures
290(C)	Warheads--General (U)
291	Surface-to-Air Missiles, Part One, System Integration
292	Surface-to-Air Missiles, Part Two, Weapon Control
293	Surface-to-Air Missiles, Part Three, Computers
294(S)	Surface-to-Air Missiles, Part Four, Missile Armament (U)
295(S)	Surface-to-Air Missiles, Part Five, Countermeasures (U)
296	Surface-to-Air Missiles, Part Six, Structures and Power Sources
297(S)	Surface-to-Air Missiles, Part Seven, Sample Problem (U)
327	Fire Control Systems--General
329	
331	Compensating Elements
335	
340	Carriages and Mounts--General
341	Cradles
342	Recoil Systems
343	Top Carriages
344	Bottom Carriages
345	Equilibrators
346	Elevating Mechanisms
347	Traversing Mechanisms
355	The Automotive Assembly (Revised)
356	Automotive Suspensions
357	

This document contains blank pages that were not filmed